Repeatability of a novel prototype surrogate neck model developed for omni-directional head impacts

by

Gabriella Faith Wynn

A thesis submitted in partial fulfillment of the requirements for the degree of

Master of Science

Department of Mechanical Engineering
University of Alberta

Abstract

Head impacts, both concussive and sub-concussive, are common in sports and can lead to adverse side effects. Since head kinematics are thought to correlate with brain injury, the implementation of protective headgear aimed to mitigate kinematics of the head during impacts. While fatal brain injuries have been reduced, concussions and other long-term effects of repetitive head impacts are still prevalent in football players at all levels. Physical surrogate models of the human head and neck are often used to assess impact severity in sports and infer the risk of brain injury, and in helmet certifications to explore the efficacy of helmets. The surrogate models can be instrumented with accelerometers to measure resultant head kinematics. Since the neck is thought to partially govern head kinematics during impact, the surrogate necks must demonstrate several performance characteristics to produce accurate results. Commercially available necks have acceptable repeatability and reproducibility, but they were not developed for the direct, multiplane loading in sports. As such, a novel prototype surrogate neck was developed for omni-directional direct head impacts. The objective of this work was to assess the repeatability and reproducibility of the neck.

Three copies of the prototype surrogate neck and one Hybrid III neck were attached to the same Hybrid III head and repeatedly impacted at 3.5 m/s using a pendulum impactor. Both the helmeted and the unhelmeted head were impacted at the front and the front boss locations. The within-neck coefficient of variation (CV_W) of the prototype surrogate neck kinematics for all impact conditions was 10% or less, which satisfies standard requirements for surrogates and is comparable to work on several standardized surrogate models. While differences between the three prototype surrogate necks were generally statistically significant, the normalized absolute differences between the neck copies were usually less than 10% and less than 20% in all cases except one. Most head and neck

certifications for current standardized models provide corridors that allow a range of ±10% on mean peak kinematics to be considered within specification - the normalized absolute differences of the prototype surrogate neck kinematics fall within that range. Further, the normalized absolute differences for other neck models were similar to what was calculated for the prototype surrogate neck. The reproducibility coefficient of variation (CV_B) values for the prototype surrogate necks were less than 15% for all kinematics and usually 10% or less, which is considered acceptable and is comparable to the reproducibility of commercially available surrogate models.

The prototype surrogate neck had CV_W values equivalent to the Hybrid III, but definitive conclusions cannot be made as to whether the kinematics differ. The Hybrid III kinematics were significantly different from the prototype surrogate neck kinematics for unprotected impacts, and the normalized absolute differences were greater than the differences calculated between the three copies of the prototype surrogate neck. In contrast, the helmeted impacts resulted in kinematics that were less significantly different between the Hybrid III and the prototype surrogate neck, with the normalized absolute differences commensurate in magnitude for the Hybrid III comparison and the prototype surrogate neck reproducibility assessment. However, the Hybrid III neck almost always had kinematics consistently greater than or less than all three of the prototype surrogate necks. Thus, the signs on the kinematics allow observation of actual differences between necks.

In summary, the prototype surrogate neck fit to a Hybrid III head and subject to multi-directional direct head impacts resulted in repeatable and reproducible kinematics. Although more testing is needed to quantify differences between the prototype surrogate neck and the Hybrid III, the prototype surrogate neck may be an effective tool for sports impact assessments.

Preface

This research is an original work by Gabriella Wynn. Parts of this thesis were first published in Annals of Biomedical Engineering, volume 49, pages 2957-2971, 2021 by Springer Nature:

> MacGillivray, S., Wynn, G., Ogle, M., Shore, J., Carey, J. P., and Dennison, C. R., 2021, "Repeatability and Biofidelity of a Physical Surrogate Neck Model Fit to a Hybrid III Head," Ann Biomed Eng, **49**, pp. 2957–2972.

The above article included information on the preceding neck model, described in Section 2.4.2 of this thesis. Thus, information on the assembly of the neck, experiments conducted, and data analysis methods are re-described in this thesis. Figure 2.2 in this thesis is also adapted from the above article.

The data presented on the front boss impacts of the helmeted and unhelmeted prototype surrogate necks and the unhelmeted Hybrid III neck were reproduced from the above article. Quasi-static compression tests on the polymer components are also duplicated. Phase 3 and Phase 4 details outlined in the methods of the above article were reproduced in this thesis, as were the data analysis methods and results related to those sections. Figures 3.4, 4.3, and 4.9 and tables 4.1, 4.3, 4.4, 4.6, and 4.16 in this thesis were reproduced/modified from the published article.

Some values in this thesis are directly replicated from the results published in the article, whereas others were derived from re-analysis of the data post-publication.

Acknowledgements

I would first like to thank Dr. Christopher Dennison for his guidance and support. I appreciate all the assistance he provided throughout the development of my experiments and the completion of this thesis. I am a more confident researcher due to the endless advice and knowledge he offered.

I would also like to thank Dr. Xinming Li, who allowed me to complete my thesis undisrupted at the University of Alberta. The feedback she provided on my thesis was invaluable, and I am grateful to have worked with her even for a short period.

My lab colleagues provided support and scholarly collaboration throughout my entire degree. My lab mates encouraged me never to give up and aspire to achieve better by helping to make my experiments run smoothly or assisting in troubleshooting when they failed. A special thank you to Lindsey Agnew and Paris Vakiel for reviewing my written thesis document.

Thank you to Megan Ogle and Samantha MacGillivray for your previous work developing the prototype surrogate neck and paving the way for my project to move forward. Also, thank you for your assistance with my project and for alleviating the anxiety I had about completing my MSc.

Finally, I would like to thank my family and friends for always supporting and encouraging me. Your faith in me motivates me to conduct my best research and succeed in my academic career. Without you, I would not be where I am today.

Table of Contents

1 Introduction 1

1.1 Motivation 1

1.2 Research Objectives 4

1.3 Thesis organization 4

2 Background Information 6

2.1 Traumatic Brain Injury 6

2.1.1 Definition of traumatic brain injury 6

2.1.2 Mechanics of Brain Injury 6

2.1.3 Reduction of TBI in sports 10

2.1.4 Importance of the Neck 13

2.2 Surrogate Models 13

2.2.1 Design requirements of surrogate models 14

2.3 Surrogate models of the neck 16

2.3.1 The Hybrid III 17

2.3.2 THOR 17

2.3.3 Side Impact Models 18

2.3.4 Limitations in repeatability and reproducibility assessments 20

2.4 Development of a new surrogate neck model 21

2.4.1 Initial neck prototype 21

2.4.2 Refined model 22

3 Methods 25

3.1 Design and Manufacture of Neck 25

3.1.1 Neck Design Refinements 25

3.1.2 Neck Manufacturing 26

3.1.3 Mechanical Properties of the Polymer Materials 27

3.2 Experimental Equipment 28

3.2.1 Pendulum and Linear Rail Assembly 28

3.2.2 Hybrid III Head 29

3.2.3 High-Speed Camera 30

3.3 Experimental Protocol 31
3.3.1 Sample Size Estimation 35
3.4 Data Analysis 35
3.4.1 Within-Neck Repeatability 36
3.4.2 Between-Neck Repeatability 37
4 Results 40
4.1 Repeatability of the three neck copies 40
4.1.1 Front boss impacts 40
4.1.2 Frontal impacts 50
4.2 Comparison with the Hybrid III neck 59
4.2.1 Front boss impacts 59
4.2.2 Frontal impacts 68
5 Discussion 77
5.1 Repeatability of prototype surrogate necks 77
5.1.1 Within-neck repeatability 77
5.1.2 Between-neck repeatability (Reproducibility) 80
5.2 Comparison to Hybrid III neck 82
5.3 Research Limitations and Future Directions 85
5.3.1 Neck Design and Manufacturing 85
5.3.2 Additive variance of helmets 86
5.3.3 Analysis Methods 87
5.3.4 Future Recommendations 88
6 Conclusion 90
6.1 Summary 90
6.2 Significance and Contributions 91
References 92

List of Tables

Table 2.1: Research studies on various models that have studied the correlation between kinematic parameters and TBI. 7

Table 2.2: Injury risk functions for brain injury based on kinematic parameters. The methods to derive each risk function are also outlined. 11

Table 3.1: Sample size for each impact scenario. 33

Table 4.1: Mean, SD, CV_W, and 95% CI values of the kinematic responses from the front boss helmeted impacts for the three prototype surrogate neck copies and the Hybrid III. The Hybrid III data is used in Section 4.2. Adapted with permission from Springer Nature, MacGillivray et al. [142] copyright 2021. 41

Table 4.2: Mean differences between the prototype surrogate necks and p-values from the ANOVAs and post-hoc statistical tests run on the full dataset and the dataset with outliers removed for all head kinematics during front boss helmeted impacts. Shaded cells represent p-values that differed due to the removal of outliers. 42

Table 4.3: Normalized absolute differences between the prototype surrogate necks for helmeted front boss impacts. Adapted with permission from Springer Nature, MacGillivray et al. [142] copyright 2021. 43

Table 4.4: Mean, SD, CV_W, and 95% CI values of the kinematic responses from the front boss unhelmeted impacts. The Hybrid III data is used in Section 4.2. Adapted with permission from Springer Nature, MacGillivray et al. [142] copyright 2021. 45

Table 4.5: Mean differences between the prototype surrogate necks and p-values from the ANOVAs and post-hoc statistical tests run on the peak head kinematics with and without outliers during front boss unhelmeted impacts. 46

Table 4.6: Normalized absolute differences between the surrogate prototype necks for unhelmeted front boss impacts. Adapted with permission from Springer Nature, MacGillivray et al. [142] copyright 2021. 47

Table 4.7: Mean, SD, CV_W, and 95% CI values of the kinematic responses from the helmeted frontal impacts. The Hybrid III data is used in Section 4.2. 50

Table 4.8: Mean differences between the prototype surrogate necks and p-values from the ANOVAs and post-hoc statistical tests run on the full dataset and the dataset with outliers removed for all head kinematics during impacts to the front of the helmeted head. Shaded cells represent p-values that differed due to the removal of outliers. 51

Table 4.9: Normalized absolute differences between the prototype surrogate necks for helmeted frontal impacts. 52

Table 4.10: Mean, SD, CV_W, and 95% CI values of the kinematic responses from the front impact condition. The Hybrid III data is used in Section 4.2. 54

Table 4.11: Mean differences between the prototype surrogate necks and p-values for the ANOVAs and post-hoc statistical tests run on the unhelmeted neck for the entire dataset and on the dataset with outliers removed for frontal head impacts. 55

Table 4.12: Normalized absolute differences between the prototype surrogate necks for unhelmeted frontal impacts. 56

Table 4.13: Mean differences between the surrogate neck prototype and the Hybrid III neck, and results of ANOVAs and post-hoc statistical tests run on the full dataset and the dataset with outliers removed for all head kinematics during front boss helmeted impacts. 60

Table 4.14: Normalized absolute differences between the Hybrid III neck and the prototype surrogate necks for helmeted front boss impacts. 61

Table 4.15: Mean differences between the Hybrid III neck and the prototype surrogate necks, as well as p-values from ANOVAs and post-hoc tests run on the full dataset and the dataset with outliers removed for all head kinematics during front boss unhelmeted impacts. 63

Table 4.16: Normalized absolute differences between the Hybrid III neck and the three prototype surrogate necks for unhelmeted front boss impacts. Adapted* with permission from Springer Nature, MacGillivray et al. [142] copyright 2021. 64

Table 4.17: Mean differences between the Hybrid III and the prototype surrogate neck kinematics during frontal helmeted impacts are reported, along with the p-values from ANOVAs and post-hoc statistical tests run on the full dataset and the dataset with outliers removed for all head kinematics. 69

Table 4.18: Normalized absolute differences between the Hybrid III and the three prototype surrogate necks for helmeted frontal impacts. 70

Table 4.19: Mean differences between the peak kinematics of the Hybrid III neck and the prototype surrogate necks reported along with the p-values from ANOVAs and post-hoc statistical tests run on the full dataset and the dataset with outliers removed for all head kinematics during front unhelmeted impacts. 72

Table 4.20: Normalized absolute differences between the Hybrid III neck and the prototype surrogate necks during unhelmeted frontal impacts. 73

List of Figures

Figure 2.1: CAD model and fully assembled prototype of the first neck iteration [52]. Left (CAD) image adapted with permission from Ogle 2018 [52]; right image adapted with permission from MacGillivray 2020 [53]. 22

Figure 2.2: The refined surrogate neck's internal and external structure [53]. Adapted with permission from MacGillivray 2020 [53] and Springer Nature, MacGillivray et al. [142] copyright 2021 23

Figure 3.1: Modifications to the prototype surrogate neck. The gimbal bracket adapter was transformed into a circular shape, and additional bolts were added to allow stronger clamping of the silicon. Not shown are the aluminum ring plates, which also had extra bolts added. The image on the left was adapted with permission from MacGillivray 2020 [53]. 25

Figure 3.2: Final assembly of the newest version of the prototype surrogate neck. The CAD model on the left displays all neck components, except the internal cables. 26

Figure 3.3: Hybrid III head-surrogate neck assembly atop a linear rail. The head-neck assembly is attached to a translating stage by an adjustable gimbal. The translating stage allows the assembly to move freely along the rail. 28

Figure 3.4: Pendulum impactor system, showing the steel pendulum arm with an MEP pad and steel plates. The Hybrid III head-neck assembly is located atop a translating linear rail. Reproduced with permission from Springer Nature, MacGillivray et al. [142] copyright 2021. 29

Figure 3.5: The Hybrid III head showing the positive coordinate system for the head COG accelerations. The x-axis is directed along the sagittal plane (anterior-posterior axis), the y-axis along the coronal plane (medial-lateral axis), and the z-axis perpendicular to the transverse plane (inferior-superior axis). 30

Figure 3.6: Impact locations on the Hybrid III head: (a) front boss impacts with a football helmet, (b) front boss impacts to the unhelmeted head, (c) frontal impacts with a football helmet, and (d) frontal impacts to the unhelmeted head. 32

Figure 3.7: Sample plot for determining peak kinematics. Red stars represent the location of chosen maxima for each curve. The peak maxima for all prototype surrogates fall within 60 ms; the Hybrid III curve increases after the initial impact region. 34

Figure 4.1: Mean and standard deviations of the (a) peak linear accelerations, (b) peak angular accelerations, and (c) peak angular velocities of all three neck copies equipped with a helmet and impacted laterally near the front boss. Significant differences between necks are denoted by an asterisk (* = p<0.05). 44

Figure 4.2: Mean and standard deviations of the (a) peak linear accelerations, (b) peak angular accelerations, and (c) peak angular velocities of all three unhelmeted necks impacted laterally near the front boss. An asterisk denotes significant differences between necks (* = p<0.05). 48

Figure 4.3: Ensemble averages of all three necks during helmeted impacts (left column) and unhelmeted impacts (right column) to the front boss of the head. Linear accelerations (first row), angular accelerations (second row), and angular velocities (third row) are shown for all three surrogate prototype necks. The figures representing helmeted impacts were reproduced with permission from Springer Nature, MacGillivray et al. [142] copyright 2021. 49

Figure 4.4: Means and standard deviations of the (a) peak linear accelerations, (b) peak angular accelerations, and (c) peak angular velocities of all three neck copies equipped with a helmet and impacted to the front of the head. Significant differences between necks are denoted by an asterisk (* = p<0.05). 53

Figure 4.5: Means and standard deviations of the (a) peak linear accelerations, (b) peak angular accelerations, and (c) peak angular velocities of all three unhelmeted necks during impacts to the front of the head. An asterisk denotes significant differences between necks (* = p<0.05). 57

Figure 4.6: Ensemble averages of all three surrogate prototype necks during helmeted impacts (left column) and unhelmeted impacts (right column) to the front of the head. Linear accelerations (first row), angular accelerations (second row), and angular velocities (third row) for all neck prototypes are displayed for the first 100 ms. 58

Figure 4.7: Means and standard deviations of the (a) peak linear accelerations, (b) peak angular accelerations, and (c) peak angular velocities of the Hybrid III neck and the three prototype surrogate necks when impacts were delivered to the front boss of the helmeted Hybrid III head. Data from Figure 4.1 is replotted alongside the new Hybrid III data. A red asterisk denotes a significant difference from the Hybrid III neck ($p<0.05$). 62

Figure 4.8: Means and standard deviations of the (a) peak linear accelerations, (b) peak angular accelerations, and (c) peak angular velocities of the Hybrid III neck and the three prototype surrogate necks when impacts were delivered to the front boss of the unhelmeted Hybrid III head. Data from Figure 4.2 is replotted alongside the new Hybrid III data. A red asterisk denotes a significant difference from the Hybrid III neck ($p<0.05$). 65

Figure 4.9: Ensemble averages of all three prototype surrogate necks and the Hybrid III neck during helmeted impacts (left column) and unhelmeted impacts (right column) to the front boss of the head. The top right miniature graphs are close-ups of the peaks for the linear and angular accelerations. Figures of the unhelmeted impacts were adapted with permission from Springer Nature, MacGillivray et al. [142], copyright 2021. 67

Figure 4.10: Means and standard deviations of the (a) peak linear accelerations, (b) peak angular accelerations, and (c) peak angular velocities of the Hybrid III neck and the three prototype surrogate necks when frontal impacts were delivered to the front of the helmeted Hybrid III head. Data from Figure 4.4 is replotted alongside the new Hybrid III data. A red asterisk denotes a significant difference from the Hybrid III neck ($p<0.05$). 71

Figure 4.11: Means and standard deviations of the (a) peak linear accelerations, (b) peak angular accelerations, and (c) peak angular velocities of the Hybrid III neck and the three prototype surrogate necks for frontal impact to the unhelmeted Hybrid III head. Data from Figure 4.5 is replotted alongside the new Hybrid III data. A red asterisk denotes a significant difference from the Hybrid III neck ($p<0.05$). 74

Figure 4.12: Ensemble averages of all three prototype surrogate necks and the Hybrid III neck during helmeted impacts (left column) and unhelmeted impacts (right column) to the front of the

head. The graphs in the top-right corner of the linear acceleration and angular accelerations plots are close-ups of the peaks for all necks. 76

1 Introduction

1.1 Motivation

Traumatic brain injury (TBI) affects approximately 70 million people worldwide annually, with the highest incidence rates reported in the United States and Canada [1]. Self-reported data from Canadians aged 12 years or older found that 508 out of 100,000 people [2] (or around 0.5% of the population [3]) experienced a "concussion or other reported brain injury" as their most serious injury in 2013/14. Estimating a population of 33 million Canadians aged 12 years or older in 2021 [4], approximately 165,000-168,000 Canadians will have sustained a brain injury last year. However, reports using national databases suggest higher rates. TBI-related emergency department (ED) visits in Ontario recorded from the National Ambulatory Care Reporting System (NACRS) determined an incidence rate of 1030.6/100,000 in 2009/10 [5]. However, based on a Public Health Agency of Canada (PHAC) report, which also used the NACRS, an estimated rate of 340/100,000 was found for the same year [6]. The difference in incidence rates is likely attributed to the inclusion of different injury types: the former article included open head wounds and other injury criteria that the PHAC report did not [5,6]. Considering both incidence rates and estimating the total population of Canada in 2021 to be 38 million people [4], approximately 129,000-392,000 Canadians had a TBI last year.

The PHAC also reported rates of TBI-related hospitalizations and ED visits over a larger time scale. The Hospital Morbidity Database and Discharge Abstract Database evaluated hospitalizations across Canada from 2006-2011 and 2011-2018, respectively. The NACRS reported ED visits from 2002-2018. From 2002-2010, the ED visits were reported in Ontario only; from 2010-2018, Alberta data was also included [6]. The combined rate of hospitalization and ED visits for the entire study period was approximately 644/100,000. However, rates increased over time, roughly stabilizing at about 945/100,000 over the final few years [6]. Using the increased rate for the 2021 population, approximately 360,000 Canadians will have experienced a TBI last year. Overall, an estimated 130,000-400,000 Canadians experience a TBI each year. However, the true estimate may be higher due to the lack of data in all Canadian provinces and the potential underreporting of mild brain injuries [6].

The Centre for Disease Control [7] reported that cognitive, behavioural/emotional, motor, sensory, and physical impairments were all associated with TBI; symptoms include deficits in memory, aggression, difficulty walking, and chronic pain. Depression, epilepsy, and post-traumatic stress disorder can also develop due to a TBI [7]. Even mild traumatic brain injuries (mTBIs), such as concussions, can lead to adverse side effects. As a result of a concussion, a person may show cognitive deficits, behavioural/emotional changes, balance issues, and trouble sleeping [8,9]. Aside from health concerns, TBI has a heavy economic burden. Based on direct medical costs and indirect costs due to lost productivity, the cost of TBI in Ontario in 2009 was estimated to be $945 million. However, the authors acknowledged that the criteria used to define TBI might differ based on the methodology used and suggested the actual cost of TBI likely fell within $279 million to $1.22 billion [5]. Considering Ontario only represents approximately 39% of the Canadian population [4], the annual cost of TBI across Canada is likely even greater.

Brain injury is a common consequence of head injury in sports. In Canada, approximately 24-50% of reported brain injuries are sports-related (or sports and recreation (SPAR) related) [2,3,6,10]. For youth, injury risk increases; one study found approximately 53% of brain injuries in those aged 10-19 are SPAR-related [6], while another suggested rates of 86% in youth aged 12-17 [3]. Further, those aged 5-24 are eight times more likely to sustain a sports-related TBI [5]. Concussions are a primary concern in sports, representing approximately 80% of the hospitalizations and ED visits due to SPAR-related TBI [6]. Football is one of the most common sports with reported TBIs in the Canadian youth population, with concussions making up 20% of all reported injuries in males [11].

In addition to concussions, repetitive hits to the head in sports are a growing concern. A recent review [12] suggested that repetitive sub-concussive head impacts, which do not lead to any clinically observable signs of concussion [12,13], are related to microstructural and functional changes in athletes' brains. Exposure to repeated head impacts can also lead to chronic traumatic encephalopathy [14], cognitive and behavioural impairment [15], and depression [15]. A review by Bailes et al. found that the average number of head impacts in one football season ranged from 100 to >1200 for athletes at all levels [13]. Studies on Canadian university football concluded that athletes sustained approximately 42-45 impacts per game on average [16,17], which results in 336-810 impacts for typical 8-game and 18-game seasons. Neurocognitive testing and task-based brain

imaging on high school students suggested that neurophysiological changes always occur when the head is impacted greater than 500 times during a season, even in players without concussion symptoms; however, even less than 500 impacts often resulted in similar adverse effects [18]. A subsequent study showed that players with greater than 900 cumulative head impacts had an increased rate of showing neurophysiological changes post-season as well [19]. Thus, the high rate of repetitive head impact and adverse effects highlights the need to mitigate the incidence and severity of head impact in sports.

Central to the research on reducing the effects of head impacts and subsequent injury in athletes is understanding impact severity levels and the role of protective gear. Research endeavours for the above often use physical models of the human, commonly referred to as anthropometric test devices (ATDs) or surrogates. Surrogates of the human head and neck are often employed for brain injury research applications because they provide repeatable and reproducible data [20–24] and can be impacted at injurious levels that would otherwise be unethical with human volunteers [20,22,24]. As such, surrogate models of the head and neck are often used (either just the head and neck components or attached to the torso/full dummy) to measure impact mechanics in laboratory reconstructions of head impacts in sports [25–32] and to evaluate helmet efficacy [33–40].

However, there are concerns regarding whether current commercially available neck models are appropriate for sports biomechanics research. Current neck models were developed for the automotive industry for specific loading directions [20–22,24,41–47]. Sports injury mechanics are arguably dissimilar to automotive injury due to factors like lack of torso restraint (seatbelts), high incidence of direct head impacts, and impacts to a broader range of the body. This limits the validity of using these surrogates in sports injury applications for which they were not intended. For example, the Hybrid III neck is most often used in sports reconstructions and helmet certifications [25–31,33–40]; however, the neck is considered to be too stiff in axial compressive loading [48,49] and along the sagittal plane [50] compared to cadavers. Further, the neck is stiffer than pre-tensed volunteers in frontal flexion, lateral flexion, and torsion [51].

Thus, there is a need for a surrogate neck model that is optimized for multi-directional loading and direct head impacts. The development of such a neck will aid in studying the biomechanics that

cause head injury in athletes, leading to refined safety regulations and protective gear to decrease the prevalence of brain injuries. The Biomedical Instrumentation Lab at the University of Alberta has developed and assessed a prototype surrogate neck designed for these objectives [52,53]. This thesis examines the repeatability and reproducibility of the resultant head kinematics when the surrogate neck is applied with a Hybrid III head in direct head impact loading scenarios.

1.2 Research Objectives

The main objective of this research is to analyze the repeatability and reproducibility of the prototype surrogate neck in multi-directional direct head impacts. This work describes design modifications to improve the neck's ease of assembly and mechanical durability during high-energy impact testing. Three copies of the prototype surrogate neck were manufactured and tested under identical experimental conditions to characterize significant differences between the resultant head kinematics. The three necks were also compared to the Hybrid III, the most common surrogate neck model used in sports injury biomechanics research.

In summary, the objectives of this research are twofold:

1) To examine any differences between three copies of a prototype surrogate neck and determine the neck's repeatability and reproducibility for standardized use across research experiments, personnel, and laboratories.
2) To compare the prototype surrogate neck to the Hybrid III neck, to ascertain whether the peak kinematics and repeatability differed between the models.

1.3 Thesis organization

Chapter 2 reviews necessary background information to supplement the work completed in this thesis. The chapter discusses the kinematics that correlate to brain injury and the applications to injury biomechanics research. Current commercially available surrogate models are outlined, focusing on the repeatability and reproducibility of the head kinematics of the models. Previous iterations of the prototype surrogate neck are summarized, and the performance requirements are presented, emphasizing the repeatability of the models. Finally, the limitations of the previous prototype surrogate neck models are addressed.

Chapter 3 describes the modifications to the prototype surrogate neck model. Specific properties of the neck are also presented. Experimental and analysis techniques to quantify repeatability and reproducibility between three copies of the prototype surrogate neck are summarized. Finally, methods to compare the prototype surrogate neck to the Hybrid III neck are detailed.

Chapter 4 outlines the results of the repeatability and reproducibility of the prototype surrogate neck and the comparisons to the Hybrid III neck. Coefficient of variation (CV) analysis is performed to determine the repeatability and reproducibility of peak head kinematics. Reproducibility is also assessed by comparing peak kinematics using an ANOVA. The normalized absolute differences are quantified between the three prototype surrogate neck copies and between the prototype surrogate neck and the Hybrid III. Visual time curve comparisons are also presented.

Chapter 5 discusses the implications of the experimental results, focusing on the repeatability and reproducibility of head kinematics the prototype surrogate neck. The repeatability and reproducibility are compared to standardized surrogate models. A more detailed discussion comparing the prototype surrogate neck and the Hybrid III neck is presented. Finally, the limitations are discussed, and recommendations for future work to further strengthen the use of the surrogate neck as an injury biomechanics model are offered.

Chapter 6 summarizes the work conducted and outlines the contributions of this thesis.

2 Background Information

2.1 Traumatic Brain Injury

2.1.1 Definition of traumatic brain injury

Traumatic and mild traumatic brain injury (TBI and mTBI) involve a disruption to the normal brain physiology caused by an external force [8,54]. For mTBIs, the brain dysfunction is briefer and less severe [8,9]. This external force can include a direct impact to the head or an indirect impact to the head, wherein impact to another region of the body leads to subsequent brain acceleration [8,9,54]. In sports, direct loading often occurs in helmet-to-helmet (or another surface) collisions. In contrast, indirect impacts are caused by impulsive loading to the head through impact to the torso or other body parts (i.e. tackling) [55]. Brain injuries are categorized as focal or diffuse depending on the area distribution of injury [56–58]; this thesis mainly focuses on diffuse brain injuries since concussions, which are common in sports [6], are diffuse injuries [56–58].

2.1.2 Mechanics of Brain Injury

Brain injuries are related to the type of forces acting on the head. Contact forces can lead to deformation of the skull tissue or pressure changes in the brain, whereas inertial forces result in accelerations that generate motion of the skull and brain [56,58]. These forces are caused by external dynamic loading to the head, which has previously been described as either direct loading, which can lead to both contact or inertial forces, or indirect loading, which results only in inertial forces [56,58,59]. These inertial forces correlate to injury by the mechanics related to the head's translational and rotational motion [30,56–59]. Linear acceleration, angular acceleration, and angular velocity have been proposed as mechanical parameters that correlate with diffuse brain injury (Table 2.1). While most research seems to suggest rotational kinematics correlate better with injury, many studies highlight the role of linear kinematics or combined mechanics as well. Further, it is generally acknowledged that linear and rotational motion always co-exist in real-world scenarios [30,55,57,60–62], suggesting that linear acceleration, angular acceleration, and angular velocity may all be important factors in brain injury.

Table 2.1: Research studies on various models that have studied the correlation between kinematic parameters and TBI.

Study	Model(s)	Kinematic parameter	Relevant Findings
Denny-brown and Russel (1941) [63]	Cats Dogs Rhesus monkeys Green monkeys	Acceleration	- Unconstrained motion of the head increases the occurrence of a concussion - A concussion can be produced by the acceleration or deceleration of the head
Holbourn (1943) [64]	Head and brain surrogate	Angular acceleration Angular velocity	- Suggested that rotation leads to injurious shear strains that cause concussions - Injury from long-duration impacts proportional to acceleration; short-duration impacts proportional to change in velocity
Ommaya et al. (1964) [65]	Rhesus monkeys	Angular acceleration	- When the rotation of the head atop the neck was limited through the use of a cervical collar, it was more difficult to produce concussion, and higher linear accelerations were necessary - Hypothesized that when the head was free to move, higher shear strains occurred in the brain due to the angular acceleration
Ommaya et al. (1966) [66]	Rhesus Monkeys	Linear acceleration	- Peak linear acceleration had a significant correlation with concussions during direct head impacts
Gurdjian, Roberts, and Thomas (1966) [67]	Cadavers	Linear acceleration	- The initial formation of the Wayne State Tolerance Curve (WSTC), wherein the risk of skull fracture depends on the average linear acceleration and the duration of impact - Skull fracture correlates with moderate to severe concussion
Hodgson et al. (1969) [68]	Stumptail monkeys	Linear acceleration	- After a direct head impact, both linear and angular acceleration are involved in head motion - Cellular evidence suggests linear acceleration is the most critical factor in causing a concussion
Unterharnscheidt (1971) [69]	Cats Squirrel Monkeys	Linear acceleration Angular acceleration	- Linear accelerations and rotational accelerations lead to different mechanisms and types of brain injury

Gennarelli, Ommaya, and Thibault (1971) [70]; Gennarelli, Thibault, and Ommaya (1972) [71]; Ommaya and Gennarelli (1974) [59]	Squirrel monkeys	Linear acceleration Angular acceleration Angular velocity	- Both accelerations caused brain lesions, but animals subject to only translational motion received fewer and more localized - Linear acceleration alone cannot cause a concussion, and rotation of the head is necessary - Hypothesized that the angular acceleration induces damaging shear strains that caused concussion (explicitly stated in [71])
Abel, Gennarelli, and Segawa (1978) [72]	Rhesus monkeys	Linear acceleration Angular acceleration	- Peak angular acceleration and peak linear acceleration are both related to injury severity - Suggested that a combination of linear and angular mechanics are factors in causing a concussion
Ono et al. (1980) [73]	Monkeys (Japanese, Rhesus, Crab-eating, and baboons) Cadavers	Linear acceleration	- In direct head impacts, concussion was highly correlated to linear head acceleration but not to angular head acceleration - Produced tolerance curve that confirmed the WSTC
Gennarelli, Adams, and Graham (1981) [74]	Monkeys (species undefined)	Angular acceleration	- Injury severity increased with angular acceleration - Resultant injuries ranged from subconcussive to immediate death
King et al. (2003) [30]	Hybrid III dummies FE Model	Linear acceleration Angular acceleration	- Both peak linear and angular acceleration were significant predictors of mTBI
Pellman et al. (2003) [29]	Hybrid III head-neck Football players	Linear acceleration Angular acceleration	- Concussions most strongly correlated with peak linear acceleration, with a weaker correlation to peak angular acceleration - No correlation between concussion and peak angular velocity
Zhang, Yang, and King (2004) [28]	Hybrid III head-neck FE model	Linear acceleration Angular acceleration	- Both linear and angular acceleration are significant predictors of mTBI, but a combination of the kinematics may be a better predictive model
Zhang et al., (2006) [75]	Cadaver head with surrogate brain FE model	Angular acceleration	- More than 90% of maximum principal strain (MPS)* is contributed by the angular acceleration
Kleiven (2007) [27]	Hybrid III FE model	Linear acceleration Angular acceleration Angular Velocity	- The combination of linear acceleration (and HIC†, a linear acceleration based metric) with angular kinematics increases the correct classification of concussion

Greenwald et al. (2008) [76]	Football Athletes	Linear acceleration Angular acceleration	-	A weighted combination of biomechanical measures that included linear and rotational acceleration (wPCS†) is generally most sensitive to the prediction of mTBI (had lowest false response rate)
Takhounts et al. (2008) [77]	Football Athletes FE model	Angular acceleration Angular velocity	-	Strain based injury metrics* correlated to angular kinematics, with a slightly better correlation to angular velocity
SAE J885 (2011, v1 1962) [78]	Animals Cadavers Volunteers	Linear Acceleration	-	Summary on the development of the WSTC, a tolerance curve for concussion based on average linear acceleration
Beckwith et al. (2013) [79]	Football Athletes	Linear acceleration	- -	Peak linear acceleration and HIC† were most sensitive to immediately diagnosed concussion Peak angular acceleration was least sensitive
Rowson and Duma (2013) [80]	Football Athletes	Linear acceleration Angular acceleration	-	Linear acceleration and CP†, a function that combines linear and rotational accelerations, are the better predictors of concussion than angular acceleration
Takhounts et al. (2014) [32]	ATDs FE Models	Angular velocity	- -	Peak angular velocity correlated best to strain measures* Angular velocity suggested as the mechanism for brain injury
Ji et al. (2014) [60]	Athletes FE Model	Angular velocity	- -	Strain measures* significantly correlated with angular velocity No significant correlation with linear acceleration
Elkin, Elliot, and Siegmund (2016) [31]	ATDs FE Model	Angular acceleration Angular velocity Linear acceleration	- -	MPS* was strongly correlated with peak angular velocity change Peak angular acceleration was slightly better correlated than peak linear acceleration, but both were moderately strong
Gabler et al. (2016) [81]	Cadavers ATDs FE Model	Angular acceleration Angular velocity	-	Angular kinematics and angular kinematic based functions are more highly correlated to strain measures* compared to translation-based metrics
Knowles and Dennison (2017) [26]	Hybrid III head-neck FE model	Angular velocity	-	Angular velocity was the best predictor of strain measures*

*Strain based measures correlate with and predict brain injury [27,30,77,82–85]; †Defined in Table 2.2

Due to the evidence supporting the correlation between kinematic parameters and injury, head kinematics are often used to assess injury risk. For example, tolerance levels for brain injury based on linear and rotational kinematics have been developed (and reviewed elsewhere [86–88]), which allow researchers to have guidelines for potential injury levels. The capabilities of these kinematic parameters in predicting injury have also led to several proposed injury risk functions that correlate the risk of injury with the acceleration or velocities experienced by the head (Table 2.2). As with the kinematics, several brain injury thresholds have been described for the injury risk functions [32,61,88,89]. Because kinematics play an essential role in assessing injury severity, researchers tend to assess protective gear using kinematics, especially looking for reductions in kinematics due to the protection. Desirable surrogate models, often used in these helmet certifications, must thus yield realistic kinematics.

2.1.3 Reduction of TBI in sports

Historically, helmet assessment methods examined helmets' ability to mitigate impact mechanics based on their ability to reduce peak translational accelerations or linear acceleration-based injury metrics (HIC and SI) to a specified threshold [22,34,35,90–94]. Although the implementation of protective headgear is credited with helping reduce the incidence of moderate and severe/fatal TBI [95–98], sports-related concussions are still prevalent [2,3,6,10,11,76]. This may be because the certifications only assessed the attenuation of linear kinematics, even though rotational kinematics also correlate to injury. Thus, certifying helmets against multiple biomechanical measures may further mitigate the risk and severity of mTBI. Several helmet certifications and assessment methods now assess peak angular acceleration or velocity in addition to linear acceleration [33–35,94]. These helmet certification methods employ a pendulum [33] or a linear impactor [34,35,94] impacting a head-neck assembly atop a sliding linear rail, which allows the generation of both translational and rotational motion [33,86]. As mentioned above, these helmet certification methods often use surrogate models. Unlike older helmet certifications, which only use a surrogate head, several current helmet testing methods also employ a surrogate neck.

Table 2.2: Injury risk functions for brain injury based on kinematic parameters. The methods to derive each risk function are also outlined.

Risk Function	Equation	Derivation method
Severity Index (SI) [78,99]	$\mathrm{SI} = \int \mathrm{a(t)}^{2.5}\,\mathrm{dt}$	WSTC
Head Injury Criteria (HIC) [78,100,101]	$\mathrm{HIC} = \left\{ (\mathrm{t_2} - \mathrm{t_1}) \left[\frac{1}{\mathrm{t_2} - \mathrm{t_1}} \int_{\mathrm{t_1}}^{\mathrm{t_2}} \mathrm{a(t)dt} \right]^{2.5} \right\}_{\max}$	WSTC
A Generalized Model for Brain Injury Threshold (GAMBIT) [102]	$\mathrm{GAMBIT} = \max_{\mathrm{t}} \sqrt{\left[\left(\frac{\mathrm{a}_{max}}{\mathrm{a_c}} \right)^2 + \left(\frac{\alpha_{max}}{\alpha_{\mathrm{c}}} \right)^2 \right]}$	Classical engineering normal and shear stress
Head Injury Power (HIP) [103]	$\mathrm{HIP} = \mathrm{m} \sum_{i=x,y,z} \mathrm{a_i} \int \mathrm{a_i dt} + \sum_{i=x,y,z} \mathrm{I_{ii}} \alpha_{\mathrm{i}} \int \alpha_{\mathrm{i}} \mathrm{dt}$	Power (rigid body dynamics)
Weighted Principal Component Score (wPCS) [76]	$\mathrm{wPCS} = 10 \left(\beta_0 \cdot \frac{\mathrm{SI} - \overline{\mathrm{SI}}}{\sigma_{\mathrm{SI}}} + \beta_1 \cdot \frac{\mathrm{HIC} - \overline{\mathrm{HIC}}}{\sigma_{\mathrm{HIC}}} + \beta_2 \cdot \frac{\mathrm{a} - \bar{\mathrm{a}}}{\sigma_{\mathrm{a}}} + \beta_3 \cdot \frac{\alpha - \bar{\alpha}}{\sigma_{\alpha}} + 2 \right)$	Principle component analysis (football player input data)
Power Rotational Head Injury Criterion (PRHIC) [82,104]	$\mathrm{PRHIC} = \left\{ (\mathrm{t_2} - \mathrm{t_1}) \left[\frac{1}{\mathrm{t_2} - \mathrm{t_1}} \int_{\mathrm{t_1}}^{\mathrm{t_2}} \mathrm{HIP_{rot}(t)dt} \right]^{2.5} \right\}_{\max}$ $\mathrm{HIP_{rot}} = \sum_{i=x,y,z} \mathrm{I_{ii}} \alpha_{\mathrm{i}} \int \alpha_{\mathrm{i}} \mathrm{dt}$	Modified HIC
Rotational Injury Criterion (RIC) [82]	$\mathrm{RIC} = \left\{ (\mathrm{t_2} - \mathrm{t_1}) \left[\frac{1}{\mathrm{t_2} - \mathrm{t_1}} \int_{\mathrm{t_1}}^{\mathrm{t_2}} \alpha(\mathrm{t})\mathrm{dt} \right]^{2.5} \right\}_{\max}$	Modified HIC

Rotational Brain Injury Criterion (BRIC) [61]	$\mathrm{BRIC} = \frac{\omega_{\max}}{\omega_c} + \frac{\alpha_{\max}}{\alpha_c}$	Best linear fit to strain-based metrics
Brain Injury Criteria (BrIC) [32]	$\mathrm{BrIC} = \left\{\sum_{i=x,y,z}\left(\frac{\omega_i}{\omega_{i,c}}\right)^2\right\}^{1/2}$	Best linear fit to strain-based metrics
Combined Probability (CP) of Concussion [80]	$\mathrm{CP} = \frac{1}{1+e^{-(\beta_0+\beta_1 a_{max}+\beta_2\alpha_{max}+\beta_3 a_{max}\alpha_{max})}}$	Multivariate logistic regression
Rotational Velocity Change Index (RVCI) [105]	$\mathrm{RVCI} = \left[\left\{\sum_{i=x,y,z} R_i\left(\int_{t_1}^{t_2}\alpha_i dt\right)^2\right\}^{1/2}\right]_{max}$	Spring-mass system deformation
Universal Brain Injury criteria (UBrIC) [106]	$\left\{\sum_{i=x,y,z}\left[\frac{\omega_i}{\omega_{i,c}} + \left(\frac{\alpha_i}{\alpha_{i,c}} - \frac{\omega_i}{\omega_{i,c}}\right)e^{-\frac{\alpha_i/\alpha_{i,c}}{\omega_i/\omega_{i,c}}}\right]^2\right\}^{\frac{1}{2}}$	Maximum deformation of excited second order system

a = linear acceleration; α = angular acceleration; ω = angular velocity; $q_{i,c}$ = critical value of q, where q refers to any kinematic; $\bar{q}$ = mean of q; σ = standard deviation, $\beta_{0,1,2,3}$ = correlation coefficient; R_i = weighting factors; m= mass; I = moment of inertia; t = time

2.1.4 Importance of the Neck

Hypotheses suggest that the neck partly governs head kinematics. The neck tethers the head to the torso such that any loading to the body can transfer through the neck to the head via the cervical spine and muscles [57]. Early research on primates showed that using a cervical collar to prevent the movement of the neck reduced the incidence of concussion [65,107]. It was hypothesized that preventing motion of the neck would reduce the tensile and shearing strains transmitted through the cervical cord to the brain. This reduction in shearing strains was thought to be due to the reduced angular acceleration acting on the brain due to the collar [65,107]. More recently, research on volunteers has examined the correlation between neck characteristics and head kinematics. The effect of neck muscle activation has been shown to affect the peak angular velocity [108,109], peak linear acceleration [108,109], and peak angular acceleration [108] of the head. Similarly, increased neck stiffness (which is proportional to improved muscle activation) significantly reduced the odds of sustaining moderate and severe head impacts as assessed by a combined linear and angular kinematic metric (wPCS, Table 2.2) [110]. As mentioned above, continued efforts to reduce the impact of TBI in sports are intertwined with the mitigation of kinematic parameters of the head during impacts. Since the neck appears to affect the resultant head kinematics, it plays a crucial role in furthering research in the field. Thus, a surrogate neck model used in helmet testing or sports reconstructions must be developed to produce accurate and reliable kinematics.

2.2 Surrogate Models

Human surrogate models have anatomical and mechanical characteristics that allow them to recreate the biomechanical responses of humans [20,22,24,111]. Surrogates of the head and neck are often coupled with instrumentation to measure the linear and rotational kinematics of the head during simulated impact scenarios [22,44,45,47,112,113]. Thus, surrogates of the head and neck (primarily the Hybrid III) are used to analyze head impact severity in laboratory reconstructions [25–31]. To ensure accurate results, the surrogate models must consistently replicate human responses to various impact scenarios; thus, the desirable attributes of surrogates include repeatability, durability, reproducibility, biofidelity, and sensitivity [20–24].

2.2.1 Design requirements of surrogate models

The repeatability of a model describes the variation between repeated measures of the same mechanics under identical test conditions on a single surrogate [21–24,41,45,114,115]. Time-independent measures (i.e. peak kinematics) are often preferred for the evaluation of repeatability since the methods of assessment are relatively straightforward [23], and even small deviations in testing conditions could alter the time-history responses between trials [114]. Repeatability of surrogate neck responses is often assessed using the coefficient of variation for repeatability (CV_W) [41,45,115–119], which is the standard deviation (SD) of a measurement divided by the mean. The smaller the CV_W, the less variation exists between tests. In general, CV_W values less than 10% are considered acceptable measures of repeatability [21,22,43–45,115,120]. Although an ANOVA has been suggested as a method to compute repeatability [23,114], no literature on existing surrogate models was found to have utilized this method.

The reproducibility of two or more surrogate models is the variation between mechanical responses of the models when tested under identical conditions [21–24,41,45,114,115]. The models should behave the same regardless of the personnel conducting the experiments, the locations of the experiments, the equipment being used, or the model manufacturers. Similar to repeatability, the coefficient of variation is often used to assess reproducibility (CV_B). In this case, the CV_B is the percent ratio of the overall standard deviation and mean across all tested models. However, current commercially available surrogate models have utilized different methods to determine the overall standard deviation. For the Hybrid III, the standard deviation between models is calculated using the mean square within and between treatments obtained from an ANOVA [41]. Other models use the standard deviation of all the models combined [45,115,116]. To differentiate between methods, the reproducibility depending on the mean square values will be denoted by $CV_{B\text{-}MS}$.

The following hypothesis has been recommended for reproducibility requirements: the variability between surrogates should not be greater than the variability of an individual surrogate [23]. Many researchers use the same criteria as the repeatability for the reproducibility; that is, the acceptable CV_B is 10% or less [21,44,115,120]. However, it has been suggested that due to the additional cumulative variance in the reproducibility assessment, the acceptable CV_B could be increased to 15% [45]. Between-subject ANOVAs are also proposed to compare performance measurements

of interest between multiple surrogate models [23,114] but are seldom used in reproducibility assessments [116].

Further, certification standards for current surrogate models suggest ranges on mechanics that must be satisfied. Most allow a difference of approximately $\pm 10\%$ on the mean value to be within specification [21,41,43,47,112,120–122]. This range can be used as a guideline to assess reproducibility since a model can vary quite a bit while still meeting certification requirements. In general, most of these certifications follow regulations outlined in Title 49 of the Code of Federal Regulations (CFR) Part 572 [47]:

1) Head drop test - The head is dropped from a specified height onto a steel plate. The impact location can be frontal or lateral, depending on the model. The speeds of these tests range from 1-3 m/s. A range of acceptable peak resultant head linear accelerations is provided for different models.
2) Neck pendulum test - The neck is attached to a headform and is directly mounted to a pendulum that falls freely from a specified height to achieve impact speeds ranging from 3-7 m/s. The pendulum is decelerated using a specified acceleration time pulse, usually achieved by an aluminum honeycomb. With this setup, the neck is free to move without the direct head impact of the head or neck. The test is oriented either frontally or laterally, depending on the model. A range of acceptable neck mechanics is provided.

Since the primary focus of this thesis is the head kinematics, only the ranges from drop tests are outlined below for existing surrogate models. While drop tests of the head do not directly replicate the experiments conducted as a part of this thesis, an estimate can be made as to whether the resultant kinematics of the impacts have acceptable ranges, even if the results between necks vary.

Although durability and biofidelity are not the primary objectives of the work presented in this thesis, they will both be described in brief. Durability refers to the surrogate's ability to resist damage after multiple impacts, even during high severity loading conditions [20–22,24]. Current requirements for durability are not standardized, but methods to determine the durability in certain surrogates have been proposed [44,115,123]. The biofidelity of a surrogate is its ability to mimic

human responses during similar loading conditions [20–22]. Several databases [124–133] have been used to develop loading corridors and response requirements that surrogate heads and necks should meet to display mechanical realism [41,44,46,113,122].

The sensitivity of a surrogate model is entwined with the previous requirements. Slight temperature changes (or other parameters in the testing environment that cannot be completely controlled) or impact angle differences should not affect the model's repeatability, biofidelity, or other performance requirements [21,22,43,44,114]. In contrast, the model should be sensitive to factors such as impact severity and impact direction since human responses may differ under these loading parameters [21,43,44,114]. Sensitivity analysis involves testing the model under different levels of severity, impact locations, and restraint/protective devices.

2.3 Surrogate models of the neck

The 50th percentile Hybrid III head developed by General Motors fulfills the above performance requirements: it has documented repeatability, durability, reproducibility and humanlike responses [41,134,135]. As such, the Hybrid III head is generally accepted as an adequate human surrogate for biomechanical testing. Although most surrogate necks display acceptable performance requirements, they were primarily tested in uni-directional loading [20–22,41,43–47,115–117]. Thus, the use of these necks in direct, multiplane impacts common in sports is questioned. As the objectives of this thesis involve the repeatability and reproducibility of the head kinematics when attached to a novel surrogate neck, these parameters will be described for standardized frontal and lateral automotive surrogate models. More comprehensive histories of existing neck models can be reviewed elsewhere [22,52,53].

The following sections present the repeatability and reproducibility of the head kinematics of previous neck models assessed in different test conditions. Where applicable, direct impacts to the head-neck assembly (usually attached to the full dummy) are reported. In other cases, indirect pendulum tests or sled tests are described. While neither of these conditions involves direct head loading, they allow an assessment of the repeatability of the kinematics when attached to a neck. In addition, drop tests with the head, which do not involve a neck, provide general guidelines to which the kinematics can vary across models.

2.3.1 The Hybrid III

The Hybrid III model is the third generation Hybrid surrogate model developed by General Motors [41]. This family of surrogates was designed for frontal automobile collisions. The Hybrid III is a major improvement over its predecessors, showing improved reproducibility, repeatability, durability, anatomical features, and fabrication costs [41]. The Hybrid III (full dummy or head and neck components) is most often used in laboratory reconstructions of sports impacts [25–31], as well as helmet testing [33–40].

Multiple Hybrid III heads were subject to frontal CFR head drop tests (Part 572 Subpart E) [41]. Based on seminal work by Hubbard and McLeod [124], the acceptable peak linear accelerations span from 225-275g [41,47], which is a range of approximately 20% (or, $\pm$10%) of 250g [41]. Further, the peak resultant head accelerations were approximated for each head based on the data presented [41], and the CV_B was calculated to be 5.7%. The Hybrid III heads subject to lateral CFR drop tests (Part 572 Subpart M) also have a range of approximately 20% around the mean (120-150 g) [47].

A seated, unhelmeted Hybrid III dummy assembly was impacted with high energy pendulum impacts (67-89 J, compared to the approximate 90 J in the present work) to the front, oblique, and side of the head (although the front and oblique targeted the jaw) [136]. The CVw values ranged from 3.6-4.5% for the resultant linear acceleration and 4.7-5.5% for the angular velocity. A helmeted Hybrid III head-neck assembly atop a linear rail was also impacted using a pendulum impactor with a mass of 15.5 kg at 3.1 m/s [38]. For frontal impacts, the CVw values were 0.6% and 6.5% for the linear and angular accelerations, respectively. Impacts to the side of the helmet resulted in CVw values of 5.6% and 3.0%.

2.3.2 THOR

The Test device for Human Occupant Restraint (THOR) model was developed to expand the frontal capabilities of the Hybrid III with lateral impacts [42,137] and additional human response data [138]. A manual was recently published [121], which outlines qualifications for the THOR head and neck mechanics. The certification specifications were derived by testing multiple THOR

surrogates in repeated impacts and forming acceptable ranges. Forehead impacts were conducted on a full-body seated surrogate at 2 m/s with a 23.4 kg impactor and frontal facial impacts at 6.73 m/s with a 13 kg impactor. Peak head resultant accelerations can range from 105.3-128.7 g and 124-152 g for the forehead and facial impacts, respectively. Both ranges allow a deviation of approximately 20% around the mean linear accelerations. Neck specifications in flexion, extension, and torsion tests were also conducted for THOR based on indirect pendulum impact tests [121]. Frontal flexion and extension tests follow CFR Part 572 Subpart E, while lateral flexion tests are based on Subpart U. Peak head angular velocity (ω_x) can range from 21.4-26.1 rad/s for lateral flexion at 3.4 m/s. In frontal flexion at 5 m/s, the peak head angular velocity (ω_y) ranged from 31.0-37.9 rad/s. In extension, the range was 32.4-39.6 rad/s. All angular velocity certifications allow a range of approximately 20% around the mean values.

To directly analyze the repeatability and reproducibility of the THOR neck, the German Road Administration (Bundesanstalt für Strassenwesen (BASt)) carried out repeated frontal impact whole body sled tests with different THOR models [139]. The repeatability of the head acceleration was approximately 2%, and the reproducibility was 6% [139]; however, the methods used by the researchers to determine these percentages were not reported.

2.3.3 Side Impact Models

There are multiple ATD's developed for side vehicle collisions that are available for commercial testing or used in a regulatory capacity: the National Highway Traffic Safety Association (NHTSA) Side Impact Dummy (SID), the European Side Impact Dummies (EuroSID-1, ES-2, ES-2re), and the Worldwide Side Impact Dummy (WorldSID).

The head and neck of the NHTSA SID are identical to the 50th percentile male surrogate model outlined in CFR part 572 Subpart B [22,23,47,140]. Thus, the acceptable range on head linear acceleration during forehead drop tests is 210-260 g, which is a range of approximately 20% around 235 g [47]. Eight part 572 necks were subject to 6-7 indirect pendulum tests for a repeatability assessment [116]. The CV_W values of all necks were less than 5% for the peak resultant head linear acceleration. The estimated overall CV_W (i.e. the pooled standard deviation of all neck models divided by the mean of all models, described by Foster [41]) value was 2.8%,

and the CV_B was 4.3%. Sled tests using seven of the head-neck assemblies were also conducted. The pooled CV_W and the CV_B values were 0.9% and 1.5%, respectively. A one-way ANOVA found that the head accelerations significantly differed between models for both the pendulum and sled tests ($p>0.001$). The significance was suggested to be partly caused by the small within-neck variability [116].

The EuroSID-1 was assessed across laboratories using multiple surrogates [117]. Two labs conducted 7 m/s lateral pendulum tests (based on CFR tests) to measure longitudinal, lateral, and vertical head accelerations of the EuroSID-1. The CV_W was 7% or less for all accelerations in both labs. However, the range of kinematics differed considerably between labs. The greatest difference between labs was seen with the longitudinal head acceleration, with an approximate 76% difference in kinematics. All other head acceleration measurements differed by 30% or more between labs. The high variation between labs was attributed to the difference in pendulum acceleration, high-speed camera set up, and definition of centre of gravity.

The ES-2 is an improvement over the EuroSID-1. Proposed ranges on the ES-2 resultant head acceleration are 100-150 g for the resultant head acceleration (range of approximately 40% around 125g) when the head is dropped laterally at 2 m/s [43]. After eight lateral drops at 2 m/s with two different ES-2 heads, the CV_W values of the peak linear acceleration were 2.8% and 3.9%, with an overall CV_W of 3.4% [45]. The ES-2 dummy biomechanical responses were also assessed [141] using head drop tests and neck calibration tests as outlined in ISO/TR 9790 [113]. The CV_W of the peak resultant head acceleration was 2.4% during head drop tests. For the neck certification, three different sled tests were conducted with varying parameters (i.e. acceleration/deceleration levels). The CV_W values measured for the head resultant, vertical, and lateral accelerations range 0.3-2.8%. Particularly for the resultant head acceleration, the CV_W was 2.5% [141].

The ES-2re is a modification to the ES-2, with rib extensions to prevent unwanted seat interactions of the torso [45]. Lateral drop tests were conducted on multiple ES-2re heads to assess repeatability and reproducibility [45,115]. After nine tests on one model, the CV_W of the peak resultant head acceleration was 4.0%. A secondary study on a different head with seven repeated impacts determined a CV_W of 4.5%. The overall CV_W of both heads was 4.2% [45]. Additional testing on

two more ES-2re heads (n=5 per neck) found that the overall CV_W for the peak head acceleration was 1.3%, and the CV_B was 5.4% [45,115]. Thus, the overall CV_W of all ES-2re heads during lateral drop tests was 3.2%. Two ES-2re models were also tested under simulated crash tests (i.e. sled tests) against two impact conditions: a flat wall and an abdomen offset [45]. One of the dummies was tested in frontal impacts, wherein the CV_W values of the resultant linear accelerations were 1.0% and 2.7% for the respective impact conditions. The other, tested in rear impacts, had CV_W values of 1.8% and 7.5%. Although a range of 100-150 g was initially suggested for the ES-2re [45,115], CFR Part 572 Subpart U states the measured peak resultant acceleration must be between 125-155 g when dropped at 2 m/s (a range of approximately 20% on 140 g) [47].

The WorldSID was developed to standardize side impact dummies globally [112]. ISO 15830-2 outlines the following allowed ranges for the WorldSID to be within specification: peak resultant head accelerations of 99-121 g in lateral tests at 2 m/s drops (range of 20% around 110 g) and 225-275 g in frontal drop tests at 2.7 m/s (range of 20% around 140 g) [112]. The repeatability and reproducibility of the WorldSID peak head acceleration during frontal and lateral drop tests was found to be 4.3% and 5.6%, respectively [44,120]. However, it is unclear whether these values represent the CV_W, CV_B, or another CV metric. Further, the WorldSID dummy was tested using the ISO/TR 9790 sled tests, and repeatability of the head acceleration metrics was provided. The CV_W values range from 2.3-6.3%, with the highest value representing the repeatability of the resultant head acceleration [119].

2.3.4 Limitations in repeatability and reproducibility assessments

The repeatability and reproducibility assessments conducted on the above neck models are limited. To the author's knowledge, only the repeatability of the angular kinematics of the Hybrid III has been directly assessed. While the angular kinematics of the THOR neck did not undergo a formal reproducibility assessment, the certification manual provides acceptable ranges on the angular velocities from tests on multiple models. All other necks only considered linear accelerations. Since angular kinematics are common in sports impacts and are thought to be correlated with the incidence of concussion, any neck used for sports applications must produce consistent angular kinematics. Further, only the THOR neck and the Hybrid III neck have assessed repeatability and reproducibility by conducting direct head impacts onto a head-neck assembly. Most other

assessments focused on drop tests with just the head, indirect pendulum impacts with the head and neck, or sled tests. As mentioned previously, none of these experimental setups are equivalent to the direct pendulum impacts conducted as a part of this thesis. Relatedly, only a single assessment could be found assessing the repeatability of helmeted impacts. This again emphasizes the disparity in the literature regarding whether the necks can provide accurate responses to sports impact applications.

2.4 Development of a new surrogate neck model

2.4.1 Initial neck prototype

A preliminary surrogate neck prototype was developed in 2018 (Biomedical Instrumentation Lab, University of Alberta) [52] (Figure 2.1). Neck anthropometry was based on a 50th percentile male. The spinal column was composed of eight 3D printed rubber (TangoBlack – Fullcure ® 970, 3D Printers Canada, Vaughan, ON) and seven aluminum (6061-T6) elements to represent the intervertebral and vertebral discs, respectively, with three steel cables running through the column to provide stability. Clamping collars were used to tension the cables. The spinal column was encased in Ecoflex ® 00-30 rubber (Smooth-on Inc., Macungie, PA). A nodding joint was used to allow compatibility of the neck with the Hybrid III headform.

Biofidelity of the neck in quasi-static bending and dynamic direct head impacts was explored by comparing the results to cadaver data. The repeatability of the neck during unhelmeted direct head impacts was also assessed. Drop tests of the head-neck assembly at the side, front, and rear were conducted at speeds ranging from 1.5 m/s – 5 m/s. Specifically considering side and frontal impacts similar to those in this thesis, 2/16 linear accelerations had unacceptable repeatability (CV_W values greater than 10%) and 5/16 angular accelerations were unacceptable.

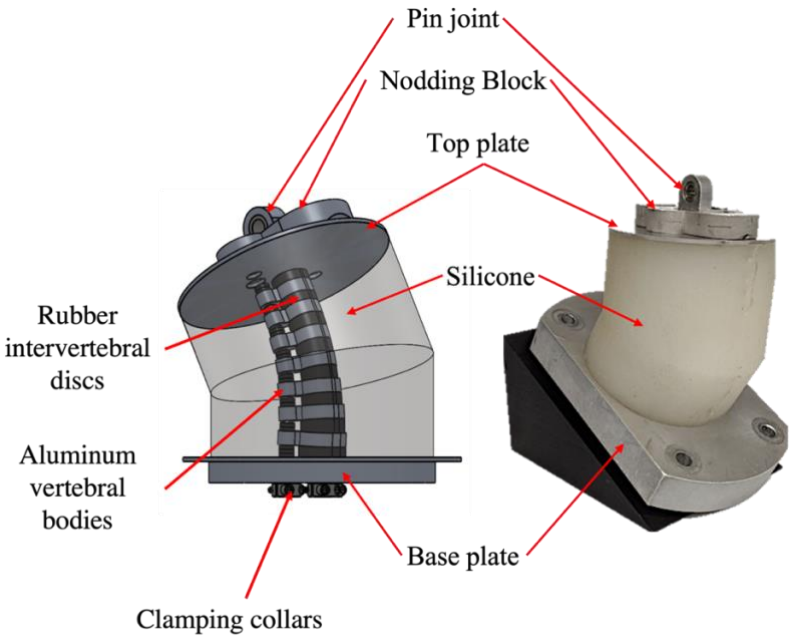

Figure 2.1: CAD model and fully assembled prototype of the first neck iteration [52]. Left (CAD) image adapted with permission from Ogle 2018 [52]; right image adapted with permission from MacGillivray 2020 [53].

The initial prototype had numerous limitations necessitating its modification. The limitations included high neck compliance due to bending in the silicon. As a result, the neck could not support the headform during drop tests (breakaway cables were used to hold the head in the correct position before impact), and hyperextension of the neck caused the silicon to separate from the base plate during impacts. Furthermore, the cable clamping collars would slip during impact tests. The above limitations could have affected the repeatability. A more in-depth overview of the design and its limitations is provided in a previous dissertation [52].

2.4.2 Refined model

The refined model was developed by MacGillivray in 2019 [53] and published in 2020 [142] (Figure 2.2). While the base design was consistent with the initial prototype, various design changes were made to address the limitations mentioned previously [53]. Since the Ecoflex silicon was too flexible, silicone with a higher shore hardness was used instead (Dragon Skin™ 20, Smooth-On Inc., Macungie, PA). The Dragon Skin™ silicone supported the helmeted headform in an upright position. Additionally, to prevent hyperextension of the neck, a silicon flange was

designed to be clamped between the aluminum plates at the base of the assembly. The steel cable assembly was also redesigned to include the steel cable, a compression ball fitting, and a hollow threaded rod welded together (Figure 2.2). Springs were added to the base of the steel cable assembly (on the hollow threaded rod) to create a changeable compression force along the internal column to tune the bending stiffness of the neck. Instead of clamping collars, locknuts were threaded onto the assembly to maintain tension in the cables.

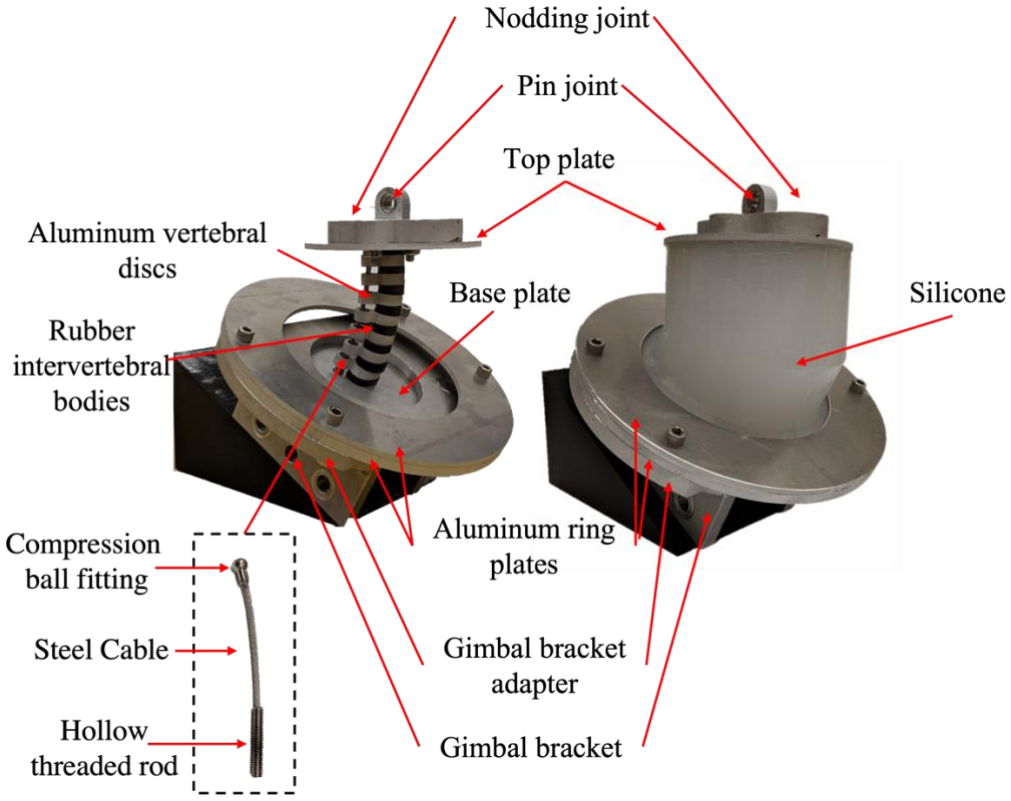

Figure 2.2: The refined surrogate neck's internal and external structure [53]. Adapted with permission from MacGillivray 2020 [53] and Springer Nature, MacGillivray et al. [142] copyright 2021.

Performance requirements of the improved model of the surrogate neck were assessed in direct head impacts to a helmeted Hybrid III headform attached to the neck [53]. Two impact speeds (2m/s and 6 m/s) were used to impact the helmeted Hybrid III head at the crown, back, and facemask (side). The repeatability of the head kinematics was assessed using the CV_W. The CV_W values for the crown and facemask (impact locations comparable to this work) were usually less than 10%, except for the peak angular accelerations during facemask impacts at both impact speeds, linear acceleration during low-speed facemask impacts, and linear accelerations of high-

speed crown impacts [53]. The durability of the neck to repeated impacts was also acceptable. The ability to tune the mechanics for crown and facemask impacts was limited, but mechanics could be adjusted for rear impacts. An initial assessment of biofidelity suggested that the surrogate neck applied with the Hybrid III head described good kinematic biofidelity relative to human subjects with passive neck muscles in low-speed impacts to the side of the head [53].

Minor limitations were noted in the design of the neck. During high-speed rear impacts to the head, it was observed that the silicon shifted out of the clamping plates on the posterior section. The top plate diameter of the surrogate neck design was also too large, resulting in difficulty assembling the head-neck assembly since the top plate would get caught on the chin of the Hybrid III head.

The previous iterations of the neck model focused on its development and characterization of the repeatability, durability, and biofidelity to different loading scenarios. This thesis expands the repeatability assessment using multiple neck models in direct head impacts and compares the prototype surrogate neck to the Hybrid III neck.

3 Methods

3.1 Design and Manufacture of Neck

Most prototype surrogate neck design characteristics are based on the refined model described in section 2.4.2 [53]. All components of the cervical spine were identical to the earlier version, including the dimensions of the intervertebral bodies and the vertebral discs. External measurements were also consistent, with the same silicon used to stabilize the neck. However, design refinements were implemented on the external aluminum structures to account for minor limitations identified in the neck model's previous iteration to improve ease of assembly.

3.1.1 Neck Design Refinements

The previous iteration of the surrogate neck introduced a silicone flange compressed between the aluminum ring plates and the base plate to prevent hyperextension of the neck. Since the flange shifted out of the clamping plates during some impacts, the neck design was slightly modified. The gimbal bracket adapter was extended into a complete circular design to more securely clamp the flange. Additional bolts were also added to the gimbal bracket adapter and the base rings to increase the clamping force on the silicon (Figure 3.1).

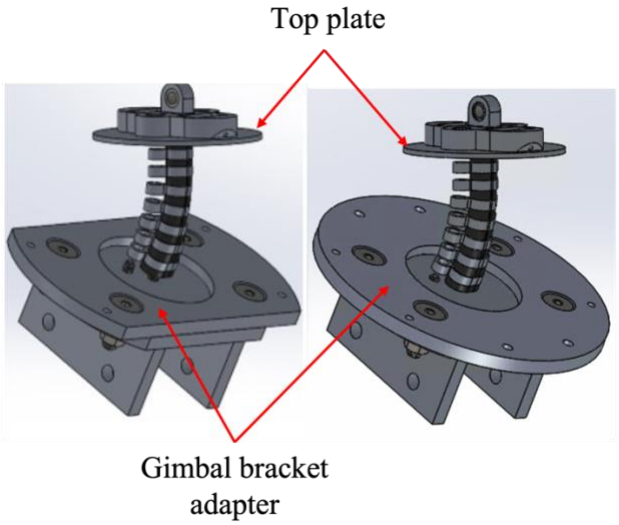

Figure 3.1: Modifications to the prototype surrogate neck. The gimbal bracket adapter was transformed into a circular shape, and additional bolts were added to allow stronger clamping of the silicon. Not shown are the aluminum ring plates, which also had extra bolts added. The image on the left was adapted with permission from MacGillivray 2020 [53].

Since the top plate diameter of the previous surrogate neck design was too large, the current neck design implements a top plate with a slightly smaller diameter. This allowed the head to attach to the neck easily. CAD models of the previous and current iterations of the neck are compared in Figure 3.1.

3.1.2 Neck Manufacturing

To assemble the neck, the internal column was placed into a neck mould sprayed with a releasing agent. However, due to the smaller top plate, the internal structure could not form a tight barrier with the bottom of the neck mould. A 3D printed mould of the nodding joint was thus created to hold the internal column in place during the curing process. The 3D mould held the nodding joint and pressed the top plate tightly against the neck mould. Dragon Skin™ silicon was then prepared. Each neck required a separate 2 lb container of silicon. A vacuum chamber was used for degassing the liquid to remove air bubbles before casting the silicon. Once the silicon was poured into the mould, the neck required several hours to cure; thus, each was manufactured on a different day. After curing, the base of the neck was assembled. The aluminum plates were clamped around the silicon flange and tightened with bolts. Compression springs with a spring constant of 8360.56N/m (9657K305 Compression Spring McMaster-Carr, Cleveland, OH) were tightened onto the base of the three cervical cables. A total neck compression force of 163 N was achieved. This compression force roughly approximates the muscle forces in the neck [143–145] and results in more repeatable results than a lower tested compression force [53]. The assembled neck is displayed in Figure 3.2.

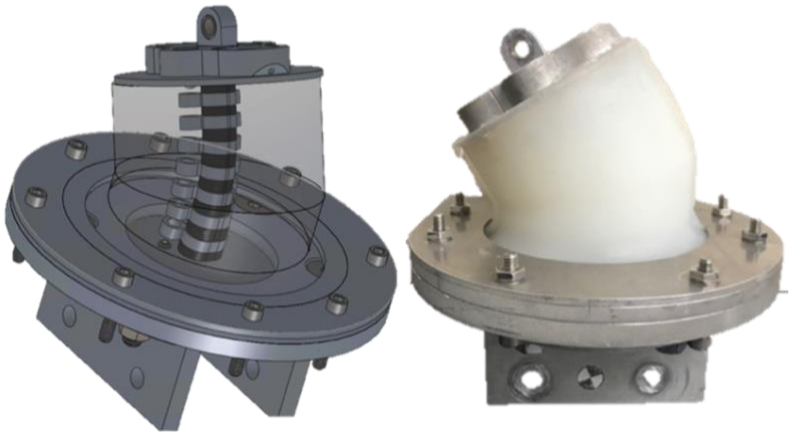

Figure 3.2: Final assembly of the newest version of the prototype surrogate neck. The CAD model on the left displays all neck components, except the internal cables.

3.1.3 Mechanical Properties of the Polymer Materials

Various sub-assemblies of the neck are composed of polymer materials: eight polymer junctions (TangoBlack-FullCure® 970, 3D Printers Canada, Vaughan, ON) represent the intervertebral discs, and the internal column is encased in Dragon Skin™ silicon. Quasi-static compression and tension tests were performed on the polymer components to document Young's modulus. To find Young's modulus, a stress-strain curve was created for each material. A load cell was used to measure the force acting on the samples. The force was converted to Newtons, and divided by the cross-sectional area of the sample to determine the stress. The strain was found by finding the relative displacement of the sample from the initial length as the load increased. The stress-strain curve was created, and a line of best fit was used to measure the slope which approximated the Young's modulus. The documentation of this material property allows for the reproducibility of these design characteristics.

For compression tests, a Dragon Skin™ silicon cube with dimensions of 11.6 mm x 11.3 mm x 11.4 mm was compressed three times. Unfortunately, the displacement rate was not recorded. The average Young's moduli in compression were 1.3 MPa and 3.6 MPa at approximately 0.2% strain and 10% strain, respectively. An annulus sector of the TangoBlack with an outer radius of 21.4 mm, an inner radius of 13.1 mm, a top length of 7.9 mm, and a bottom length of 4.8 mm was also compressed three times. The displacement rate was also not recorded for these tests. The average Young's modulus at approximately 0.2% strain in compression was 1.7 MPa, and approximately 10% strain was 9.4 MPa. For tension tests, a rectangular sample of Dragon Skin™ with a cross-sectional area of 5.3 mm x 8.5 mm and an initial length of 8.4 mm was stretched three times using a rate of 0.1 mm/s. The average Young's modulus was found to be 0.38 MPa. A rectangular sample of TangoBlack with a cross-sectional area of 5.3 mm x 5.5 mm was also tested in tension three times at a rate of 0.05 mm/s. The initial length depended on the trial number since the sample was modified between tests due to slippage but ranged from 4.4 – 4.7 mm. The tension was applied lengthwise, parallel to the grain. The average Young's modulus was found to be 2.4 MPa.

3.2 Experimental Equipment

3.2.1 Pendulum and Linear Rail Assembly

A 50th percentile Hybrid III head was fixed to the prototype surrogate neck(s) and mounted to a linear rail using a gimbal (Figure 3.3). The gimbal design allowed the head-neck assembly to be rotated and positioned at multiple angles, such that different impact locations could be achieved. The head-neck assembly could move along the linear rail to allow realistic translation after impact. For helmeted tests, a Schutt F7 football helmet was donned on the Hybrid III head (Schutt Sports, Litchfield IL, size large).

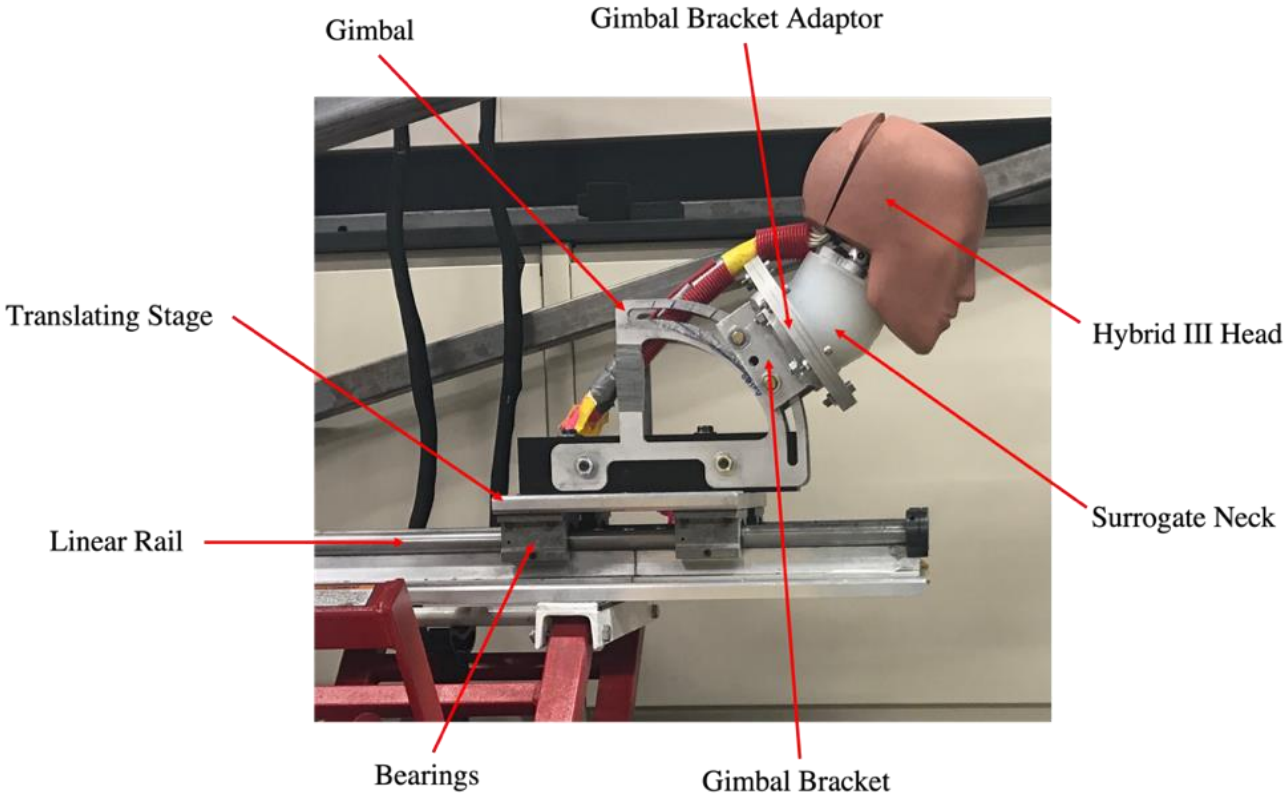

Figure 3.3: Hybrid III head-surrogate neck assembly atop a linear rail. The head-neck assembly is attached to a translating stage by an adjustable gimbal. The translating stage allows the assembly to move freely along the rail.

A pendulum impactor system (Figure 3.4) was used to achieve direct head impacts to the Hybrid III head. The steel impactor arm was equipped with a Modular Elastomer Programmer (MEP) pad and steel plates to achieve an effective mass of approximately 15 kg. The MEP impact surface is

the same as specified in specific helmet testing certifications [94,146,147]. The pendulum impactor arm was raised electromechanically to a predetermined height and released to impact the Hybrid III head at a chosen impact speed.

Figure 3.4: Pendulum impactor system, showing the steel pendulum arm with an MEP pad and steel plates. The Hybrid III head-neck assembly is located atop a translating linear rail. Reproduced with permission from Springer Nature, MacGillivray et al. [142] copyright 2021.

3.2.2 Hybrid III Head

The 50th percentile male Hybrid III head (mass ≈ 4.54 kg) [41] was instrumented with a nine uniaxial accelerometer array (Measurement Specialities Inc., Hampton VA, model 64C-2000-360). The accelerometers were mounted to the inner surface of the Hybrid III skin in a 3-2-2-2 configuration, with three accelerometers at the head centre of gravity (COG) and six accelerometers located at the crown, front, and left side of the head (two at each location). The

sensors were connected to a data acquisition system hardware (PX1 6251, National Instruments, Austin TX) and LabView software (LabVIEW v8.5, National Instruments, Austin TX). All data acquisition and filtering techniques were chosen to meet SAE standard J211-1 recommendations for surrogate models in impact testing [148]. Data were collected with a sampling frequency of 100 kHz. An anti-aliasing hardware filter with a 4 kHz corner frequency was initially applied to the analog voltages. During post-processing in MATLAB R2020a (MathWorks Inc., MA United States), a subsequent 4th order low-pass Butterworth filter was applied at a cut-off frequency of 1650 Hz, as per Channel Frequency Class (CFC) 1000 for head COG linear acceleration signals. Head COG linear accelerations were directly measured from the accelerometers, while head COG angular accelerations were calculated through equations proposed by Padgaonkar [149]. Angular velocity was determined by integrating the angular accelerations. The positive coordinate system for the kinematics of the Hybrid III headform is used as described in SAE Standard J211-1 (Figure 3.5).

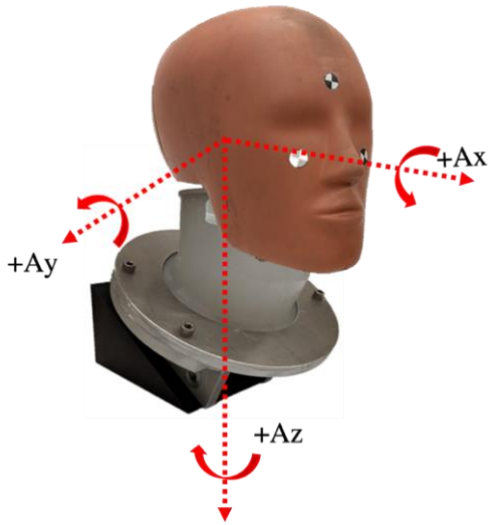

Figure 3.5: The Hybrid III head showing the positive coordinate system for the head COG accelerations. The x-axis is directed along the sagittal plane (anterior-posterior axis), the y-axis along the coronal plane (medial-lateral axis), and the z-axis perpendicular to the transverse plane (inferior-superior axis).

3.2.3 High-Speed Camera

High-speed video was used to confirm impact speed. A high-speed camera (Phantom v611, Vision Research, Wayne NJ) was positioned lateral to the head-neck assembly. A Carl Zeiss (Jena, Germany) 50 mm f/1.4 macro lens was used for imaging. The camera recorded at a sample rate of

3000 frames per second, with a 1280 x 800 resolution and 330 μs exposure time. Impact speed was determined using the Phantom CineViewer Software (v3.4, Vision Research, Wayne NJ). Calibration of the high-speed camera was first conducted by placing a ruler in the impact region of interest and measuring a known distance in the frame. Following calibration, the cameras remained stationary. A high-contrast marker near the pendulum impacting end was used for consistent pixel tracking for impact speed determination. The central point on the high-contrast marker was manually selected ten frames before impact. The same point on the marker was then chosen in the impact frame. The CineViewer software automatically calculated the speed between the two selected points by dividing the measured distance by the time difference between the two points.

3.3 Experimental Protocol

Three prototype surrogate necks were fabricated and then applied in repeat impact experiments, along with one Hybrid III neck. The necks were attached to the Hybrid III head and fixed to the linear rail (Figure 3.3). The pendulum arm was released from a predetermined height to impact the head at 3.5 m/s at two impact locations: (1) lateral impacts near the front boss (n=20/neck) and (2) frontal/forehead impacts (n=10/neck) (Figure 3.6).

(a)

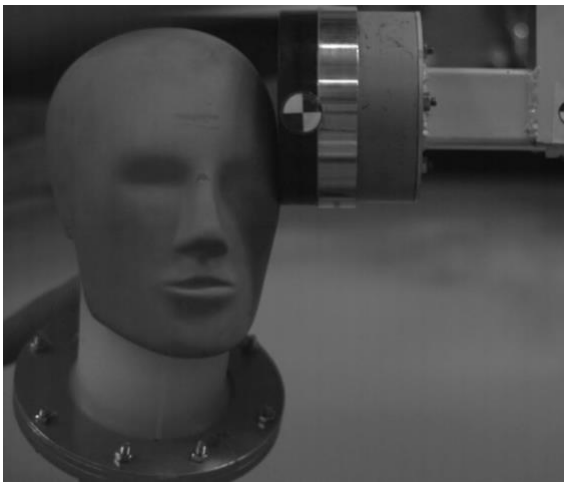

(b)

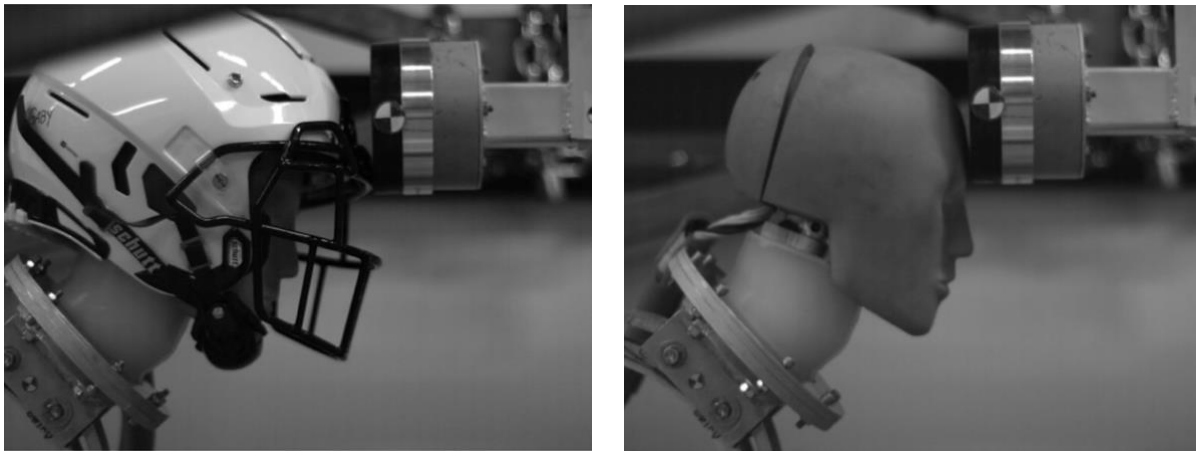

(c) (d)

Figure 3.6: Impact locations on the Hybrid III head: (a) front boss impacts with a football helmet, (b) front boss impacts to the unhelmeted head, (c) frontal impacts with a football helmet, and (d) frontal impacts to the unhelmeted head.

The impact locations were chosen since they are common helmet impact locations in football [150,151] and helmet certification studies [33–35,37]. Front boss impacts also allowed a combined loading scenario with neck axial rotation and extension. The pendulum's effective mass and impact speed were chosen to mimic impact energies often seen in football impacts [79,152–155] while keeping the unhelmeted impacts <200 g as not to dislodge the accelerometers in the headform.

Generally, the 50th percentile peak linear accelerations, angular accelerations, and angular velocities for collegiate football players are 20-21 g [79,152,153,155], 848-1400 rad/s^2 [79,152,153,155], and approximately 4 rad/s [154], respectively. The 95th percentile peaks are 47-64 g [79,152,153,155], 2050-4380 rad/s^2 [79,152–155], and approximately 13 rad/s [154]. On days of diagnosed concussion, the 50th percentile kinematics were 22.5 g at 875 rad/s^2, and the 95th percentile peaks were 82 g and 3376 rad/s^2. Further, for concussive impacts, the 50th percentile peaks were 4948 rad/s^2 and 22 rad/s [154] and the 95th percentile peaks were 7688 rad/s^2 and 34 rad/s [154]. In this thesis, the mean linear accelerations ranged from 30-57 g, the mean angular accelerations from 2950-3289 rad/s^2, and the mean angular velocities from 16-21 rad/s (see "Section 4 – Results"). Thus, the impact energies in this thesis are comparable to those seen in real-life football impacts; more precisely, the resultant kinematics mostly fell within the prescribed 50th to 95th percentile kinematics seen in football collisions.

The Hybrid III head was initially helmeted with a football helmet and impacted laterally near the front boss (n=20/neck). Impacts were delivered to the head-neck assembly with the three prototype necks then the Hybrid III neck, with all 20 trials completed on each neck before testing another. Tests were conducted on the three prototype necks on the same day, but Hybrid III testing was done a different day. To allow assessment of repeatability when a helmet was absent, the unhelmeted Hybrid III head was also attached to the prototype surrogate necks and Hybrid III neck, and impacted with the same parameters as the helmeted impacts (n=20/neck). Again, all tests were completed on each individual neck before moving onto the next. All tests were conducted over two days. Frontal impacts were also performed with the protected head and the unprotected head (n=10/neck). All helmeted and unhelmeted frontal impacts were conducted on the same day, completing each set of tests on each neck before testing another. A full breakdown of experiments is shown in Table 3.1.

Table 3.1: Sample size for each impact scenario.

Location	Neck	Sample Size	
		Helmeted	Unhelmeted
Front Boss	Neck 1	20	20
	Neck 2	20	20
	Neck 3	20	20
	Hybrid III	20	20
Frontal	Neck 1	10	10
	Neck 2	10	10
	Neck 3	10	10
	Hybrid III	10	10

The impact metrics used to evaluate the neck response during head impacts were the peak values of the resultant COG linear acceleration (a), angular acceleration (α), and angular velocity (ω). These metrics were chosen due to their correlation with brain injury, as described in section 2.1.3. Peak values were defined as the maximum peak within a 60 ms time frame for each dataset. As seen in Figure 3.7, the maximum peaks did not correlate with the first peak in the angular velocity-time curves. Thus, the maximum peak was chosen instead of the first peak since it was

hypothesized that the largest angular velocity value would lead to the greatest variance. Since repeatability was the main objective of this thesis, choosing the value with the largest variance would provide a generous estimate of repeatability (i.e. a higher CV value). A time period of 60 ms was chosen since most maximum peaks occurred within this period; however, for Hybrid III frontal impacts, the time series data increased after the initial impact region (Figure 3.7). This increase was not indicative of the impact kinematics, so the peak kinematics were chosen as the local maximum within the first 60 ms. The peak was determined for each test and averaged to find the mean peak kinematics for all test scenarios.

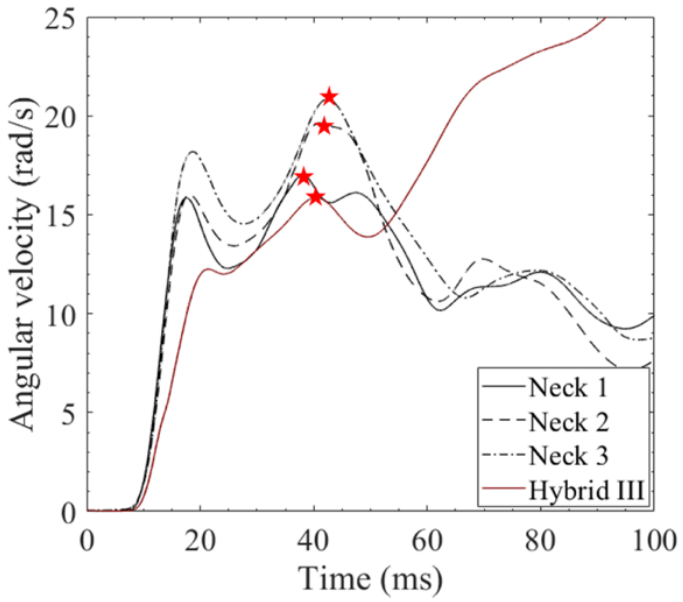

Figure 3.7: Sample plot for determining peak kinematics. Red stars represent the location of chosen maxima for each curve. The peak maxima for all prototype surrogates fall within 60 ms; the Hybrid III curve increases after the initial impact region.

Ensemble series time data were also presented to describe the neck performance. It is important to note that the peak kinematics described as the average of the maxima of each data set is not equivalent to the peaks seen on the ensemble time series curves. This is because the time location of the peak is variable between datasets, so the peak of the ensemble will not be the arithmetic mean of all the datasets.

3.3.1 Sample Size Estimation

Since this is the first study to analyze the differences between models of the prototype surrogate neck, there was no pre-existing data on between-neck differences; thus, estimates of required sample size for determining potential statistical significance between necks were made. Using previous studies as guidelines [41,45,115–117,121,136], three neck replicates were used in this work. A sample size of n=20 impacts per neck was initially chosen for the front boss impacts as a generous sample size estimation. The front boss data was then used to run an *a priori* power analysis for the frontal impact experiments. A sample size of n<10 was acceptable for all kinematics except one (the angular acceleration of the unhelmeted head, n=37), for a power of 0.8 and significance level of 0.05 (G*Power 3.1 [156]). Thus, the sample size was reduced to 10 for the frontal impacts. In addition, a sensitivity power analysis with a power of 0.8 and a significance level of 0.05 was performed, identifying the following minimum effect sizes that the ANOVAs could reliably detect:

- Front boss impacts – just prototype surrogate necks: Cohen's $f > 0.41$
- Front boss impacts – prototype surrogate necks and Hybrid III: Cohen's $f > 0.38$
- Front impacts - just prototype surrogate necks: Cohen's $f > 0.60$
- Front impacts – prototype surrogate necks and Hybrid III: Cohen's $f > 0.55$

All effects sizes were acceptable, except for the angular acceleration between the three prototype surrogate necks in front boss unhelmeted impacts (Cohen's $f = 0.3 < 0.41$), the angular acceleration for the helmeted prototype surrogate necks during frontal impacts (Cohen's $f = 0.53 < 0.6$), and the angular accelerations between the protected prototype surrogate necks and the Hybrid III in front impacts (Cohen's $f = 0.34 < 0.55$). Overall, the experiments were considered sufficiently powered to determine statistical differences between the necks.

3.4 Data Analysis

The means and standard deviations (SD) of all peak head kinematics (linear acceleration, angular velocity, and angular acceleration) were reported and analyzed via multiple data analysis methods. Repeatability was determined in two ways: (1) within-neck repeatability; and (2) between-neck repeatability. The between-neck repeatability was further classified as (i) reproducibility between the three necks and (ii) comparisons between neck models (the prototype surrogate and Hybrid

III). Within-neck repeatability was assessed using the coefficient of variation of repeatability (CV_W). The reproducibility of the head kinematics between neck surrogates was evaluated by statistical tests (ANOVAs and post-hoc tests), normalized absolute differences, and the coefficient of variation of reproducibility (CV_B). The kinematics of the prototype surrogate were also compared to the Hybrid III via statistical tests, mean comparisons, and normalized absolute differences.

3.4.1 Within-Neck Repeatability

Within-neck repeatability was determined by quantifying the variability between repeat impacts for peak head kinematics using the coefficient of variation for repeatability (CV_W) (Equation 1). In equation 1, σ is the standard deviation and $\bar{x}$ is the mean, where x is an arbitrary variable representing all peak kinematics (peak a, peak α, and peak ω).

$$CV_W = \frac{\sigma}{\bar{x}} \times 100\% \tag{1}$$

The average overall CV_W of the prototype surrogate neck was also determined by calculating the percent ratio of the estimated pooled standard deviation of all three prototype surrogate necks (S_P) and the mean of all three necks ($\bar{X}$), where X describes the peak kinematics from all necks (Equation 2) [41]. The estimated pooled standard deviation is presented in equation 3, where s_i represents the standard deviation of the ith neck model and n is the number of necks being compared. The result from equation 2 represents the approximate CV_W of the prototype surrogate neck in general.

$$CV_W = \frac{S_P}{\bar{X}} \times 100\% \tag{2}$$

$$S_P = \left[\sum_{i=1}^{n} \frac{s_i^2}{n}\right]^{1/2} \tag{3}$$

CV_W values of 10% or less were deemed acceptable [21,22,43–45,115,120].

3.4.2 Between-Neck Repeatability

Statistical analyses were performed to investigate between-neck repeatability. Statistical tests were conducted using IBM SPSS Statistics V 26.0 (Armonk, New York, USA) with a significance of $p<0.05$. Separate one-way ANOVAs were performed on all peak head kinematics for the following cases:

(1) To compare the response of three prototype surrogate necks attached to a Hybrid III head, directly impacted at two impact locations for two helmet scenarios (i.e. reproducibility of the prototype surrogate model).
(2) To compare three prototype surrogate necks and the Hybrid III neck, using the same experimental parameters as (1) (i.e. comparison of the prototype surrogate neck to the Hybrid III).

Boxplots of each dataset were inspected to determine outliers. When outliers were detected, they were removed, beginning with the most extreme. Then, a second ANOVA was run to assess the effect of the outlier on the results. The results of the ANOVA with removed outliers did not differ sufficiently for different conclusions to be drawn; thus, the ANOVA results were reported for each full dataset. A Shapiro-Wilk test was used to assess the normality of each dependent variable. Most datasets were normally distributed ($p>0.05$); however, there were cases where the data was non-normal. The removal of outliers did make most datasets normal. As mentioned before, the removal of outliers did not substantially affect the ANOVA; thus, the results of the ANOVA do not appear to be affected by the underlying distributions. In addition, even in the scenarios in which the datasets remained non-normal, the ANOVA was considered an acceptable statistical test since it is relatively robust to violations in normality [157,158].

Levene's test for equality of variances based on the median ($p<0.05$) was used to test the variance of each dependent variable. A one-way Welch ANOVA and Games-Howell post hoc tests were conducted for any variable that violated Levene's test. Otherwise, the standard one-way ANOVA and Tukey's HSD (honestly significant difference) post-hoc tests were conducted. Effect sizes were reported as Cohen's *f* for the ANOVA and Cohen's *d* for the post-hoc comparisons. Cohen's

f effect sizes are defined as 0.10 = small, 0.25 = medium, and 0.40 = large [159]. Similarly, Cohen's *d* values of 0.20, 0.50, and 0.80 refer to small, medium, and large effect sizes, respectively [160].

In addition to statistical tests, the between-neck repeatability of the three prototype surrogates was assessed by defining a metric called the normalized absolute difference (Equation 4).

$$\frac{|x_j - x_k|}{\frac{1}{3}\sum_{i=1}^{3} x_i} \times 100\% \begin{cases} j,k = 1,2,3 \\ j \neq k \end{cases} \tag{4}$$

In equation 4, *i,j,k* refer to the neck number. The current standard for neck certifications in impact allows a range of peak linear head accelerations and angular velocities spanning approximately 20% [41,47,112,121]. Thus, a normalized absolute difference of ≤20% was defined as acceptable.

The CV of reproducibility (CV_B) was also used to determine the between-neck repeatability of the prototype surrogate neck. As mentioned in section 2.2.1, there is a lack of standardized methods for the CV_B calculation. Foster calculated CV_{B-MS}, which is defined as the percent ratio of the estimated standard deviation between the three surrogate models (S_B) and the means of the three models ($\bar{X}$) (Equation 5) [41]. The estimated standard deviation between the three models is derived from the mean squares obtained from the ANOVA, shown in equation 6, where MSB is the mean square between treatments, MSW is the mean square within treatments, and n is the number of trials for each neck.

$$CV_B = \frac{S_B}{\bar{X}} \times 100\% \tag{5}$$

$$S_B = \left[\frac{MSB - MSW}{n}\right]^{\frac{1}{2}} \tag{6}$$

However, most other necks calculated the CV_B by dividing the total standard deviation (derived from tests across all models) by the means of all models. Since this method was most common in the literature and could be easily used by the author to assess reproducibility given raw data, results from the second method are presented in this thesis. CV_B values of 10% or less are proposed as being acceptable [21,44,115,120], although values up to 15% may be tolerable [45].

To compare the Hybrid III neck and the surrogate prototype necks, the normalized absolute differences were calculated using equation 7, where x_j represents mean kinematics of the prototype surrogate and x_{Hy3} the Hybrid III. Equation 7 is similar to equation 5, except the Hybrid III kinematics are always present in the numerator.

$$\frac{\left|x_j - x_{Hy3}\right|}{\frac{1}{3}\sum_{i=1}^{3} x_i} \times 100\% \{ j = 1,2,3 \tag{7}$$

Finally, time series kinematics were presented between necks by plotting the ensemble averages of the head kinematics. The curves compare the three prototype surrogate necks to each other and the Hybrid III neck.

The following section outlines the results for the within-neck and between-neck repeatability assessment methods outlined above. Section 4.1 focuses on the repeatability between the prototype surrogate necks, whereas section 4.2 compares the prototype surrogate neck to the Hybrid III neck.

4 Results

4.1 Repeatability of the three neck copies

Three copies of the neck were tested with both an unprotected and protected head in repeat experiments considering several impact locations. Within-neck repeatability CV_W values were always less than 10%, indicating repeatability that is considered acceptable [21,22,43–45,115,120]. Although statistically significant differences between necks were noted, the CV_B values and the normalized absolute differences between necks were generally 10% or less. Overall, between-neck repeatability was lesser than what is deemed allowable in current literature [21,41,44,45,47,112,115,120,121]. The numbers supporting these general findings are presented below.

4.1.1 Front boss impacts

Helmeted Impacts

The means, SDs, CV_W values, and 95th percentile confidence intervals (CIs) of all head kinematics are reported for the three prototype surrogate necks subject to lateral impacts near the front boss when the head was equipped with a helmet (Table 4.1) (Hybrid III kinematics are also reported, but those will be referenced in Section 4.2.1). One-way ANOVAs and post-hoc comparisons were run on data sets with and without outliers (Table 4.2). Figure 4.1 shows graphical comparisons of the mean kinematics between the necks. The normalized absolute differences were calculated to determine the differences between the kinematics of the necks (Table 4.3). To further assess reproducibility, the CV_B values were also reported. Finally, the supplemental time series kinematic curves (Figure 4.3) are provided.

The means and SDs were used to calculate the CV_W values of all prototype surrogate neck kinematics, which were always less than 10% (Table 4.1). The overall CV_W was calculated to be 3.3% for the linear acceleration, 6.7% for the angular acceleration, and 5.9% for the angular velocity. An ANOVA was run to assess statistical differences between the mean kinematics outlined in Table 4.1.

Table 4.1: Mean, SD, CV_W, and 95% CI values of the kinematic responses from the front boss helmeted impacts for the three prototype surrogate neck copies and the Hybrid III. The Hybrid III data is used in Section 4.2. Adapted with permission from Springer Nature, MacGillivray et al. [142] copyright 2021.

Neck model		Peak a (g)	Peak α (rad/s^2)	Peak ω (rad/s)
1	Mean±SD	34.2 ± 0.9	2954.8 ± 154.5	17.2 ± 0.9
	CV_W	2.6%	5.2%	5.2%
	95% CI	(33.8, 34.6)	(2882.5, 3027.1)	(16.8, 17.7)
2	Mean±SD	32.2 ± 1.0	3145.2 ± 287.0	19.8 ± 1.2
	CV_W	3.2%	9.1%	6.2%
	95% CI	(31.7, 32.7)	(3010.9, 3279.6)	(19.2, 20.4)
3	Mean±SD	34.0 ± 1.3	3446.6 ± 178.8	21.1± 1.3
	CV_W	3.9%	5.2%	6.0%
	95% CI	(33.4, 34.6)	(3362.9, 3530.3)	(20.5, 21.7)
Hybrid III	Mean±SD	30.2 ± 1.3	3038.3 ± 304.0	16.0 ± 0.7
	CV_W	4.2%	10.0%	4.3%
	95% CI	(29.6, 30.8)	(2896.0, 3180.5)	(15.7, 16.4)

First, the assumptions of the ANOVA were checked. The following distributions were non-normal, as assessed by a Shapiro-Wilk test (p<0.05): the linear accelerations of necks 2 and 3, the angular velocities of necks 1 and 3, and the angular acceleration of neck 3. Inspection of the boxplots showed at least one outlier in each neck dataset for all three head kinematics. The outliers were removed, and a second ANOVA was run to determine if the results were affected (Table 4.2). The removal of outliers made all datasets normally distributed. In addition, only the post-hoc test between the angular accelerations of necks 1 and 2 showed statistical differences when the outlier was removed (Table 4.2). Even so, the mean difference changes were small (i.e. approximately 3% of the mean angular accelerations). Thus, the outliers were kept in the analysis since the results are not substantially affected by the outliers or underlying distributions. The assumption of homogeneity of variances was violated for angular accelerations, as assessed by Levene's test for equality of variance based on the median (p=0.041); thus, a one-way Welch ANOVA and Games-Howell post-hoc tests were conducted for the angular accelerations.

Table 4.2: Mean differences between the prototype surrogate necks and p-values from the ANOVAs and post-hoc statistical tests run on the full dataset and the dataset with outliers removed for all head kinematics during front boss helmeted impacts. Shaded cells represent p-values that differed due to the removal of outliers.

		With outliers		Without outliers	
		Mean Difference	p-value	Mean difference	p-value
Linear acceleration (g)	ANOVA	-	$p < 0.001$	-	$p < 0.001$
	Neck 1 - Neck 2	2.03	$p < 0.001$	2.17	$p < 0.001$
	Neck 1 - Neck 3	0.20	$p = 0.836$	0.41	$p = 0.190$
	Neck 2 - Neck 3	-1.83	$p < 0.001$	-1.76	$p < 0.001$
Angular Velocity (rad/s)	ANOVA	-	$p < 0.001$	-	$p < 0.001$
	Neck 1 - Neck 2	-2.57	$p < 0.001$	-2.61	$p < 0.001$
	Neck 1 - Neck 3	-3.86	$p < 0.001$	-3.87	$p < 0.001$
	Neck 2 - Neck 3	-1.29	$p = 0.002$	-1.26	$p < 0.001$
Angular Acceleration (rad/s^2)*†	ANOVA	-	$p < 0.001$	-	$p < 0.001$
	Neck 1 - Neck 2	-190.39	$p = 0.036$	-115.04	$p = 0.158$
	Neck 1 - Neck 3	-491.78	$p < 0.001$	-441.20	$p < 0.001$
	Neck 2 - Neck 3	-301.39	$p = 0.001$	-326.16	$p < 0.001$

* Welch's ANOVA; † Games-Howell post-hoc tests

The three prototype surrogate necks were significantly different (Table 4.2). However, the magnitude of the differences in means were less than 20% of the average of all three necks and less than 10% for most cases (Table 4.3). The one-way ANOVA showed statistically significant differences between the linear accelerations ($p<0.001$, Cohen's $f = 0.9$), angular velocities ($p<0.001$, Cohen's $f=1.4$), and angular accelerations ($p<0.001$, Cohen's $f=1.0$) of all three neck models (Table 4.2). The linear accelerations between necks 1 and 2 were 6.1% different ($p<0.001$, Cohen's $d=2.1$), and necks 2 and 3 were 5.5% different ($p<0.001$, Cohen's $d=1.5$) (Table 4.2 and Table 4.3). The angular accelerations between all three necks were also different: necks 1 and 2 were 6.0% different ($p=0.036$, Cohen's $d=0.8$), necks 2 and 3 were 9.5% different ($p=0.001$, Cohen's $d=1.3$), and necks 1 and 3 were 15.5% different ($p<0.001$, Cohen's $d=2.9$) (Table 4.2 and Table 4.3). Angular velocities were significantly different between necks 1 and 2 ($p<0.001$, Cohen's $d=2.4$), necks 2 and 3 ($p=0.002$, Cohen's $d=1.0$), and necks 1 and 3 ($p<0.001$, Cohen's $d=3.5$) (Table 4.2), with normalized absolute differences of 13.2%, 6.7%, and 19.9%, respectively

(Table 4.3). A graphical comparison of the mean kinematics between the three prototype surrogate necks subject to front boss impacts is displayed in Figure 4.1.

On average, the linear accelerations differed by 4.0% between necks for helmeted impacts. The angular kinematics of the head showed greater discrepancies between models, with 10.3% and 13.3% average differences for angular acceleration and angular velocity, respectively (Table 4.3). The linear accelerations, angular accelerations, and angular velocities between necks had CV_B values of 4.2%, 9.2%, and 10.1%, respectively.

Table 4.3: Normalized absolute differences between the prototype surrogate necks for helmeted front boss impacts. Adapted with permission from Springer Nature, MacGillivray et al. [142] copyright 2021.

	Δa (%)	Δα (%)	Δω (%)
Neck 1 - Neck 2	6.1	6.0	13.2
Neck 2 - Neck 3	5.5	9.5	6.7
Neck 1 - Neck 3	0.6	15.5	19.9
Average	4.0	10.3	13.3

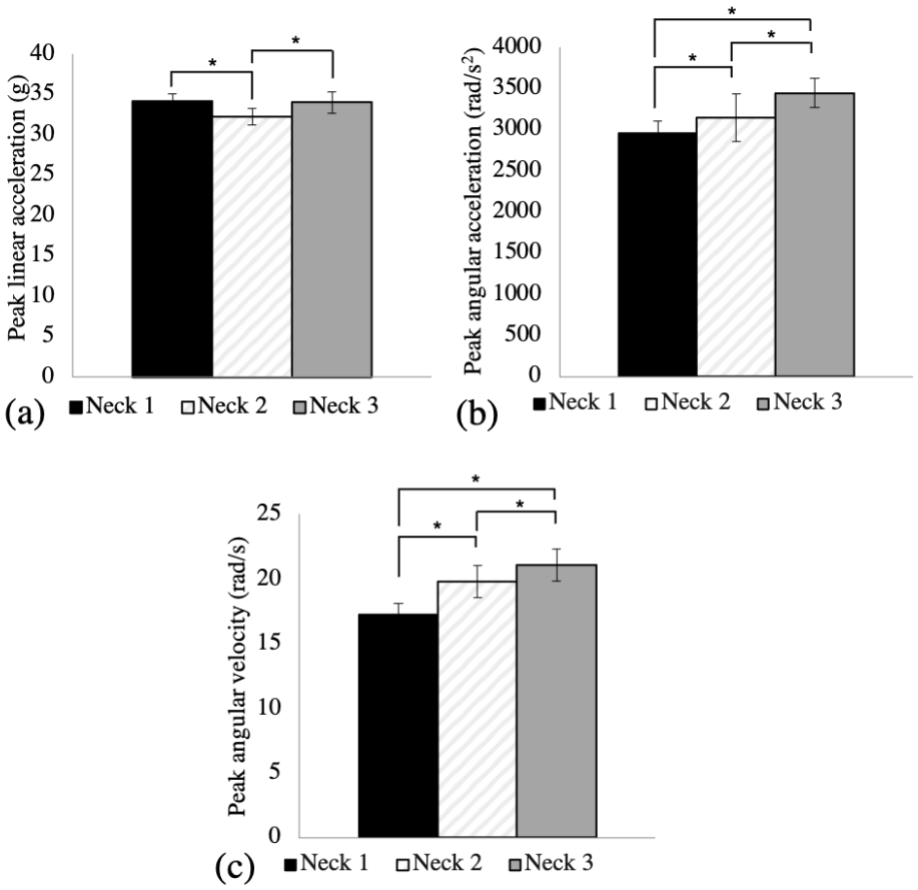

Figure 4.1: Mean and standard deviations of the (a) peak linear accelerations, (b) peak angular accelerations, and (c) peak angular velocities of all three neck copies equipped with a helmet and impacted laterally near the front boss. Significant differences between necks are denoted by an asterisk (* = $p<0.05$).

Unhelmeted Impacts

For lateral impacts near the front boss of the unhelmeted Hybrid III head, the means, SDs, CV_W values, and 95th percentile CIs of the head kinematics are reported for each of the three prototype surrogate necks and the Hybrid III neck (which will be assessed in section 4.2.1) (Table 4.4). One-way ANOVAs and post-hoc comparisons run on data sets with and without outliers were compared in Table 4.5. Graphical comparisons of the mean kinematics between the necks are also presented (Figure 4.2). The normalized absolute differences (Table 4.6) and the CV_B values were reported. Again, the supplemental time series kinematic curves (Figure 4.3) are provided.

The CV_W values were 6% or less for all kinematics (Table 4.4), with the overall CV_W values calculated to be 1.4%, 4.7%, and 1.3% for the linear accelerations, angular accelerations, and angular velocities. An ANOVA was again run to determine statistical differences between the peak kinematics of the prototype surrogate necks. Thus, the normality, outliers, and equality of variance were assessed.

Table 4.4: Mean, SD, CV_W, and 95% CI values of the kinematic responses from the front boss unhelmeted impacts. The Hybrid III data is used in Section 4.2. Adapted with permission from Springer Nature, MacGillivray et al. [142] copyright 2021.

Neck model		Peak a (g)	Peak α (rad/s^2)	Peak ω (rad/s)
1	Mean±SD	151.5 ± 2.1	7501.4 ± 316.2	27.6 ± 0.2
	CV_W	1.4%	4.2%	0.9%
	95% CI	(150.5, 152.5)	(7353.4, 7649.4)	(27.4, 27.7)
2	Mean±SD	154.2 ± 2.0	7444.5 ± 257.7	26.5 ± 0.4
	CV_W	1.3%	3.5%	1.4%
	95% CI	(153.2, 155.1)	(7323.9, 7565.1)	(26.3, 26.7)
3	Mean±SD	144.6 ± 2.3	7684.9 ± 458.2	26.6 ± 0.4
	CV_W	1.6%	6.0%	1.5%
	95% CI	(143.6, 145.7)	(7470.5, 7899.3)	(26.4, 26.8)
Hybrid III	Mean±SD	165.8 ± 1.8	8743.2 ± 283.8	22.5 ± 0.2
	CV_W	1.1%	3.2%	0.8%
	95% CI	(164.9, 166.6)	(8610.4, 8876.1)	(22.4, 22.6)

Outliers were detected in the linear acceleration dataset of neck 2 and the angular velocity datasets of necks 2 and 3. An ANOVA performed on the datasets with outliers removed showed results were unchanged (Table 4.5). The distribution of data for the angular velocity of neck 2 was non-normal (p=0.04); however, the removal of outliers normalized the distribution. Thus, the outliers were kept in the analysis, and a one-way ANOVA was run with Tukey post-hoc tests. Results of Welch's ANOVA and Games-Howell post-hoc tests are reported for the angular acceleration, as the assumption of homogeneity of variance was violated (p=0.03).

Table 4.5: Mean differences between the prototype surrogate necks and p-values from the ANOVAs and post-hoc statistical tests run on the peak head kinematics with and without outliers during front boss unhelmeted impacts.

		With outliers		Without outliers	
		Mean Difference	p-value	Mean difference	p-value
Linear acceleration (g)	ANOVA	-	$p < 0.001$	-	$p < 0.001$
	Neck 1 - Neck 2	-2.63	$p = 0.001$	-2.38	$p = 0.002$
	Neck 1 - Neck 3	6.89	$p < 0.001$	6.89	$p < 0.001$
	Neck 2 - Neck 3	9.52	$p < 0.001$	9.27	$p < 0.001$
Angular Velocity (rad/s)	ANOVA	-	$p < 0.001$	-	$p < 0.001$
	Neck 1 - Neck 2	1.06	$p < 0.001$	1.16	$p < 0.001$
	Neck 1 - Neck 3	0.99	$p < 0.001$	1.08	$p < 0.001$
	Neck 2 - Neck 3	-0.07	$p = 0.775$	-0.08	$p = 0.632$
Angular Acceleration (rad/s^2) *†	ANOVA	-	$p = 0.143$	-	-
	Neck 1 - Neck 2	56.90	$p = 0.808$	-	-
	Neck 1 - Neck 3	-183.50	$p = 0.316$	-	-
	Neck 2 - Neck 3	-240.40	$p = 0.119$	-	-

* Welch's ANOVA; † Games Howell post hoc tests

Only the linear accelerations (p<0.001, Cohen's f=1.9) and angular velocities (p<0.001, Cohen's f=1.5) of the unhelmeted necks were significantly different (Table 4.5), and the normalized absolute differences between the necks were usually smaller than the helmeted impacts (Table 4.6). The linear accelerations were significantly different between necks 1 and 2 (p=0.001, Cohen's d=1.3), necks 1 and 3 (p<0.001, Cohen's d=3.1), and necks 2 and 3 (p<0.001, Cohen's d=4.4). The normalized absolute differences between the necks were 1.8%, 4.6%, and 6.3% for each neck pair above, respectively (Table 4.6). The angular velocity of neck 1 was 3.9% different than neck 2 (p<0.001, Cohen's d=3.4) and 3.7% different than neck 3 (p<0.001, Cohen's d=3.0) (Table 4.5 and Table 4.6). The angular accelerations were not significantly different between the necks (Table 4.5). Figure 4.2 presents a graphical representation of the mean peak kinematics from the three prototype surrogate necks during unhelmeted front boss impacts.

In general, unhelmeted impacts to the front boss had average normalized absolute differences of 4.2% for linear acceleration, 2.6% for angular velocity, and 2.1% for angular acceleration (Table 4.6). The CV_B was 3.0%, 4.6%, and 2.2% for the linear acceleration, angular acceleration, and angular velocity.

Table 4.6: Normalized absolute differences between the surrogate prototype necks for unhelmeted front boss impacts. Adapted with permission from Springer Nature, MacGillivray et al. [142] copyright 2021.

	Δa (%)	Δα (%)	Δω (%)
Neck 1 - Neck 2	1.8	0.8	3.9
Neck 2 - Neck 3	6.3	3.2	0.3
Neck 1 - Neck 3	4.6	2.4	3.7
Average	4.2	2.1	2.6

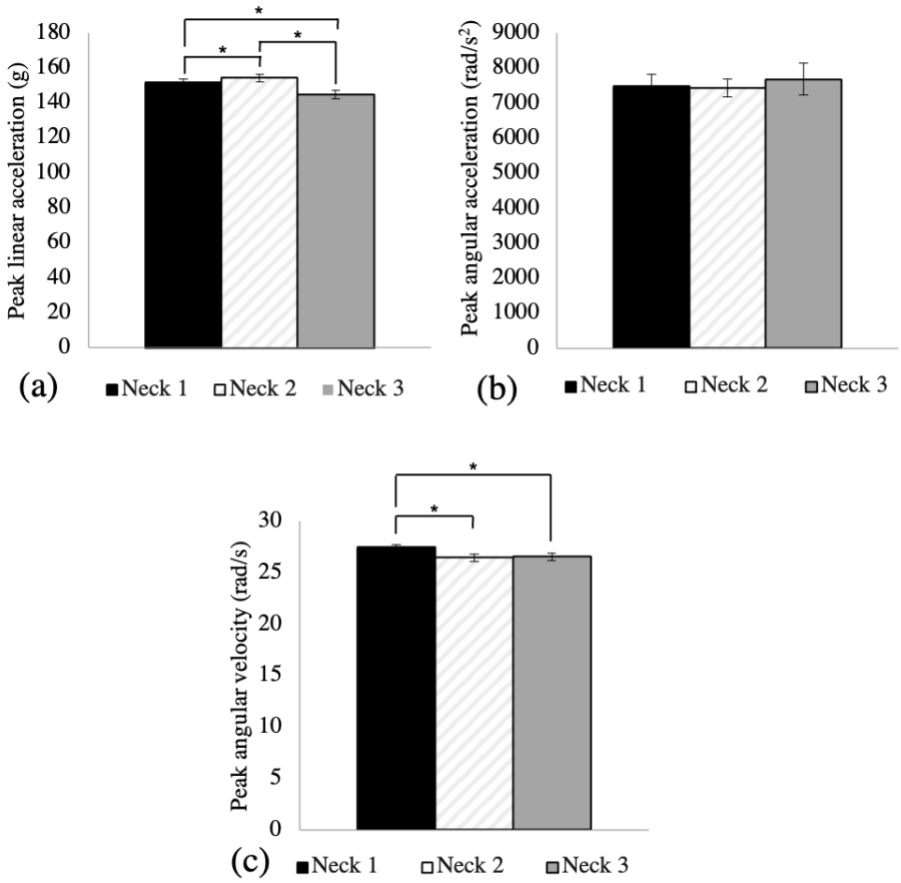

Figure 4.2: Mean and standard deviations of the (a) peak linear accelerations, (b) peak angular accelerations, and (c) peak angular velocities of all three unhelmeted necks impacted laterally near the front boss. An asterisk denotes significant differences between necks (* = p<0.05).

Summary

Although the statistical results suggest significant differences between the neck models, direct comparisons between individual neck prototypes suggest minor differences between the kinematics of the necks. The normalized absolute differences were 20% or less for all kinematics and less than 10% for most cases when a helmet was used (Table 4.3); for unhelmeted impacts, the normalized absolute differences were less than 7% (Table 4.6). The CV_B was always 10% or less for helmeted impacts and less than 5% for unhelmeted impacts. Furthermore, the low variance within groups is thought to be partly responsible for causing significant differences. The calculated CV_W values were less than 10% for all helmeted cases and 7% for unhelmeted impacts, showing high repeatability within groups.

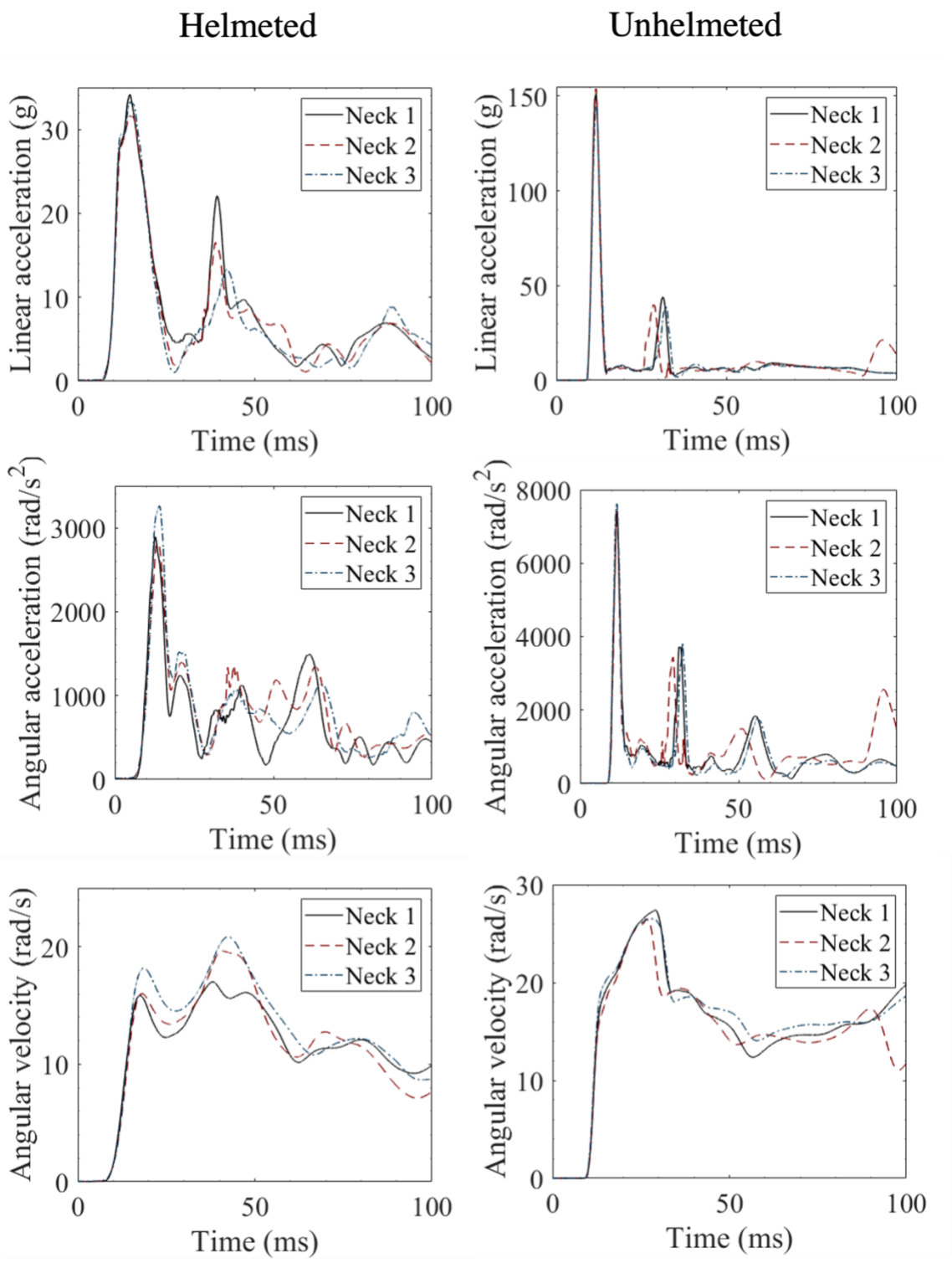

Figure 4.3: Ensemble averages of all three necks during helmeted impacts (left column) and unhelmeted impacts (right column) to the front boss of the head. Linear accelerations (first row), angular accelerations (second row), and angular velocities (third row) are shown for all three surrogate prototype necks. The figures representing helmeted impacts were reproduced with permission from Springer Nature, MacGillivray et al. [142] copyright 2021.

4.1.2 Frontal impacts

Helmeted

Mean, SD, CV_W, and 95% CI values of all head kinematics are reported for the three prototype surrogate necks during frontal impacts for the protected Hybrid III head (Table 4.7) (Hybrid III neck kinematics are used in Section 4.2.2). ANOVAs were conducted on the data with and without outliers (Table 4.8). The peak head kinematics for each neck are visually compared in Figure 4.4. The normalized absolute differences between the necks are outlined in Table 4.9, and the CV_B values are provided for reproducibility assessment. The supplemental time series kinematic curves are displayed in Figure 4.6.

Table 4.7: Mean, SD, CV_W, and 95% CI values of the kinematic responses from the helmeted frontal impacts. The Hybrid III data is used in Section 4.2.

Neck model		Peak a (g)	Peak α (rad/s^2)	Peak ω (rad/s)
1	Mean±SD	57.0 ± 1.1	3184.9 ± 202.5	21.8 ± 0.9
	CV_W	1.9%	6.4%	4.2%
	95% CI	(56.2, 57.8)	(3040.1, 3329.7)	(21.1, 22.4)
2	Mean±SD	53.8± 0.7	3489.1 ± 303.5	18.8 ± 0.5
	CV_W	1.4%	8.7%	2.9 %
	95% CI	(53.2, 54.3)	(3272.0, 3706.2)	(18.4, 19.2)
3	Mean±SD	49.6 ± 0.8	3251.0 ± 261.4	16.7 ± 0.8
	CV_W	1.7%	8.0%	5.1%
	95% CI	(49.0, 50.2)	(3064.0, 3438.0)	(16.1, 17.4)
Hybrid III	Mean±SD	51.1± 2.3	3230.3 ± 575.3	16.2 ± 0.5
	CV_W	4.5%	17.8%	3.3%
	95% CI	(49.4, 52.7)	(2818.7, 3641.8)	(15.8, 16.6)

The CV_W values are less than 10% for all copies of the prototype surrogate neck (Table 4.7). The average overall CV_W for helmeted impacts was calculated to be 1.7% for the linear accelerations, 7.8% for the angular accelerations, and 4.1% for the angular velocities. Before running an ANOVA, the assumptions were checked.

The following distributions were determined to be non-normal (p<0.05): the linear acceleration of necks 1 and 3, the angular velocity of neck 3, and the angular accelerations of necks 1 and 2. At least one outlier was detected in the non-normal datasets, except for the linear acceleration of neck

3. Table 4.8 describes the results of the ANOVA with and without outliers and shows only the angular acceleration between necks 2 and 3 is affected (p=0.119 with outliers; p=0.01 without outliers), but the change in mean difference is minimal. The removal of outliers also made all datasets normal, except the linear acceleration of neck 3. Since the results are not substantially affected by outliers or underlying distribution, the results are reported for the complete datasets with outliers included. Aside from the angular velocity and angular acceleration datasets with outliers removed, all other datasets had equal variance, so the standard one-way ANOVA and Tukey post-hoc tests were conducted.

Table 4.8: Mean differences between the prototype surrogate necks and p-values from the ANOVAs and post-hoc statistical tests run on the full dataset and the dataset with outliers removed for all head kinematics during impacts to the front of the helmeted head. Shaded cells represent p-values that differed due to the removal of outliers.

		With outliers		Without outliers	
		Mean Difference	p-value	Mean difference	p-value
Linear acceleration (g)	ANOVA	-	$p < 0.001$	-	$p < 0.001$
	Neck 1 - Neck 2	3.21	$p < 0.001$	2.93	$p < 0.001$
	Neck 1 - Neck 3	7.41	$p < 0.001$	7.13	$p < 0.001$
	Neck 2 - Neck 3	4.20	$p < 0.001$	4.20	$p < 0.001$
Angular Velocity (rad/s)	ANOVA	-	$p < 0.001$	-	$p < 0.001$*
	Neck 1 - Neck 2	3.01	$p < 0.001$	3.01	$p < 0.001$†
	Neck 1 - Neck 3	5.05	$p < 0.001$	4.70	$p < 0.001$†
	Neck 2 - Neck 3	2.04	$p < 0.001$	1.69	$p < 0.001$†
Angular Acceleration (rad/s^2)	ANOVA	-	$p = 0.035$	-	$p < 0.001$*
	Neck 1 - Neck 2	-304.18	$p = 0.036$	-361.19	$p = 0.001$†
	Neck 1 - Neck 3	-66.10	$p = 0.837$	-35.31	$p = 0.905$†
	Neck 2 - Neck 3	238.08	$p = 0.119$	325.88	$p = 0.010$†

*Welch's ANOVA; †Games-Howell

The three necks had statistically different kinematics (Tale 4.8), but most normalized absolute differences between necks were less than 20% (Table 4.9). ANOVA results show that the linear accelerations (p<0.001, Cohen's f=3.6), angular velocities (p<0.001, Cohen's f=2.8), and angular accelerations (p=0.035, Cohen's f=0.5) between all three neck models were different. The linear

accelerations were significantly different between necks 1 and 2 (p<0.001, Cohen's d=3.5), necks 1 and 3 (p<0.001, Cohen's d=7.7), and necks 2 and 3 (p<0.001, Cohen's d=5.3) (Table 4.8); the normalized differences between the pairs were 6.0%, 13.9% and 7.9%, respectively (Table 4.9). The angular velocity was 15.8% different between necks 1 and 2 (p<0.001, Cohen's d=4.0), 10.7% different between necks 2 and 3 (p<0.001, Cohen's d=2.9), and 26.4% different between necks 1 and 3 (p<0.001, Cohen's d=5.7) (Table 4.8 and Table 4.9). The angular accelerations were only different between necks 1 and 2 (p=0.036, Cohen's d=1.2), with a normalized absolute difference of 9.2% (Table 4.8 and Table 4.9). The mean peak head kinematics for all three prototype surrogate necks subject to frontal helmeted impacts are presented visually in Figure 4.4.

The average normalized absolute difference between the linear accelerations of the necks during helmeted frontal impacts was 9.2%. For the rotational kinematics, the necks' angular accelerations were 6.1% different, and the angular velocities were 17.6% different (Table 4.9). Regarding the CV_B, the linear accelerations between necks had a variance of 6.0%, the angular acceleration had a variance of 8.6%, and the angular velocity had a variance of 11.7%.

Table 4.9: Normalized absolute differences between the prototype surrogate necks for helmeted frontal impacts.

	Δa (%)	Δα (%)	Δω (%)
Neck 1 - Neck 2	6.0	9.2	15.8
Neck 2 - Neck 3	7.9	7.2	10.7
Neck 1 - Neck 3	13.9	2.0	26.4
Average	9.2	6.1	17.6

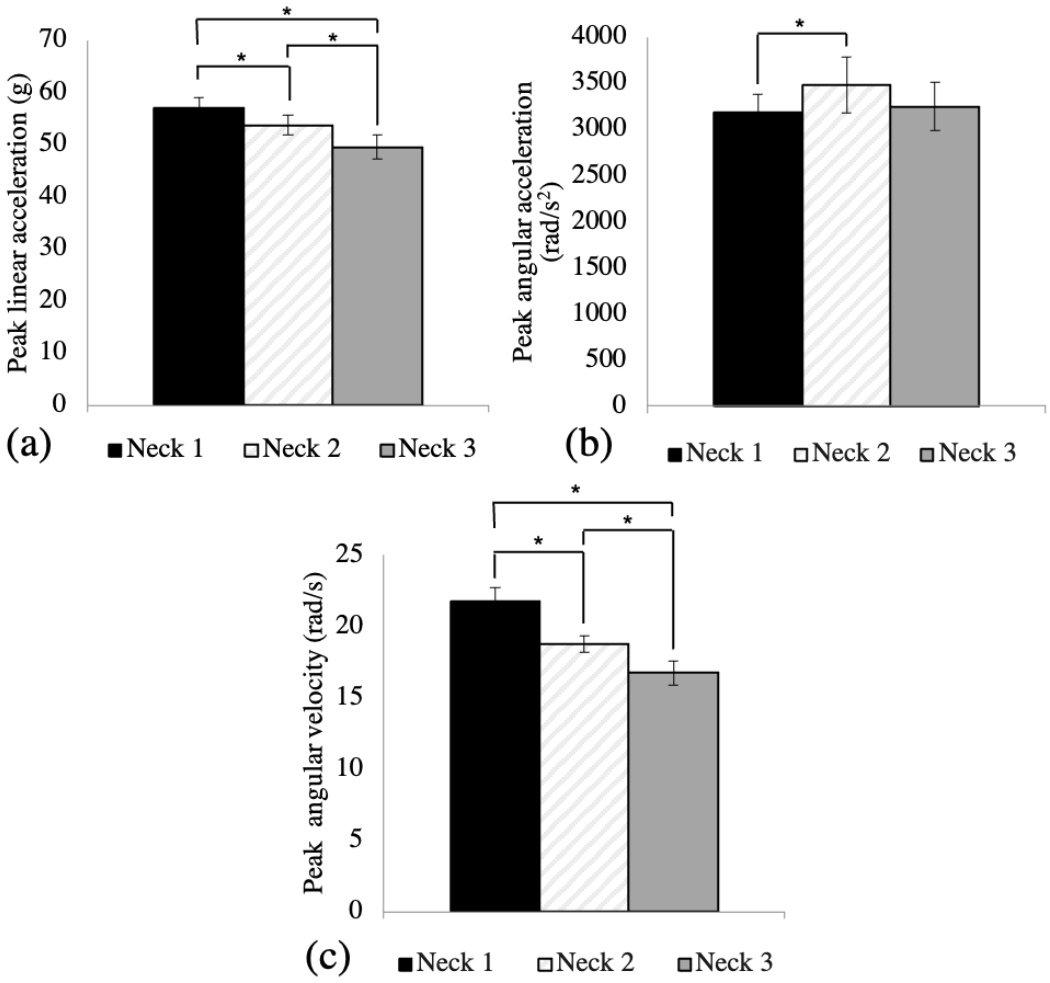

Figure 4.4: Means and standard deviations of the (a) peak linear accelerations, (b) peak angular accelerations, and (c) peak angular velocities of all three neck copies equipped with a helmet and impacted to the front of the head. Significant differences between necks are denoted by an asterisk (* = p<0.05).

Unhelmeted

The means, SDs, CV_W values, and 95% CIs of all head kinematics are reported for the necks during frontal impacts when the Hybrid III head was unprotected; Hybrid III neck kinematics were also reported and will be used in Section 4.2.2 (Table 4.10). ANOVAs were conducted on the data with and without outliers for the protected head (Table 4.11). The means and standard deviations of the head kinematics for each neck are presented in Figure 4.5. For reproducibility assessment, the normalized absolute differences between necks are outlined in Table 4.12, and the CV_B values are provided. The supplemental time series curves are displayed in Figure 4.6.

Table 4.10: Mean, SD, CV_W, and 95% CI values of the kinematic responses from the unhelmeted front impact condition. The Hybrid III data is used in Section 4.2.

Neck model		Peak a (g)	Peak α (rad/s^2)	Peak ω (rad/s)
1	Mean±SD	127.4± 3.0	5664.3 ±231.4	31.1 ± 0.4
	CV_W	2.4%	4.1%	1.3%
	95% CI	(125.3, 129.6)	(5498.7, 5829.9)	(30.9, 31.4)
2	Mean±SD	126.7± 1.9	5639.0 ±158.9	30.6± 0.2
	CV_W	1.5%	2.8%	0.8%
	95% CI	(125.4, 128.1)	(5525.3, 5752.7)	(30.4, 30.8)
3	Mean±SD	117.9 ± 1.6	5182.5 ±116.3	27.8 ± 0.5
	CV_W	1.4%	2.2%	1.8%
	95% CI	(116.7, 119.1)	(5099.3, 5265.7)	(27.5, 28.2)
Hybrid III	Mean±SD	131.7 ±1.4	6418.6±288.1	33.4 ± 0.3
	CV_W	1.1%	4.5%	0.9%
	95% CI	(130.7, 132.7)	(6212.5, 6624.7)	(33.2, 33.6)

All CV_W values are less than 5% (Table 4.10). The overall CV_W values were 1.8%, 3.2%, and 1.3% for the linear accelerations, angular accelerations, and angular velocities, respectively. In general, neck 3 seems to display mean kinematics lower than the other two necks (Table 4.10), but an ANOVA was run to determine any statistical differences. The outliers, normality, and variances were assessed before running an ANOVA.

All datasets were normal except the angular velocity of neck 3 (p=0.042). Only the linear acceleration of neck 2 had one outlier. Nevertheless, the ANOVA was run twice on the linear acceleration dataset (with and without outliers) to ensure the presence of the outlier was not affecting the results (Table 4.11). The results were not affected by the removal of the outlier. Levene's test for equality of variance based on the median suggested the angular acceleration dataset and linear acceleration without outliers dataset violated the assumption of homogeneity of variance (p=0.045); thus, Welch's ANOVA and Games-Howell post-hoc tests were run on these data.

Table 4.11: Mean differences between the prototype surrogate necks and p-values for the ANOVAs and post-hoc statistical tests run on the unhelmeted necks for the entire dataset and on the dataset with outliers removed for frontal head impacts.

		With outliers		Without outliers	
		Mean Difference	p-value	Mean difference	p-value
Linear acceleration (g)	ANOVA	-	$p < 0.001$	-	$p < 0.001$*
	Neck 1 - Neck 2	0.72	$p = 0.759$	0.23	$p = 0.972$†
	Neck 1 - Neck 3	9.57	$p < 0.001$	9.57	$p < 0.001$†
	Neck 2 - Neck 3	8.84	$p < 0.001$	9.33	$p < 0.001$†
Angular Velocity (rad/s)	ANOVA		$p < 0.001$		-
	Neck 1 - Neck 2	0.56	$p = 0.010$	-	-
	Neck 1 - Neck 3	3.30	$p < 0.001$	-	-
	Neck 2 - Neck 3	2.74	$p < 0.001$	-	-
Angular Acceleration (rad/s^2)*†	ANOVA		$p < 0.001$		-
	Neck 1 - Neck 2	25.26	$p = 0.956$	-	-
	Neck 1 - Neck 3	481.80	$p < 0.001$	-	-
	Neck 2 - Neck 3	456.54	$p < 0.001$	-	-

* Welch's ANOVA; † Games-Howell

The unhelmeted frontal impacts resulted in significant differences between head kinematics for all necks (Table 4.11). However, the normalized absolute differences were lower than their helmeted counterparts (Table 4.12). Linear accelerations (p<0.001, Cohen's f=2.0), angular velocities (p<0.001, Cohen's f=3.9), and angular accelerations (p<0.001, Cohen's f=1.3) were significantly different for all necks during unhelmeted frontal impacts (Table 4.11). The linear accelerations of necks 1 and 3 (p<0.001, Cohen's d=3.9) and necks 2 and 3 (p<0.001, Cohen's d=5.0) were significantly different, as were the angular accelerations between the neck pairs (p<0.001, Cohen's d=2.6 and Cohen's d=3.3, respectively) (Table 4.11). The normalized absolute differences between the linear accelerations were 7.7% and 7.1%, respectively, and were 8.8% and 8.3% for the angular accelerations (Table 4.12). The angular velocities differed by 1.9% between necks 1 and 2 (p=0.01, Cohen's d=1.7), 9.2% between necks 2 and 3 (p<0.001, Cohen's d=7.1), and 11.1% between necks 1 and 3 (p<0.001, Cohen's d=7.4) (Table 4.11 and Table 4.12). In Figure 4.5, the peak kinematics of the three prototype surrogate necks are presented.

The linear accelerations between necks during unhelmeted frontal impacts differed by 5.1% on average, the angular accelerations differed by 5.8%, and the angular velocities differed by 7.4% (Table 4.12). The CV_B values were 4.0%, 5.1%, and 5.1% for the linear acceleration, angular acceleration, and angular velocity.

Table 4.12: Normalized absolute differences between the prototype surrogate necks for unhelmeted frontal impacts.

	Δa (%)	Δα (%)	Δω (%)
Neck 1 - Neck 2	0.6	0.5	1.9
Neck 2 - Neck 3	7.1	8.3	9.2
Neck 1 - Neck 3	7.7	8.8	11.1
Average	5.1	5.8	7.4

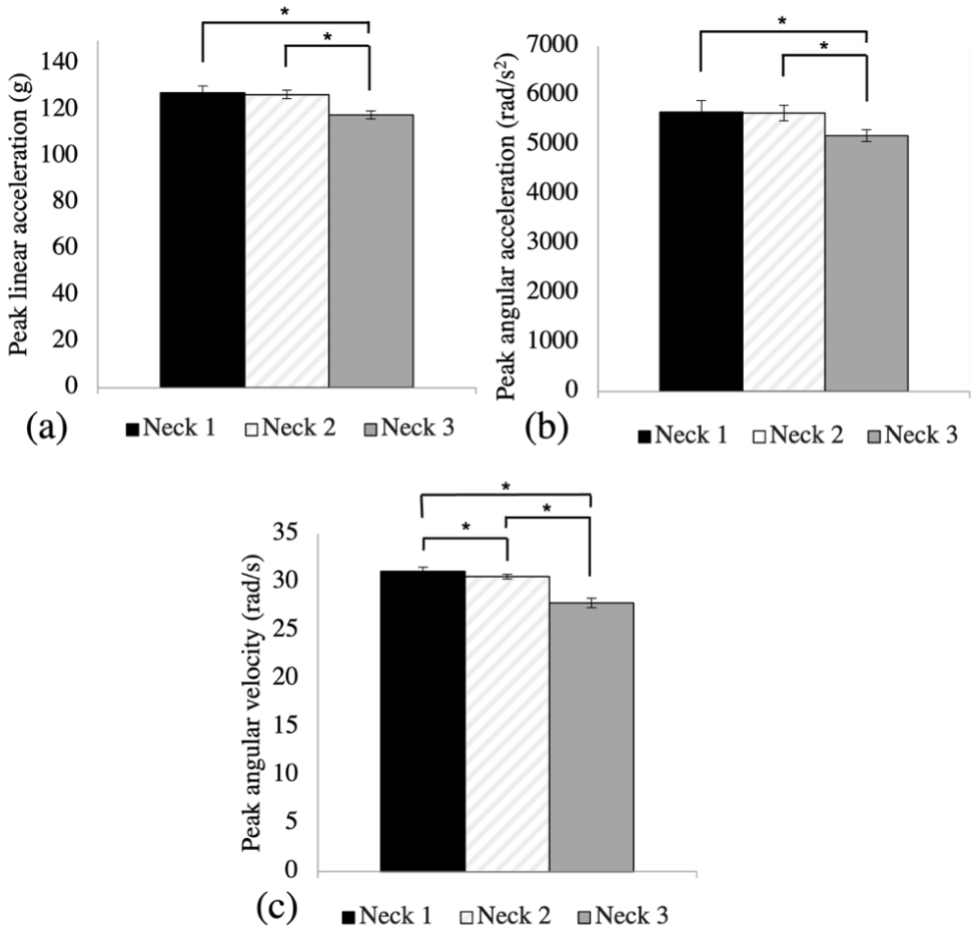

Figure 4.5: Means and standard deviations of the (a) peak linear accelerations, (b) peak angular accelerations, and (c) peak angular velocities of all three unhelmeted necks during impacts to the front of the head. An asterisk denotes significant differences between necks (* = p<0.05).

Summary

As before, statistical results suggested significant differences between necks, but the normalized absolute differences and CV_B values are considered acceptable. Except for the angular velocities between necks 1 and 3, the normalized absolute differences between the three neck models were less than 16% when a helmet was used (Table 4.9). When unhelmeted, the normalized absolute differences were always 11% or less (Table 4.12). For most kinematics in both protected and unprotected impacts, the CV_B values were 10% or less, and all were less than 15%. The calculated CV_W values were less than 9% for all helmeted cases (Table 4.7) and 5% for unhelmeted impacts (Table 4.10), once again showing high repeatability within groups.

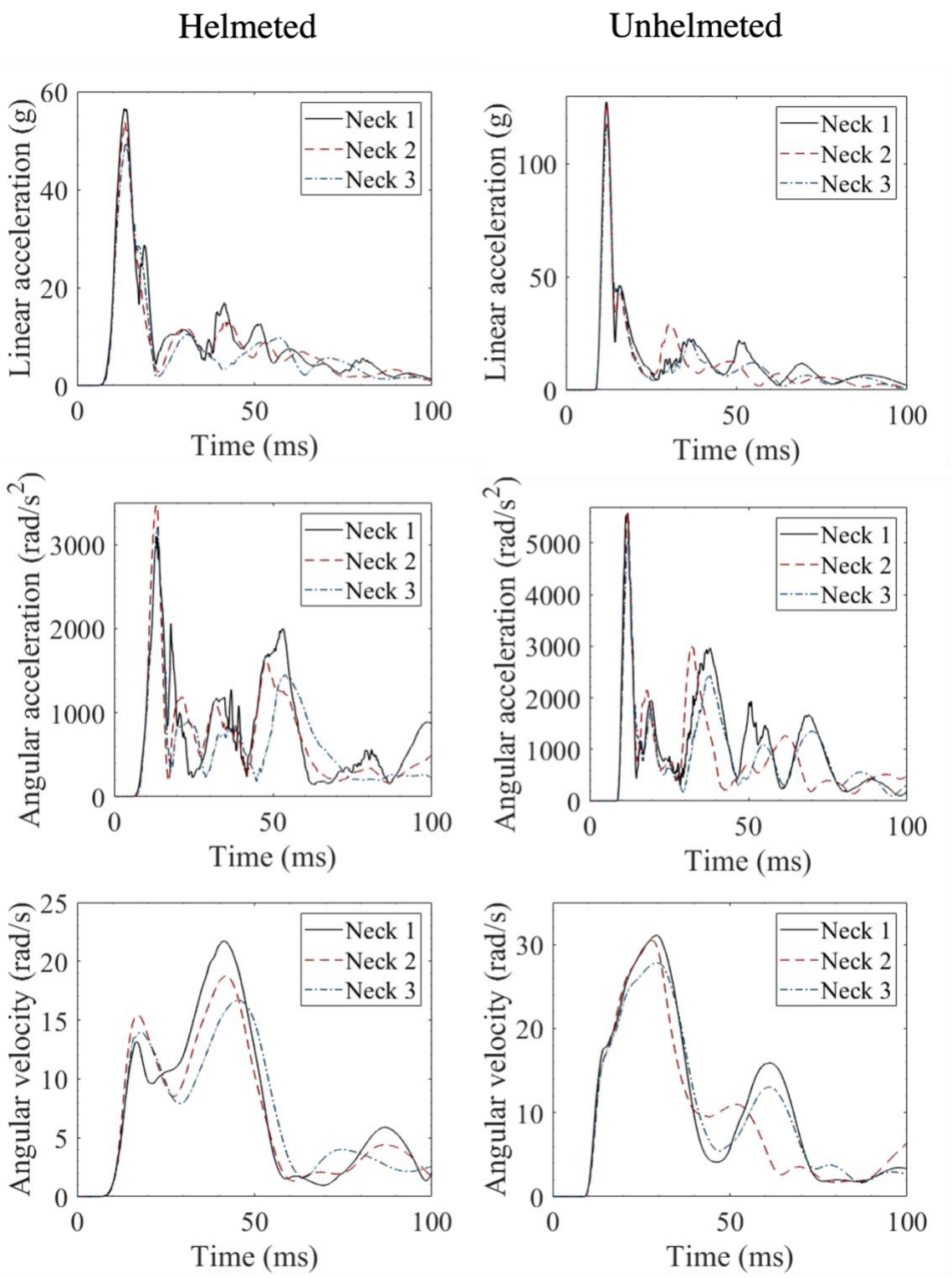

Figure 4.6: Ensemble averages of all three surrogate prototype necks during helmeted impacts (left column) and unhelmeted impacts (right column) to the front of the head. Linear accelerations (first row), angular accelerations (second row), and angular velocities (third row) for all neck prototypes are displayed for the first 100 ms.

4.2 Comparison with the Hybrid III neck

A Hybrid III neck was tested under the same conditions as the three prototype surrogate necks to quantify differences between the mechanics and variance of the Hybrid III and the prototype surrogate neck. Within-neck repeatability of the Hybrid III was commensurate with the prototype surrogate neck, with all CV_W values 10% or less except the angular acceleration of helmeted frontal impacts. Statistical significance indicated a difference between the head kinematics of the prototype surrogate and the Hybrid III. For unhelmeted impacts at both impact locations, the normalized absolute differences between the Hybrid III neck and each prototype surrogate neck were greater than the differences between the three copies of the prototype surrogate neck, suggesting the Hybrid III and prototype surrogate necks may lead to different kinematics in this test condition. In contrast, the Hybrid III neck and the prototype surrogate appear to have more similar kinematics during helmeted impacts. Overall, the unhelmeted impacts suggest the necks may lead to different kinematics. However, using a helmet increases the variance and makes it less clear if the kinematics substantially differ. In addition, the Hybrid III neck almost always had kinematics that were greater or less than all three of the surrogate necks. Below, numerical results are presented that support these general findings.

4.2.1 Front boss impacts

Helmeted

Head kinematics are reported for the Hybrid III neck impacted at the front boss on the head equipped with a helmet (Table 4.1). Figure 4.7 shows graphical comparisons of the Hybrid III neck and the three prototype surrogates. Table 4.13 compares the results of the ANOVA run on the complete datasets versus the datasets with outliers removed for the helmet cases. Normalized absolute differences were also calculated between the Hybrid III neck and each prototype surrogate (Table 4.14). The time series kinematics of all four necks are shown in Figure 4.9.

The Hybrid III CV_W values were 10% or less for all Hybrid III kinematics, which matches the prototype surrogate neck repeatability (Table 4.1). For both the peak linear accelerations and the angular velocities, the Hybrid III kinematics are consistently less than the kinematics of the surrogate necks. The Hybrid III neck resulted in lower peak angular accelerations that two of the

prototype surrogate necks (Figure 4.7 and Table 4.14). An ANOVA was run to determine any statistical differences between the neck types.

A Shapiro-Wilk test showed the following distributions were non-normal (p<0.05): the linear accelerations of necks 2 and 3, the angular velocities of necks 1,3 and the Hybrid III, and the angular acceleration of neck 3 and the Hybrid III. The Hybrid III neck datasets had no outliers, but all prototype surrogate neck datasets had at least one outlier. Removal of the outliers made the distributions of the prototype surrogate neck normal but did not affect the normality of the Hybrid III datasets. However, since the ANOVA is robust to violations in normality, the ANOVA was still considered an acceptable test. Further, the removal of outliers did not affect the overall results of the neck comparisons (Table 4.13), so results were reported for the complete datasets. The assumption of homogeneity of variances was violated for the angular accelerations and the linear acceleration dataset without outliers, as assessed by Levene's test based on the median (p=0.016); thus, a Welch's ANOVA and Games-Howell post-hoc tests were conducted for these datasets.

Table 4.13: Mean differences between the surrogate neck prototype and the Hybrid III neck, and results of the ANOVAs and post-hoc statistical tests run on the full dataset and the dataset with outliers removed for all head kinematics during front boss helmeted impacts.

		With outliers		Without outliers	
		Mean Difference	p-value	Mean difference	p-value
Linear acceleration (g)	ANOVA	-	p < 0.001	-	p < 0.001*
	Hy3 – Neck 1	-4.02	p < 0.001	-3.90	p < 0.001†
	Hy3 – Neck 2	-1.99	p < 0.001	-1.73	p < 0.001†
	Hy3 – Neck 3	-3.82	p < 0.001	-3.49	p < 0.001†
Angular Velocity (rad/s)	ANOVA	-	p < 0.001	-	p < 0.001
	Hy3 – Neck 1	-1.19	p = 0.003	-0.96	p < 0.001
	Hy3 – Neck 2	-3.75	p < 0.001	-3.57	p < 0.001
	Hy3 – Neck 3	-5.04	p < 0.001	-4.83	p < 0.001
Angular Acceleration (rad/s^2)*†	ANOVA		p < 0.001		p < 0.001
	Hy3 – Neck 1	83.42	p = 0.696	45.55	p = 0.922
	Hy3 – Neck 2	-106.97	p = 0.665	-69.49	p = 0.856
	Hy3 – Neck 3	-408.36	p < 0.001	-395.65	p < 0.001

* Welch's ANOVA; † Games-Howell

When the Hybrid III head was equipped with a helmet, the linear accelerations (p<0.001, Cohen's f=1.5), angular velocities (p<0.001, Cohen's f=2.0), and angular accelerations (p<0.001, Cohen's f=0.8) differed between the Hybrid III neck and the prototype surrogate necks (Table 4.13). The linear acceleration of the Hybrid III neck was 12.0% less than neck 1 (p<0.001, Cohen's d=3.7), 6.0% less than neck 2 (p<0.001, Cohen's d=1.7), and 11.4% less than neck 3 (p<0.001, Cohen's d=2.9) (Table 4.13 and Table 4.14). Only the angular accelerations between the Hybrid III and neck 3 were significantly different (12.8% different; p<0.001, Cohen's d=1.6) (Table 4.13 and Table 4.14). The angular velocity of the Hybrid III neck was 6.1% less than neck 1 (p=0.003, Cohen's d=1.5), 19.4% less than neck 2 (p<0.001, Cohen's d=3.8), and 26.0% less than neck 3 (p<0.001, Cohen's d=5.0) (Table 4.13 and Table 4.14).

Table 4.14: Normalized absolute differences between the Hybrid III neck and the prototype surrogate necks for helmeted front boss impacts.

	Δa (%)	Δα (%)	Δω (%)
Hybrid III – Neck 1	12.0	2.6	6.1
Hybrid III – Neck 2	6.0	3.4	19.4
Hybrid III – Neck 3	11.4	12.8	26.0
Average	9.8	6.3	17.2

The differences between the kinematics of the Hybrid III and the prototype surrogate necks (Table 4.14) are similar in magnitude to the normalized absolute differences between the three prototype surrogate necks during helmeted front boss impacts (Table 4.3). During the Hybrid III comparisons, the normalized absolute differences were 5.8% greater for linear accelerations and 3.9% greater for angular velocities than the reproducibility assessments between the surrogate prototype necks. However, the normalized absolute difference of the angular acceleration between copies of the prototype surrogate neck was approximately 4% larger than the average difference between the prototype surrogate neck and the Hybrid III neck. This may be partly attributed to the more considerable variance of the angular accelerations compared to the other kinematics (Table 4.1).

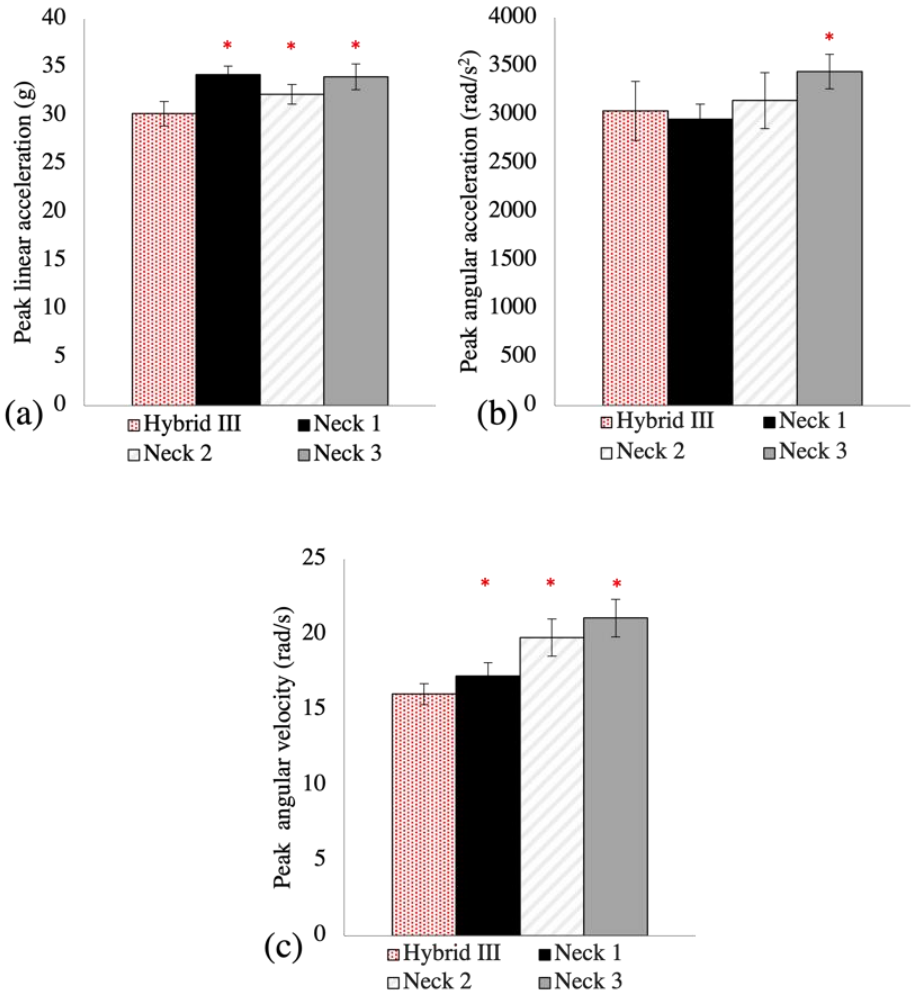

Figure 4.7: Means and standard deviations of the (a) peak linear accelerations, (b) peak angular accelerations, and (c) peak angular velocities of the Hybrid III neck and the three prototype surrogate necks when impacts were delivered to the front boss of the helmeted Hybrid III head. Data from Figure 4.1 is replotted alongside the new Hybrid III data. A red asterisk denotes a significant difference from the Hybrid III neck (p<0.05).

Unhelmeted

The means, SDs, CV_W values, and 95% CIs of the Hybrid III head kinematics are reported for impacts to the front boss of the unprotected head (Table 4.4). Comparisons of the Hybrid III neck with the three prototype surrogates are also shown visually in Figure 4.8. Table 4.15 compares the results of the ANOVA run on the complete datasets and the datasets with outliers removed. Normalized absolute differences were calculated between the Hybrid III neck and each prototype surrogate (Table 4.16). The time series kinematics of all four necks are also presented (Figure 4.9).

The Hybrid III CVw values are less than 5% for all kinematics, and there appear to be more evident mean differences between the Hybrid III and the prototype surrogate necks than the helmeted tests (Table 4.4). The Hybrid III peak linear and angular accelerations are greater than all prototype surrogate necks; in contrast, the peak angular velocity of the Hybrid III is lesser than the prototype surrogate necks (Figure 4.8 and Table 4.15). As before, an ANOVA was run to determine statistical differences between necks. The outliers, normality, and variance assumptions were first checked. Only the linear acceleration (neck 2) and angular velocity datasets (neck 1 and neck 2) had outliers. In addition, the linear acceleration of the Hybrid III and the angular velocity of neck 2 were non-normal datasets (p<0.05). Although the removal of outliers only made the angular velocity of neck 2 normal, the Hybrid III outlier did not affect the conclusions drawn from the results (Table 4.15); thus, the ANOVA was considered an acceptable test. A Welch's ANOVA and Games-Howell post hoc tests were conducted for the angular accelerations since Levene's test for equality of variance based on the median showed unequal variances (p=0.037).

Table 4.15: Mean differences between the Hybrid III neck and the prototype surrogate necks, as well as p-values from the ANOVAs and post-hoc tests run on the full dataset and the dataset with outliers removed for all head kinematics during front boss unhelmeted impacts.

		With outliers		Without outliers	
		Mean Difference	p-value	Mean difference	p-value
Linear acceleration (g)	ANOVA	-	p < 0.001	-	p < 0.001
	Hy3 – Neck 1	14.23	p < 0.001	14.23	p < 0.001
	Hy3 – Neck 2	11.60	p < 0.001	11.85	p < 0.001
	Hy3 – Neck 3	21.12	p < 0.001	21.12	p < 0.001
Angular Velocity (rad/s)	ANOVA	-	p < 0.001	-	p < 0.001
	Hy3 – Neck 1	-5.09	p < 0.001	-5.09	p < 0.001
	Hy3 – Neck 2	-4.03	p < 0.001	-3.93	p < 0.001
	Hy3 – Neck 3	-4.10	p < 0.001	-4.01	p < 0.001
Angular Acceleration (rad/s^2)*†	ANOVA	-	p < 0.001	-	-
	Hy3 – Neck 1	1241.84	p < 0.001	-	-
	Hy3 – Neck 2	1298.74	p < 0.001	-	-
	Hy3 – Neck 3	1058.34	p < 0.001	-	-

*Welch's ANOVA; † Games-Howell

The Hybrid III showed significantly different head kinematics from the prototype surrogate neck for unhelmeted impacts; linear accelerations (p<0.001, Cohen's f=3.8), angular velocities (p<0.001, Cohen's f=6.5), and angular accelerations (p<0.001, Cohen's f=1.6) were all different (Table 4.15). The linear acceleration of the Hybrid III neck was 9.5% greater than neck 1 (p<0.001, Cohen's d=7.3), 7.7% greater than neck 2 (p<0.001, Cohen's d=6.2), and 14.1% greater than neck 3 (p<0.001, Cohen's d=10.2) (Table 4.15 and Table 4.16). The angular acceleration of the Hybrid III neck was also 16.5% greater than neck 1 (p<0.001, Cohen's d=4.1), 17.2% greater than neck 2 (p<0.001, Cohen's d=4.8), and 14.0% greater than neck 3 (p<0.001, Cohen's d=2.8) (Table 4.15 and Table 4.16). The angular velocity of the Hybrid III was 18.9% (p<0.001, Cohen's d=24.3), 15% (p<0.001, Cohen's d=13.8), and 15.3% (p<0.001, Cohen's d=13.4) less than all three prototype surrogate necks, respectively (Table 4.15 and Table 4.16). Comparisons of the mean peak kinematics between the Hybrid III neck and the surrogate prototype necks are also graphically displayed (Figure 4.8).

Table 4.16: Normalized absolute differences between the Hybrid III neck and the three prototype surrogate necks for unhelmeted front boss impacts. Adapted* with permission from Springer Nature, MacGillivray et al. [142] copyright 2021.

	Δa (%)	Δα (%)	Δω (%)
Hybrid III – Neck 1	9.5	16.5	18.9
Hybrid III – Neck 2	7.7	17.2	15.0
Hybrid III – Neck 3	14.1	14.0	15.3
Average	10.4	15.9	16.4

*The analysis method in this thesis was slightly different from the article, but the results were similar.

Comparing Table 4.16 to Table 4.6 shows the normalized absolute differences are greater between the Hybrid III neck and the prototype surrogate neck versus between the three prototype surrogate necks. The normalized absolute difference was 6% greater when comparing the peak linear accelerations between the Hybrid III necks and the prototype surrogate necks than the differences between the three prototype neck copies; the differences were 14% greater for the angular kinematics during the Hybrid III comparisons.

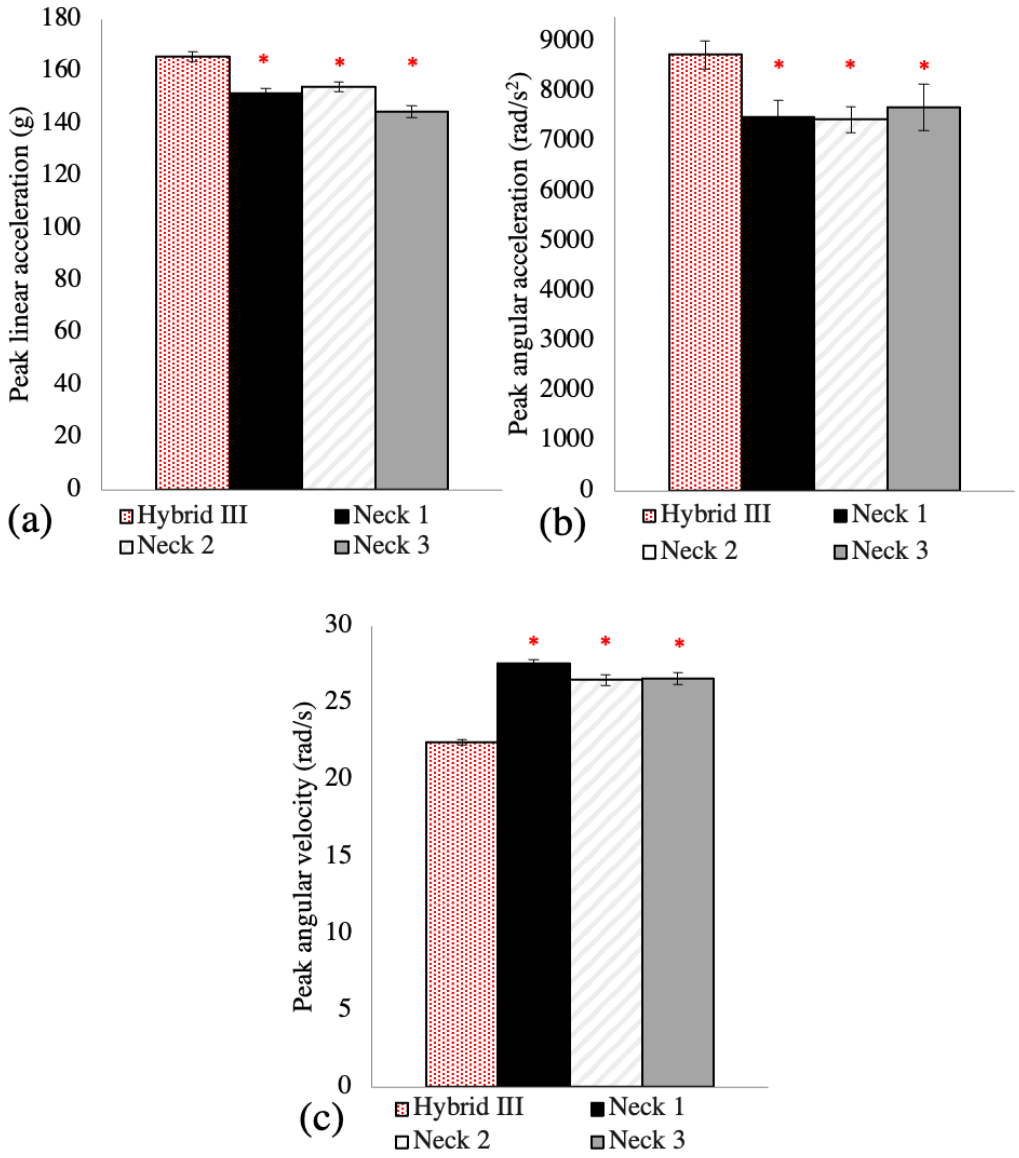

Figure 4.8: Means and standard deviations of the (a) peak linear accelerations, (b) peak angular accelerations, and (c) peak angular velocities of the Hybrid III neck and the three prototype surrogate necks when impacts were delivered to the front boss of the unhelmeted Hybrid III head. Data from Figure 4.2 is replotted alongside the new Hybrid III data. A red asterisk denotes a significant difference from the Hybrid III neck ($p<0.05$).

Summary

The statistical results and normalized absolute differences between neck types suggest the Hybrid III neck and the prototype surrogate neck differ during unhelmeted impacts. For the unhelmeted impacts, the average difference between the Hybrid III neck and the prototype surrogate necks was 14.2%, whereas the average difference between just the prototype surrogate necks was 3.0%. In contrast, the normalized absolute differences between the helmeted Hybrid III neck and each prototype surrogate neck were similar to the differences calculated between three copies of the prototype surrogate neck. The average difference between the head kinematics of the Hybrid III and the prototype surrogate necks was 11.1%, compared to the average difference between the three prototype surrogate necks of 9.2%. Further, the Hybrid III peak kinematics were consistently greater or less than the three surrogate necks, except for the angular acceleration of helmeted impacts.

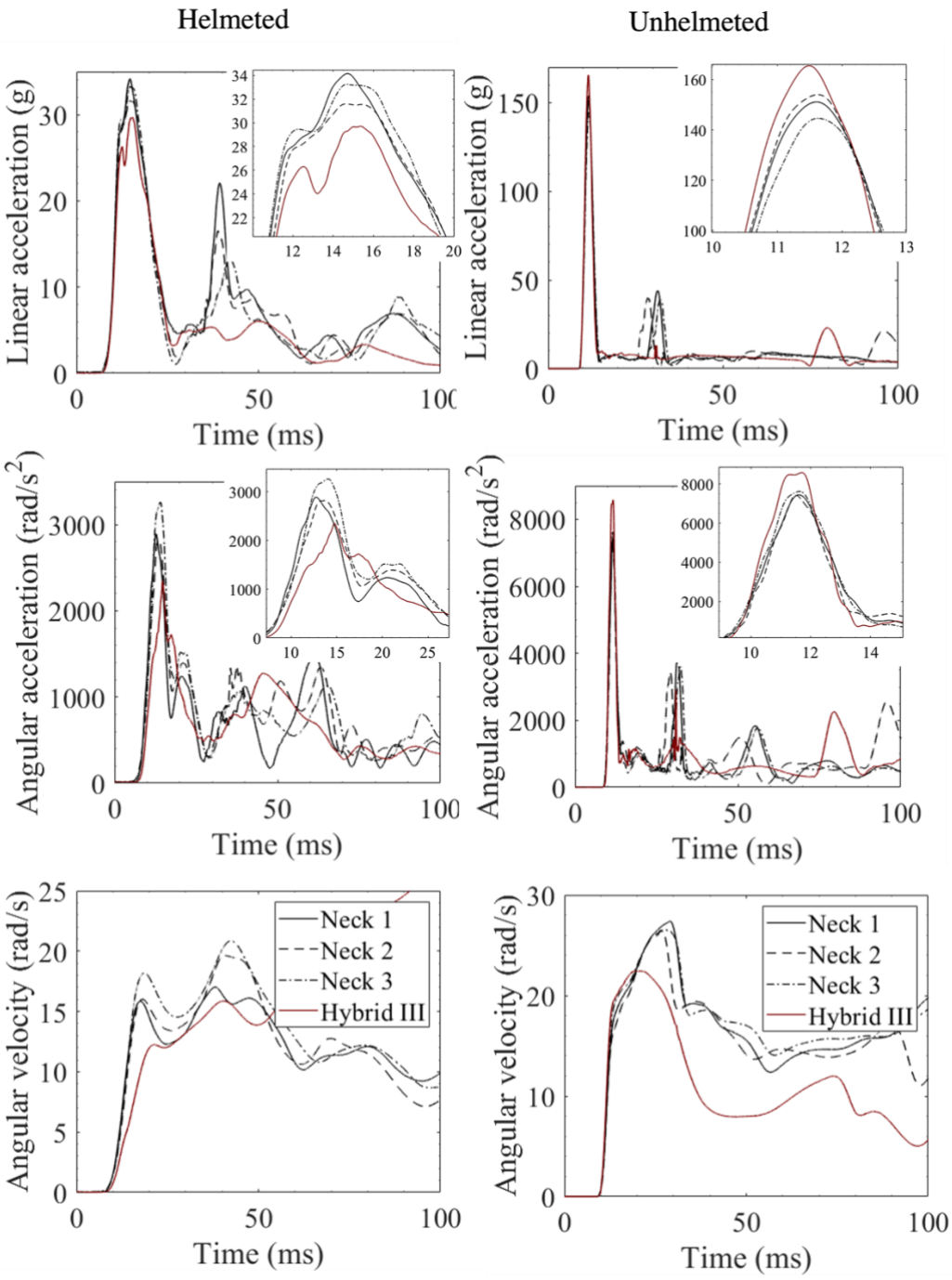

Figure 4.9: Ensemble averages of all three prototype surrogate necks and the Hybrid III neck during helmeted impacts (left column) and unhelmeted impacts (right column) to the front boss of the head. The top right miniature graphs are close-ups of the peaks for the linear and angular accelerations. Figures of the unhelmeted impacts were adapted with permission from Springer Nature, MacGillivray et al. [142], copyright 2021.

4.2.2 Frontal impacts

Helmeted

Means, SDs, CV_w values, and 95% CIs of all head kinematics are reported for the Hybrid III neck attached to the protected Hybrid III head during frontal impacts (Table 4.7). The Hybrid III neck and the three prototype surrogates are also compared graphically (Figure 4.10). Results of ANOVAs run with and without outliers are presented in Table 4.17. Normalized absolute differences were calculated between the Hybrid III neck and each prototype surrogate neck (Table 4.18). The time series mechanics were compared by plotting the kinematic curves for each neck (Figure 4.12).

The CV_w values for the linear acceleration and angular velocity were less than 5%, but the angular acceleration had a CV_w greater than 10% (Table 4.7). The Hybrid III mean angular velocity was smaller than all prototype surrogate necks (Table 4.17 and Figure 4.10). The peak linear accelerations and angular accelerations showed no trends in magnitude differences, but the Hybrid III kinematics were less than two of the prototype surrogate necks (Table 4.17 and Figure 4.10). An ANOVA was run to detect significant differences between the Hybrid III and the prototype surrogate neck. As required, the ANOVA assumptions were first checked.

The linear acceleration of necks 1 and 3, the angular velocity of neck 3, and the angular accelerations of necks 1 and 2 datasets were non-normal ($p<0.05$). Outliers were detected in all the above datasets, except the linear acceleration of neck 3. A second ANOVA was run on the data with outliers removed (Table 4.17). The removal of outliers made most datasets normal except the linear acceleration of neck 3 but did affect some of the results. The angular accelerations between necks were not significantly different when outliers were included, but the differences were significant once the outliers were removed. However, post-hoc comparisons between the Hybrid III and the three prototype surrogates were not affected (Table 4.17). The conclusions of the ANOVA are thus unchanged, as the Hybrid III shows similarity to all the necks regardless of the outliers. The angular velocity between the Hybrid III and neck 3 also showed different results when outliers were removed, but the mean difference changes were minor. Since the results do not differ sufficiently for different conclusions to be reached, the outliers were kept in the datasets,

and a one-way ANOVA with Tukey post-hoc tests were conducted. A Welch's ANOVA and Games-Howell post-hoc tests were conducted for the linear acceleration and angular acceleration data, since Levene's test for equality of variance based on the median was significant for both (p<0.05).

Table 4.17: Mean differences between the Hybrid III and the prototype surrogate neck kinematics during frontal helmeted impacts are reported, along with the p-values from ANOVAs and post-hoc statistical tests run on the full dataset and the dataset with outliers removed for all head kinematics.

		With outliers		Without outliers	
		Mean Difference	p-value	Mean difference	p-value
Linear acceleration (g)*†	ANOVA	-	p < 0.001	-	p < 0.001
	Hy3 – Neck 1	-5.90	p < 0.001	-5.62	p < 0.001
	Hy3 – Neck 2	-2.69	p = 0.022	-2.69	p = 0.022
	Hy3 – Neck 3	1.50	p = 0.266	1.50	p = 0.266
Angular Velocity (rad/s)	ANOVA	-	p < 0.001	-	p < 0.001
	Hy3 – Neck 1	-5.57	p < 0.001	-5.57	p < 0.001
	Hy3 – Neck 2	-2.56	p < 0.001	-2.56	p < 0.001
	Hy3 – Neck 3	-0.52	p = 0.399	-0.87	p = 0.029
Angular Acceleration (rad/s^2)*†	ANOVA	-	p = 0.120	-	p < 0.001
	Hy3 – Neck 1	45.38	p = 0.995	14.59	p = 1.000
	Hy3 – Neck 2	-258.80	p = 0.603	-346.60	p = 0.306
	Hy3 – Neck 3	-20.72	p = 1.000	-20.72	p = 1.000

*Welch's ANOVA; †Games-Howell

For impacts to the helmeted head, the linear accelerations (p<0.001, Cohen's f=2.1) and angular velocities (p<0.001, Cohen's f=3.2) were significantly different between the Hybrid III and the three prototype surrogates (Table 4.17). The linear acceleration of the Hybrid III neck was 11.0% less than neck 1 (p<0.001, Cohen's d=3.3) and 5.0% less than neck 2 (p=0.022, Cohen's d=1.6) (Table 4.17 and Table 4.18). The angular velocity of the Hybrid III neck was also 29.1% less than neck 1 (p<0.001, Cohen's d=7.5) and 13.4% less than neck 2 (p<0.001, Cohen's d=4.7) (Table 4.17 and Table 4.18). The Hybrid III neck and neck 3 were not significantly different for any head

kinematics, nor were the angular accelerations different between the Hybrid III and any prototype surrogate neck (Table 4.17 and Table 4.18).

Table 4.18: Normalized absolute differences between the Hybrid III and the three prototype surrogate necks for helmeted frontal impacts.

	Δa (%)	Δα (%)	Δω (%)
Hybrid III – Neck 1	11.0	1.4	29.1
Hybrid III – Neck 2	5.0	7.8	13.4
Hybrid III – Neck 3	2.8	0.6	2.7
Average	6.3	3.3	15.1

Comparing Table 4.18 with Table 4.9, it is evident that the normalized absolute differences between the Hybrid III and the prototype surrogate necks are not greater than the differences between the three surrogate prototype necks. The average normalized absolute differences between the Hybrid III and the prototype surrogate necks 8.2%. In contrast, the average normalized absolute difference between the three prototype surrogate necks was 11.0%. Thus, the Hybrid III necks comparisons to the prototype surrogate neck result in normalized absolute differences of all kinematics 3% smaller than those between the three prototype necks.

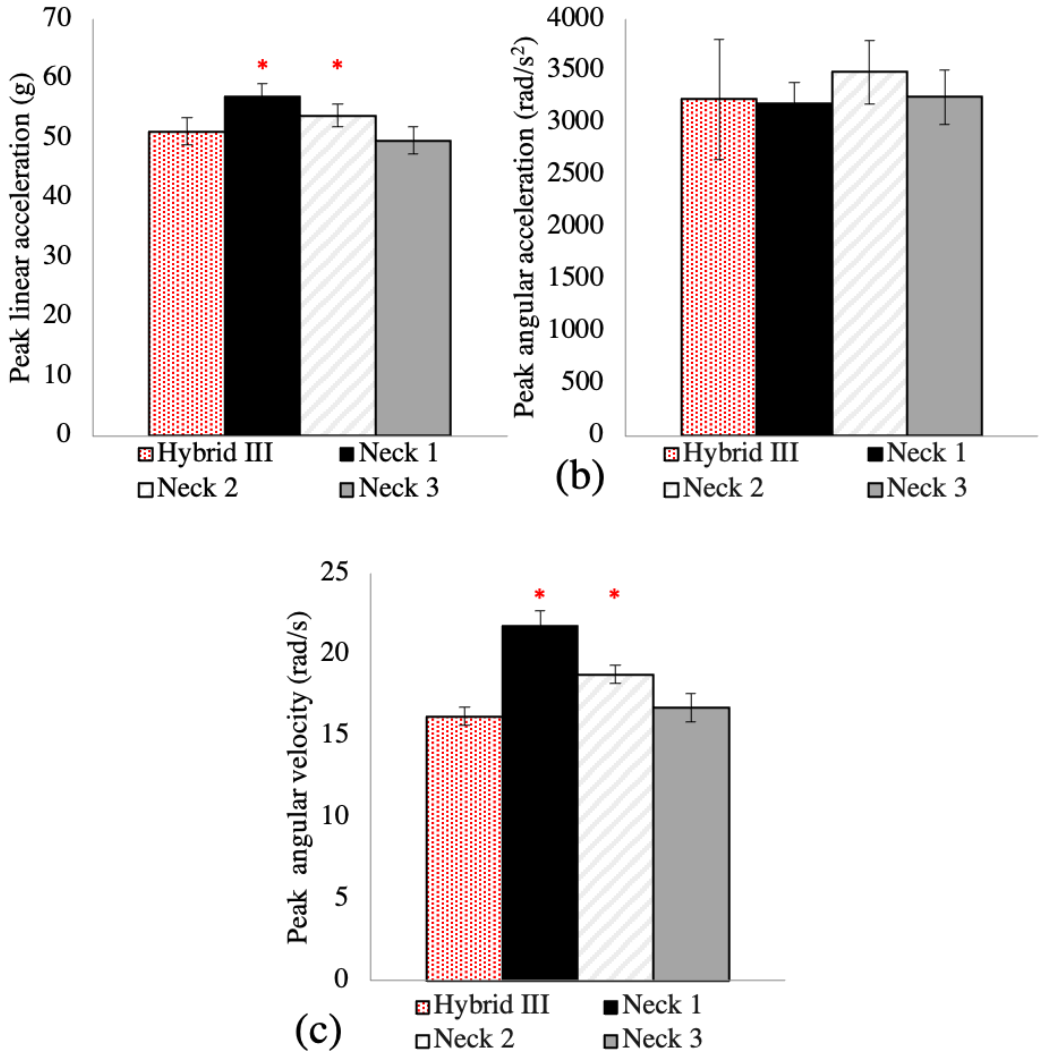

Figure 4.10: Means and standard deviations of the (a) peak linear accelerations, (b) peak angular accelerations, and (c) peak angular velocities of the Hybrid III neck and the three prototype surrogate necks when frontal impacts were delivered to the front of the helmeted Hybrid III head. Data from Figure 4.4 is replotted alongside the new Hybrid III data. A red asterisk denotes a significant difference from the Hybrid III neck ($p<0.05$).

Unhelmeted

Means, SDs, CV_w values, and 95% CIs of all head kinematics are reported for the Hybrid III neck attached to the unprotected Hybrid III head during frontal impacts (Table 4.10). Figure 4.11 shows graphical comparisons of the Hybrid III neck mean peak kinematics with the three prototype surrogates. Comparisons between an ANOVA with and without outliers are shown in Table 4.19.

Normalized absolute differences were calculated between the Hybrid III neck and each prototype surrogate neck (Table 4.20). The time series mechanics of all necks are presented in Figure 4.12.

Table 4.19: Mean differences between the peak kinematics of the Hybrid III neck and the prototype surrogate necks reported along with the p-values from ANOVAs and post-hoc statistical tests run on the full dataset and the dataset with outliers removed for all head kinematics during front unhelmeted impacts.

		With outliers		Without outliers	
		Mean Difference	p-value	Mean difference	p-value
Linear acceleration (g)	ANOVA	-	$p < 0.001$	-	$p < 0.001$*
	Hy3 – Neck 1	4.29	$p < 0.001$	4.29	$p = 0.007$†
	Hy3 – Neck 2	5.01	$p < 0.001$	4.52	$p < 0.001$†
	Hy3 – Neck 3	13.85	$p < 0.001$	13.85	$p < 0.001$†
Angular velocity (rad/s)	ANOVA	-	$p < 0.001$	-	-
	Hy3 – Neck 1	2.21	$p < 0.001$	-	-
	Hy3 – Neck 2	2.77	$p < 0.001$	-	-
	Hy3 – Neck 3	5.52	$p < 0.001$	-	-
Angular Acceleration (rad/s^2)	ANOVA	-	$p < 0.001$	-	$p < 0.001$
	Hy3 – Neck 1	754.28	$p < 0.001$	829.87	$p < 0.001$
	Hy3 – Neck 2	779.53	$p < 0.001$	855.13	$p < 0.001$
	Hy3 – Neck 3	1236.08	$p < 0.001$	1311.67	$p < 0.001$

*Welch's ANOVA; † Games-Howell

The CV_W for all Hybrid III kinematics was less than 5% (Table 4.10). Further, the Hybrid III always had greater kinematics than the prototype surrogate necks (Table 4.19 and Figure 4.11). An ANOVA was run to determine significant differences between head kinematics. All assumptions were checked before running an ANOVA to determine statistical differences. Only the angular velocity of neck 3 showed non-normal distribution ($p<0.05$). Outliers in the linear acceleration of the neck 2 dataset and the angular acceleration of the Hybrid III dataset were removed, and a second ANOVA was run. Removal of outliers did not affect the results (Table 4.19), so they were kept in the analysis. All datasets except the linear acceleration with outliers had equal variance.

All kinematics differed between the Hybrid III neck and the prototype surrogate necks: linear accelerations (p<0.001, Cohen's f=2.5), angular accelerations (p<0.001, Cohen's f=2.2), and angular velocities (p<0.001, Cohen's f=5.6) (Table 4.19). The linear acceleration of the Hybrid III neck was 3.5% greater than neck 1 (p<0.001, Cohen's d=1.8), 4.0% greater than neck 2 (p<0.001, Cohen's d=3.0), and 11.2% greater than neck 3 (p<0.001, Cohen's d=9.1) (Table 4.19 and Table 4.20). The angular acceleration of the Hybrid III was 13.7% greater than neck 1 (p<0.001, Cohen's d=2.9), 14.2% greater than neck 2 (p<0.001, Cohen's d=3.4), and 22.5% greater than neck 3 (p<0.001, Cohen's d=5.6) (Table 4.19 and Table 4.20). The angular velocity of the Hybrid III was also greater than all three neck copies: 7.4% greater than neck 1 (p<0.001, Cohen's d=6.3), 9.3% greater than neck 2 (p<0.001, Cohen's d=10.4), and 18.5% greater than neck 3 (p<0.001, Cohen's d=13.7) (Table 4.19 and Table 4.20).

Table 4.20: Normalized absolute differences between the Hybrid III neck and the prototype surrogate necks during unhelmeted frontal impacts.

	Δa (%)	Δα (%)	Δω (%)
Hybrid III – Neck 1	3.5	13.7	7.4
Hybrid III – Neck 2	4.0	14.2	9.3
Hybrid III – Neck 3	11.2	22.5	18.5
Average	6.2	16.8	11.7

In Table 4.12, the normalized absolute differences between the three prototype surrogate necks are presented. Comparing the results of that table to Table 4.20, it is apparent that the normalized absolute differences between the Hybrid III neck and the prototype surrogate necks are larger than the differences between the three prototype surrogate necks. The average difference for the Hybrid III comparison to the prototype surrogate necks was 11.6%; in contrast, the average difference between the prototype surrogate necks was 6.1%. While the linear acceleration difference was only 1.1% greater when the neck types were compared, the angular acceleration and velocity were 11.0% and 4.4% greater for the Hybrid III comparison.

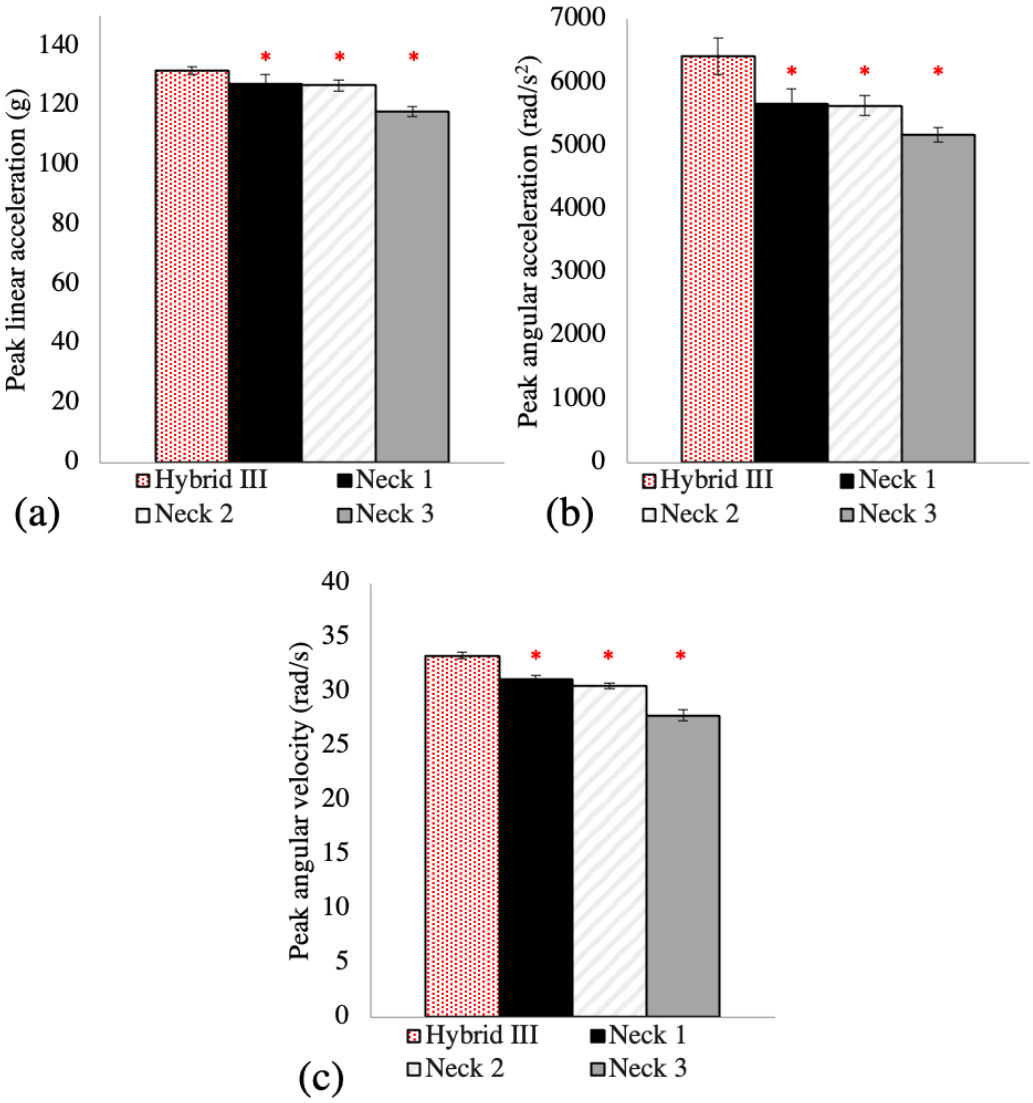

Figure 4.11: Means and standard deviations of the (a) peak linear accelerations, (b) peak angular accelerations, and (c) peak angular velocities of the Hybrid III neck and the three prototype surrogate necks for frontal impact to the unhelmeted Hybrid III head. Data from Figure 4.5 is replotted alongside the new Hybrid III data. A red asterisk denotes a significant difference from the Hybrid III neck ($p<0.05$).

Summary

While the statistical tests and normalized absolute differences suggest differences between the neck models for both head protection cases, the differences are more evident for the unprotected head impacts. There was no significant difference between the angular accelerations of the Hybrid III and the surrogate prototype models for the helmeted impacts, nor did the Hybrid III neck or neck 3 show any significant kinematic differences. In addition, the normalized absolute differences were greater between the three surrogate prototype necks (average of 11.0%) than the differences from the comparisons of the Hybrid III neck to the surrogate prototype necks (average of 8.2%) during helmeted impacts. In contrast, the Hybrid III comparisons resulted in greater differences than the neck differences between the prototype surrogate neck copies for the unhelmeted impacts. On average, the normalized absolute differences for the Hybrid III comparisons were 11.6%, whereas the differences between the prototype surrogate necks were 6.1%. Further, while the Hybrid III neck always resulted in peak kinematics larger than the prototype surrogate necks during unhelmeted impacts, the protected impacts do not have clear consistency; however, the Hybrid III does seem to have lesser peak values than two of the necks for all kinematics. In general, the Hybrid III neck and the prototype surrogate neck do not result in substantially different kinematics during helmeted impacts to the front of the head, but the unhelmeted impacts may lead to differing kinematics.

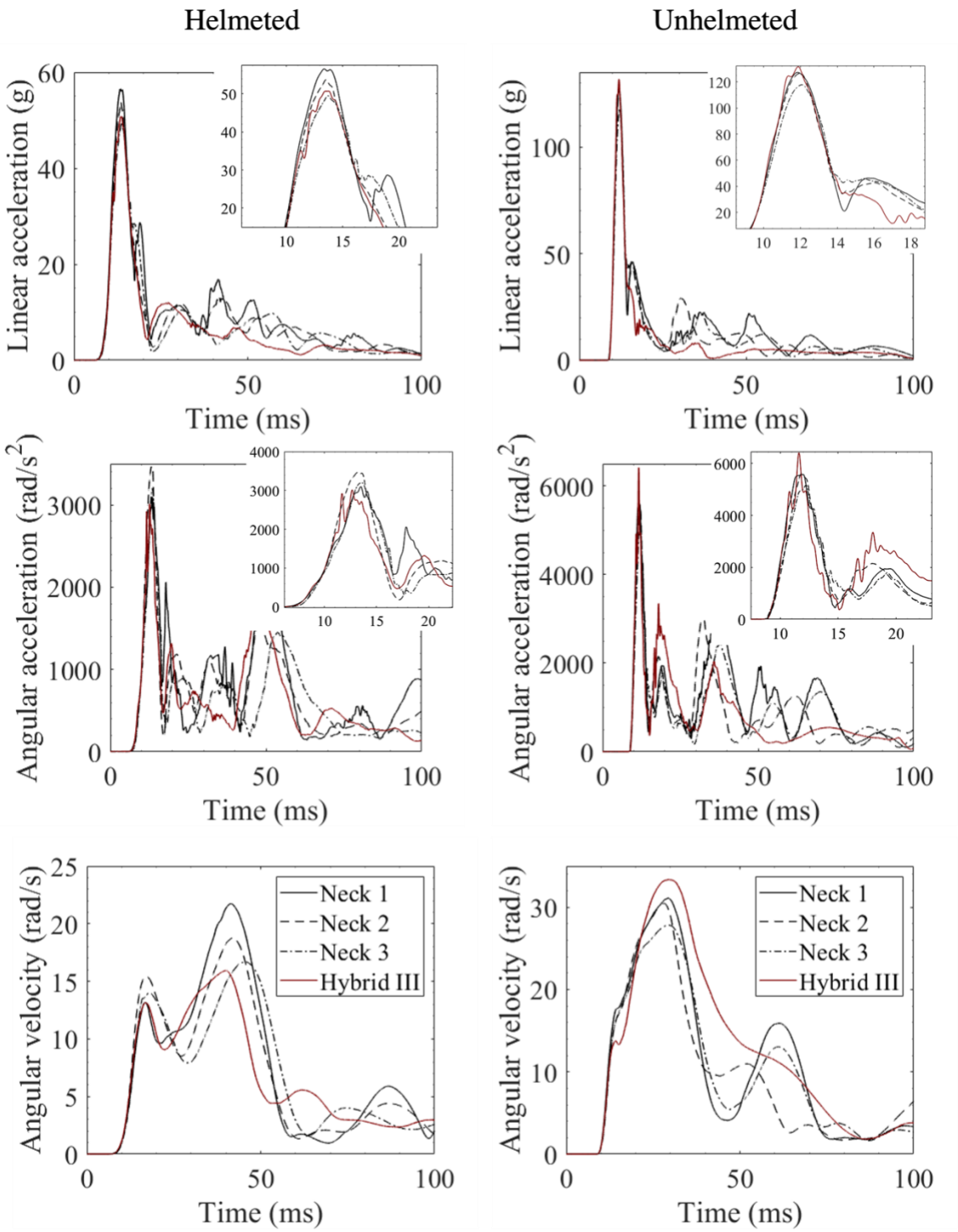

Figure 4.12: Ensemble averages of all three prototype surrogate necks and the Hybrid III neck during helmeted impacts (left column) and unhelmeted impacts (right column) to the front of the head. The graphs in the top-right corner of the linear acceleration and angular accelerations plots are close-ups of the peaks for all necks.

5 Discussion

5.1 Repeatability of prototype surrogate necks

5.1.1 Within-neck repeatability

Compared to current regulatory guidelines and existing surrogate models, the prototype surrogate neck displays acceptable repeatability for direct head impacts applied to the front and front boss of an unprotected and protected Hybrid III head.

The CV_W values for all head kinematics are less than or equal to 10%, which is acceptable for surrogate models [21–23,43–45,115,120]. For impacts to the protected head, the variance was 9% or less (average of 4.8%); impacts to the unprotected head had variances of 6% or less (average of 2.2%). The use of a helmet did increase the variance, but the additive variance did not lead to unacceptable repeatability of the model. The overall CV_W was defined using the average mean and pooled standard deviation of all three necks for the overall prototype surrogate neck response. The overall CV_W of linear acceleration for helmeted impacts at both impact locations impacts was 3% or less, less than 8% for angular acceleration, and less than 6% for angular velocity. The unhelmeted necks' linear and angular acceleration overall CV_W values were less than 2%, and the angular velocity was less than 5%. Thus, the prototype surrogate neck can be classified as having acceptable repeatability of less than 8% for all head kinematics for frontal and front boss impacts, with greater repeatability displayed during unhelmeted impacts.

The repeatability of the current prototype surrogate neck is similar to the previous iteration, which is expected since the neck changes were minor; however, both iterations are improvements over the initial neck prototype. The first neck model had multiple linear and angular acceleration measures that exhibited unacceptable CV_W values greater than 10% [52]. The second neck model generally had CV_W values of 10% or less with only a few linear and angular acceleration measures resulting in values greater than 10% [53]. In contrast, the current prototype surrogate neck did not exhibit any unacceptable repeatability measures. While the neck itself is considered an improvement over the previous model since it addressed its limitations, the differences between the repeatability of the current prototype and the previous iteration may be due to the change in

experimental equipment. Unlike the manual raising of the pendulum impactor, which was credited with potentially causing outlier responses in the previous model [53], this thesis implemented an automated pendulum raise and release process as suggested by MacGillivray, which likely decreased impact location variation. The impact locations were also different, and the facemask location may have led to greater variances.

The repeatability of the peak linear accelerations of other commercially available surrogate head and neck models has previously been assessed using drop tests, sled tests, pendulum deceleration tests, and direct head impacts. Although the tests used in previous studies are not directly comparable to the experiments presented in this thesis, the CV_W values from these studies can be compared to the CV_W values of the prototype surrogate neck to examine general trends. In addition, although the exact impact locations (i.e. side of the head vs laterally near the front boss) may lead to slightly different loading scenarios, conservative comparisons can be made to the repeatability of standard surrogate models. As described in the following paragraphs, impacts to the front and front boss of the prototype surrogate neck resulted in CV_W values similar to available standardized models.

The repeatability of the resultant peak head kinematics from the prototype surrogate neck subject to front-boss impacts was similar to that of commercially available necks tested in lateral impacts. Pendulum impact tests to the oblique and side of the unhelmeted Hybrid III head attached to a Hybrid III neck resulted in CV_W values of 4.5% and 3.6% for the linear accelerations and 4.7% and 5.5% for the angular velocities [136]. Lateral pendulum impacts to the unhelmeted EuroSID-1 head-neck assembly produced CV_W values of 3.0-7.2% for the linear acceleration, depending on the direction measured and the laboratory [117]. Lateral head drop tests were also conducted on several ES-2 and ES-2re models. The CV_W values for the linear acceleration of the ES-2 models were calculated to be 2.8% and 3.9% (overall CV_W of 3.4%) [45]. A test on another ES-2 head reported a CV_W of 2.4%. For the ES-2re models, the CV_W values ranged 1.1-4.5%, with an overall CV_W of 3.2% [45,115]. Lateral sled tests were also conducted on the ES-2, ES-2re, and WorldSID ATDs. The CV_W of the resultant linear head accelerations for the ES-2 was 2.5% [141] and for the WorldSID was 6.3% [119]. In comparison, lateral impacts near the front boss of the Hybrid III head attached to the unhelmeted prototype surrogate resulted in overall CV_W values of 1.4% for

the linear acceleration and 1.3% for the angular velocity. Thus, the CV_W values of the head kinematics of the prototype surrogate neck during unhelmeted front boss impacts were generally smaller than the values reported for other surrogate models.

The repeatability of head kinematics during unhelmeted frontal impacts of the prototype surrogate neck was also comparable to commercially available models. When eight unhelmeted part 572 50th percentile male head-neck assemblies (used in the SID) were subject to indirect pendulum tests, the overall CV_W value was 2.8% for the linear acceleration [116]. Further, repeated direct pendulum impacts to an unhelmeted Hybrid III headform attached to the Hybrid III neck on a seated full-body model resulted in CV_W values of 3.9% for linear acceleration and 4.8% for angular velocity [136]. For the ES-2re in frontal sled tests, the CV_W values were 1.0% and 2.4% for different impact conditions; rear impacts led to CV_W values of 1.8% and 7.5% [45]. The overall CV_W of the prototype surrogate neck's linear acceleration and angular velocity during unhelmeted frontal impacts were 1.8% and 1.3%, respectively, which are less than the values determined for the SID and Hybrid III necks.

There are limited repeatability assessments using helmeted head-neck assemblies. However, one study by Cobb et al. used a pendulum impactor with a mass of 15.5 kg to impact a helmeted head-neck assembly atop a linear slider table at a speed of 3.1 m/s, which is comparable to the parameters used in this thesis [38]. Repeated impacts onto the front of the helmeted Hybrid III head-neck assembly resulted in CV_W values of approximately 0.6% for the linear accelerations and 6.5% for the angular accelerations [38]. Impacts to the side of the head resulted in CV_W values of 5.6% for the linear accelerations and 3.0% for the angular accelerations. In comparison, the overall CV_W values for helmeted impacts onto the surrogate prototype head-neck assembly in frontal impacts were 1.7% for the linear acceleration and 7.8% for the angular acceleration. In impacts to the front boss, the values were 3.3% and 6.7%, respectively. The CV_W values for helmeted impacts were slightly greater for the prototype surrogate neck but were generally similar to the Hybrid III.

5.1.2 Between-neck repeatability (Reproducibility)

In general, the ANOVA found significant differences between the kinematics of the three prototype surrogate necks, especially in the helmeted impacts. Front boss impacts to the helmeted head resulted in significant differences in nearly all kinematics, with only the linear accelerations between two of the necks not showing significant differences; in contrast, the angular accelerations during unhelmeted impacts were not significantly different between any of the necks, nor was the angular velocity between two of the necks. For frontal impacts, impacts to the protected head resulted in significant differences between the peak linear accelerations and peak angular velocities for all necks and the angular accelerations between two necks. Unprotected frontal impacts resulted in significant differences between the peak angular velocities of all necks. In addition, peak linear acceleration and peak angular acceleration of one of the necks (neck 3) was significantly different from the other two necks. As mentioned previously, the low variance within groups (i.e. low CV_W values) may be in part responsible for the significant differences between necks. This rationale was also suggested for the part 572 50^{th} percentile male neck reproducibility, wherein statistical significance was determined for the linear acceleration between neck models, but the within-neck variance was small [116]. Further, no evidence suggested one neck was responsible for the significant results (i.e. one of the necks was substantially different from the other two).

The normalized absolute differences between the prototype surrogate necks during unhelmeted impacts were 11% or less for all kinematics measured at both impact locations and were 20% or less for all helmeted impacts except one (the angular velocity differences between necks 1 and 3 for front boss helmeted impacts). Current surrogate head and neck certifications have suggested acceptable ranges of 20-40% on peak kinematics, with most allowing a range of approximately 20% of the mean [41,43,45,47,112,113,115,121]. Perhaps most comparable to the present work is the forehead and facial impacts conducted on the seated THOR [121]. The THOR impacts include the head, neck, and whole body, which can be approximated by the linear rail, and led to peak head resultant accelerations comparable to the unhelmeted results in the present work. The ranges on the resultant linear accelerations and angular velocities from both impact scenarios for the THOR allowed a deviation of approximately 20% of the mean.

It should be noted that the acceptable ranges in the literature are estimated based on certification ranges provided for existing models during unhelmeted impacts, which usually involve acceptable corridors ranging from 105-275 g and 21-40 rad/s. While this is comparable to the unhelmeted neck impacts in this thesis (118-154 g and 27-31 rad/s), helmeted impacts had lower kinematics (32 - 57 g and 17 - 22 rad/s). The certification ranges may not adequately represent acceptable ranges for lower severity impacts.

A comparison to existing literature was also conducted using the normalized absolute differences. Multiple replicates of existing surrogate models have been assessed under identical test parameters to determine the reproducibility of the linear accelerations. Thus, the normalized absolute differences could be calculated from each model's means and standard deviations. This data is not directly comparable to the experiments conducted in this thesis, as drop tests did not incorporate a neck and thus assessed differences in kinematics between different head models. Further, sled tests, which did incorporate the neck, did not conduct direct head impacts. However, this assessment does provide guidelines to which the kinematics between the prototype surrogate necks can reasonably vary.

Normalized absolute differences of 3.5-11.1% (average of 7.4%) were calculated between the peak linear head accelerations of three Hybrid III heads during frontal drop tests [41]. For part 572 head drop tests, the normalized absolute difference ranged from 0.1-12.6% for the resultant head acceleration in frontal impacts (average of 4.0%). For the sled tests, the differences were 0.1-4.0% (average of 1.9%). Comparatively, the normalized absolute differences between the linear accelerations of the prototype surrogate necks during frontal unhelmeted impacts ranged from 0.6%-7.7%, with an average of 5.1%. Thus, the differences between the three prototype surrogate necks were comparable to the differences between multiple copies of other surrogate models in frontal loading scenarios.

The linear accelerations of the prototype surrogate necks during front boss impacts between models of the prototype surrogate were generally less than what has been calculated for current standard lateral ATDs, although the data is limited. The linear accelerations of ES-2re heads subject to lateral drop tests differed by 10.1% for one pair but only 0.8% for another [45]. Two

ES-2 heads also tested in lateral drop tests differed by 12.7% [43]. For unhelmeted front boss impacts, the linear accelerations between the prototype surrogate necks ranged from 1.8-6.3%, describing between-model differences generally less than the ES-2(re) models. Overall, the average normalized absolute differences of all kinematics in all impact conditions were comparable to the normalized absolute differences from available data on current surrogate models.

Finally, using the reproducibility coefficient of variation (CV_B), the prototype surrogate neck's resultant head kinematics were found to have acceptable reproducibility. While most researchers have recommended a CV_B value of 10% represents the limit of acceptable reproducibility [21,44,115,120], a higher threshold of 15% has been suggested as well [45]. Unhelmeted impacts had CV_B values of 5% or less for all kinematics for frontal and front boss impacts. Helmeted impacts had slightly greater variance between neck models, but all were less than 12% (all except the helmeted frontal impacts were 10% or less).

The CV_B values for the linear accelerations of the prototype surrogate neck also fell in line with existing surrogate model reproducibility. The CV_B value for linear accelerations of multiple part 572 necks during pendulum and sled tests was calculated to be 4.3% and 1.5%, respectively [116]. In addition, the ES-2re head reproducibility was also assessed using lateral drop tests, wherein the CV_B for the linear acceleration was 5.4%. Finally, the Hybrid III reproducibility in drop tests was estimated to be 5.7% [41]. The reproducibility of the prototype surrogate in unhelmeted frontal ($CV_B = 4.0\%$) and unhelmeted front boss impacts ($CV_B = 3.0\%$) is similar to the reproducibility of existing surrogate head and neck models. However, the available data is limited.

5.2 Comparison to Hybrid III neck

In general, the within-neck repeatability of the Hybrid III neck was commensurate with the repeatability of the prototype surrogate neck, with all except one case defined as acceptable as per current requirements. As with the prototype surrogate necks, the calculated CV_W values are smaller for the unhelmeted impacts (average of 1.9%) than for the helmeted impacts (average of 7.3%). In general, CV_W values for both the Hybrid III and prototype surrogate necks' linear accelerations and angular velocities fell below 6%. In both the Hybrid III and the prototype surrogate neck, the

angular acceleration variation was greater; however, the Hybrid III had an unacceptable CV_W value. The reason why the unhelmeted angular acceleration of the Hybrid III had CV_W values greater than 10% is unclear. Examination of the data showed no outliers that could explain the variance. Similar impact tests conducted on the Hybrid III head-neck assembly equipped with a Riddell football helmet calculated the CV_W values of the angular acceleration to be 3.0% for the side impacts (as compared to 10.0% for the front boss impacts in this work) and 6.5% for frontal impacts (as compared to the 17.8% found in this work) [38]. Thus, the high variation in this study is not replicated in the limited literature on the helmeted Hybrid III neck; however, the helmets used were different and may act differently during impacts. The higher variance in the angular accelerations of the helmeted impacts may be due to the additive variance due to the helmet described as a limitation below (Section 5.3.2). More research is required to analyze the repeatability of the angular kinematics of the Hybrid III neck.

General trends suggest that when the head is not protected, the Hybrid III neck and the prototype surrogate necks lead to differing kinematics; however, when the head is helmeted, the variance increases, and it is less clear if the kinematics substantially differ. Post-hoc statistical results suggest that the Hybrid III kinematics differ from all three prototype surrogate neck copies for unprotected impacts, for both front boss and frontal impacts. In contrast, the helmeted impacts more often resulted in similar kinematics between neck models. Impacts to the front boss resulted in Hybrid III peak linear and angular velocities that significantly differed from all three surrogate necks, but the angular acceleration differed from just one of the necks. For frontal impacts, the Hybrid III peak linear acceleration and peak angular velocity only significantly differed from two of the necks, and none of the angular accelerations differed between neck models. The use of helmets may have affected the results of the ANOVA in that the additional variance could have made it more challenging to ascertain differences between mean kinematics of the neck types.

The normalized absolute differences between the three prototype surrogate necks were always smaller than the differences between the Hybrid III neck and the prototype surrogate neck during unhelmeted impacts. The kinematics differed by an average of 14.2% between the Hybrid III and the prototype surrogate neck during unhelmeted front boss impacts, whereas normalized absolute differences between the three copies of the prototype surrogate neck averaged at 3.0%. Similarly,

the differences were 11.6% and 6.1% for the frontal unhelmeted impacts, respectively. In contrast, the helmeted front boss impacts led to kinematics that differed by an average of 11.1% between the Hybrid III and the prototype surrogate neck, whereas differences between copies of the prototype surrogate neck were 9.2%. The Hybrid III and surrogate prototype neck differences were lower (8.2%) than the surrogate prototype necks (11.0%) for the helmeted frontal impacts. Overall, although the differences were sometimes minimal, the normalized absolute differences between the Hybrid III and the prototype surrogate neck were generally greater than those between copies of the prototype surrogate neck, except for the helmeted frontal impacts.

Since the normalized absolute differences of the prototype surrogate neck were compared to certification ranges for current surrogate model head kinematics, the normalized absolute differences between the Hybrid III and prototype surrogate neck were also compared in this way. As mentioned previously, the Hybrid III certification allows a range of ~20% of 235g (225-275 g) [41,47]. The normalized absolute differences between the Hybrid III and prototype surrogate neck kinematics were less than 20% for most cases, which falls within the above range. As such, the difference between the Hybrid III neck and prototype surrogate neck often fell within the certification range provided for a single model. This suggests that using the prototype surrogate neck would not produce different kinematics from repeated tests with multiple Hybrid III models. Based on this analysis, the prototype surrogate neck would not give results that significantly differ from the Hybrid III. However, as explained before, the peak linear accelerations in the Hybrid III certifications are larger than the peaks reported in this thesis. The normalized absolute differences between different neck models may require a more standardized allowable range, which could be determined with future large-scale experimentation using multiple neck models.

The most conclusive result drawn from the Hybrid III comparison to the prototype surrogate neck is that the Hybrid III neck almost always had kinematics that were consistently greater than or less than all three of the surrogate necks, especially for the unhelmeted impacts. To provide context, Figure 4.8 shows that the peak linear acceleration and angular acceleration of the Hybrid III are always greater than the prototype surrogate necks, and the peak angular velocity is always smaller than the prototype surrogate necks. For front boss impacts, the peak angular velocity of the Hybrid III was always less than the prototype surrogate necks for both protected and unprotected head

impacts. The peak linear acceleration of the Hybrid III was less than all the prototype surrogate necks for the helmeted impacts, while the peak angular acceleration was less than two of the necks. The unhelmeted impacts to the front boss resulted in Hybrid III peak linear and angular accelerations that were always greater than all three of the prototype surrogate necks. For frontal impacts, the kinematics of the unprotected head impacts were consistently greater for the Hybrid III. The helmeted impacts led to Hybrid III accelerations that were less than two of the necks for the, and an angular velocity less than all of the necks.

Thus, although the mean differences between the Hybrid III and the prototype surrogate neck kinematics were sometimes statistically insignificant or led to small normalized absolute differences, the signs on the kinematics allow general differences between the neck models to be observed. As such, the necks would produce differing kinematics in sports biomechanics research. For example, when tested in the same loading scenario, the prototype surrogate neck could result in higher kinematics, suggesting a higher injury risk or less effective helmet protection than calculated with the Hybrid III. This is important because it strengthens the argument for the development of a prototype surrogate neck optimized for multi-directional loading scenarios, and thus substantiates the continuation of this research. As mentioned, the Hybrid III neck is commonly used in sports biomechanics research even though it was only originally developed for indirect frontal loading in sled tests. This work was shown that in other impact conditions (i.e. front boss impacts to the helmeted head and unhelmeted impacts to both impact locations), the Hybrid III neck produces kinematics that differ from the novel surrogate neck. Thus, it is important to continue the development of neck models that are reliable in measuring head kinematics for several different loading scenarios.

5.3 Research Limitations and Future Directions

5.3.1 Neck Design and Manufacturing

Although durability was not a primary objective of this thesis, the neck was examined after completing experiments. A superficial visual inspection of the neck components indicated no obvious breakage or failure of the internal column, aluminum plates, or silicon. However, it was noted that the nuts compressing the springs had loosened. Although the kinematics appear to be

consistent over repeated impacts, the loosening of the springs may have negatively affected the reported repeatability (both within- and between-neck). It is recommended that future iterations of the surrogate neck implement a thread locker to prevent the loosening of the nuts and improve the repeatability of the design.

As mentioned in Chapter 3, each neck required an individual container of Dragon Skin© silicon. It is possible that the properties of the silicon were slightly different in each container. This parameter cannot be controlled entirely since the intrinsic properties of the silicon will be apparent in different batches of material. However, for reproducibility assessments, the design process could be standardized to quantify how much the silicon affects the reproducibility. A larger container of the silicon could be used to make all copies of the neck, such that the silicon has similar properties in all copies. In addition, since the silicone was poured on different days, environmental changes could have affected the degassing and curing processes. Multiple 3D neck moulds could be manufactured to build the necks simultaneously.

5.3.2 Additive variance of helmets

The unhelmeted impacts resulted in more repeatable and reproducible kinematics than helmeted ones. While unhelmeted conditions allow for a direct assessment of the neck repeatability without protective devices, it is still essential to analyze the performance characteristics of the helmeted head since potential applications of this neck include helmet certifications and laboratory reconstructions of sports impacts. Helmets appeared to contribute additively to the head-neck assembly variance in direct head impact experiments. While helmeted impacts resulted in acceptable repeatability in all kinematics, the added variance may have affected the between-neck assessments (both the reproducibility and the comparison to Hybrid III) since the added variance may have affected the results of the ANOVA. In addition, for the surrogate prototype necks, the linear acceleration resulted in the lowest CV_W values during helmeted impacts, whereas the angular velocities were smallest during the unhelmeted impacts. The increased CV_W values for the angular kinematics during helmeted impacts could be attributed to the variable movement of the helmet on the head during impacts, leading to slightly different measured angular kinematics at the head centre of gravity during helmeted impacts. Although care was taken to ensure the helmet placement was consistent using visual markers on the Hybrid III headform, the helmet had to be re-aligned

after every impact due to slight shifting. A helmet positioning procedure could be used in the future to ensure consistent helmet fit and impact location [34].

5.3.3 Analysis Methods

Sample Size Estimates

The power of an ANOVA is affected by the sample size – low sample sizes can lead to underpowered analyses. While *a priori* power analyses are often conducted prior to experimentation to ensure studies are sufficiently powered, no preliminary data were available for this to be done for the current study. Thus, *post hoc* sensitivity power analyses were conducted instead, which suggested the tests did have sufficient power to provide reasonable results.

To further strengthen the sample size estimations, the methods to assess the repeatability and reproducibility of other surrogate models were examined. The Hybrid III was tested in sled and drop tests wherein three surrogate heads and necks were subject to at least two tests each [41]. Six repeated impacts onto the Hybrid III head-neck were also conducted to assess repeatability [136]. The THOR performance specifications were determined by testing three different models five times each, with two additional models tested at other laboratories [121]. In a repeatability assessment on part 572 ATDs, eight necks were subjected to at least six impacts [116]. Two different labs conducted twenty impact tests on two EuroSID-1 models to assess repeatability and reproducibility [117]. The ES-2 and ES-re heads were impacted eight times [45] and up to nine times [45,115], respectively. Finally, for the WorldSID and ES-2 sled tests, the necks were tested 3-6 times, with most tests using three repeats [44,119,120,141]. Thus, using three replicates with a sample size of $n \geq 10$ in this work is comparable to what has been used in other studies.

ANOVA

The ANOVA was applied as one method to explore the data objectively. Although the violations to the ANOVA assumptions were addressed, they still exist. Even so, the mean differences between necks were not substantially affected by the outliers, suggesting the presence of outliers did not affect the results. The normality of the data was also usually achieved by removing the outliers. Along with the general robustness of ANOVAs to violations in normality [157,158], this suggests the results are not affected by the underlying distributions.

Furthermore, other methods used to assess neck reproducibility did not rely on the underlying assumptions. The normalized absolute differences only depended on the mean kinematics and suggested the neck offers reproducibility that aligns with prevailing norms in impact assessment. In addition, the CVs only require the standard deviations and averages of the kinematics and are not subject to the same assumptions as the ANOVA.

Effect Sizes

Most significant relationships determined via the ANOVA were defined as having large effects (Cohen's $f > 0.4$ and Cohen's $d > 0.8$), which would suggest the results of the ANOVA are meaningful (i.e. the kinematics between necks were truly substantially different). However, the effect size guidelines are only suggestions for when effect size estimates in a specific field are unknown [161]. Thus, the proposed effect sizes may not adequately represent small, medium, or large effect sizes necessary for impact experiment assessments. It may be more relevant to directly compare the effect sizes between the reproducibility assessment of the three prototype surrogate necks and the comparison of the prototype surrogate and the Hybrid III, to examine whether the differences between the neck models are larger than the difference between copies of the neck. The Cohen's d for the prototype surrogate neck differences ranged from 0.13 – 7.73 (mean of 2.65), whereas the average for the Hybrid III comparison ranged from 0.05 – 24.29 (mean of 5.09). On average, the effect sizes were larger when comparing the prototype surrogate neck to the Hybrid III neck than for the differences between prototype surrogate necks. Thus, although the results of the ANOVA were significant with large effects, the effect sizes were greater between the Hybrid III and the prototype surrogate than between the three prototype surrogate necks.

5.3.4 Future Recommendations

As mentioned above, one design refinement to improve the repeatability and reproducibility of the model is to implement a thread locker to the base of the springs to ensure consistent compression during all impacts. A helmet positioning tool can also ensure consistent helmet fit during repeated impacts.

Different impact parameters should be tested to expand the analysis of the repeatability and reproducibility of the prototype surrogate neck. The neck should be tested in other impact locations

common in accident reconstructions and helmet certifications, such as impacts to the rear and top of the head. Other helmets could be used to expand the capabilities of the neck to multiple applications as well. The neck should also be assessed in indirect loading scenarios, which can be done by conducting sled tests or experiments similar to the CFR pendulum tests. This will allow the omni-directionally and the sensitivity of the neck to a multitude of different impact scenarios to be further assessed. Further, different personnel or laboratories could develop multiple versions of the neck to assess reproducibility in this way.

The above assessments can be conducted with the Hybrid III neck or other neck models to further explore the differences between neck types. Continued research on differences between the surrogate prototype neck and the Hybrid III neck is highly suggested, as this work only encompasses a small subsection of potential research applications. As discussed, the helmet may have obscured differences between the Hybrid III neck and the prototype surrogate neck. A potential way to discern more meaningful differences between neck types is to conduct higher severity impacts. Previous research has suggested that lower impact energies lead to greater variability within-neck models [116,136]; thus, increasing severity may result in less variability and allow greater differences to be deduced between necks. Further, to determine acceptable percent differences between the Hybrid III neck and the prototype surrogate neck, it may be beneficial to compare the normalized absolute differences of different commercially available necks. This will provide a guideline for how similar the kinematics can be between different neck models.

It is also suggested that future studies that compare the prototype surrogate neck model to other necks models should include multiple copies of each neck. As discussed, current certifications for head kinematics allow a range of 20%. Thus, the kinematics can vary quite substantially while still being acceptable. This could mean that, for example, the kinematics obtained for only one Hybrid III neck may not represent the average overall mechanics of the Hybrid III. Using multiple neck models will allow for a more general conclusion on the kinematics of the necks to be made, such that comparisons between necks may be more accurate.

6 Conclusion

6.1 Summary

The overarching goal of the prototype surrogate neck is to be the first model developed for omni-directional direct head impacts, as current commercially available surrogate necks are typically only validated for indirect motion along a single plane. As such, the prototype surrogate neck describes a model that is likely better suited for use in research that involves multiplane loading in direct head impacts, such as assessing the impact severity in sports impacts to infer risk of brain injury. A critical stage for any surrogate model developed for impact biomechanics applications is to satisfy specific design requirements. The model must provide reliable results, regardless of where the experiment is conducted or who manufactured the model. As such, the objective of this thesis was to examine the repeatability and reproducibility of the resultant head kinematics of the protected and unprotected Hybrid III head when attached to the prototype surrogate model and directly impacted on the forehead and front boss. This thesis provided a cohesive overview of the repeatability of the head kinematics to various impact parameters common in sports scenarios, thus strengthening the neck's practicality for use in sports biomechanics research. Comparisons to the Hybrid III neck were also conducted since the Hybrid III is the neck model most often used in sports injury biomechanics and helmet assessments. The results suggesting that the Hybrid III and prototype surrogate neck kinematics differ in certain loading scenarios also emphasize the importance of developing and continuing to test the capabilities of the novel surrogate neck model in representing human responses to alternate loading scenarios, such as those seen in sports impacts.

The main results of this thesis were:

1) The neck exhibited repeatability and reproducibility that met current requirements for standardized ATDs, and;
2) The neck produced head kinematics that were different from the Hybrid III neck for unhelmeted impacts, while the variances between necks were comparable, but further testing is needed to draw stronger conclusions.

6.2 Significance and Contributions

Standardized models often used in sports injury assessment, like the Hybrid III, were not designed for direct, multiplane loading often seen in sports. As such, the repeatability and reproducibility of the head kinematics of most standardized surrogate models have only been assessed through uni-directional indirect head impacts or drop tests without a neck. To the author's knowledge, the Hybrid III neck is the only neck that evaluated the repeatability of kinematics during direct impacts onto the head-neck assembly. The reproducibility of head kinematics during impacts to a head-neck assembly were not assessed for any of the neck models. Since the neck is thought to govern head kinematics, direct head impacts to the head-neck assembly are often used in sports applications; thus, the repeatability and reproducibility of the head-neck assembly should be assessed during direct head impacts. The prototype surrogate neck is the only model with acceptable repeatability and reproducibility of the resultant head kinematics during direct head impacts involving a surrogate head-neck assembly.

Further, only the repeatability and reproducibility of the linear acceleration have been measured for most commercially available surrogate models. Only the Hybrid III neck directly assessed the repeatability of the resultant angular accelerations, but the reproducibility was not evaluated. This is concerning, as the rotational motions are thought to correlate to brain injury (Section 2.1.2); thus, the repeatability and reproducibility of these angular metrics should be assessed to ensure each model can be used to ascertain injury risk, especially for use in helmet certifications and sports reconstructions. The novel prototype surrogate neck is the only model tested to confirm acceptable repeatability and reproducibility of rotational kinematics. It is thus arguably the best neck for biomechanical testing that employs rotational kinematics.

Finally, the signs on the kinematics for the Hybrid III neck were almost always systematically different from the prototype surrogate neck. Using the prototype surrogate neck in the place of the Hybrid III neck in laboratory reconstructions could lead to an injury risk inference that is substantially different between models. In addition, the prototype surrogate neck used in helmet certification studies could suggest that the reduction in kinematics is lesser than what is determined when the Hybrid III is used.

References

[1] Dewan, M. C., Rattani, A., Gupta, S., Baticulon, R. E., Hung, Y.-C., Punchak, M., Agrawal, A., Adeleye, A. O., Shrime, M. G., Rubiano, A. M., Rosenfeld, J. V., and Park, K. B., 2018, "Estimating the Global Incidence of Traumatic Brain Injury," Journal of Neurosurgery, **130**(4), pp. 1080–1097.

[2] Gordon, K. E., and Kuhle, S., 2018, "'Reported Concussion' Time Trends within Two National Health Surveys over Two Decades," Brain Injury, **32**(7), pp. 843–849.

[3] Rao, D. P., McFaull, S., Thompson, W., and Jayaraman, G. C., 2017, "Trends in Self-Reported Traumatic Brain Injury among Canadians, 2005-2014: A Repeated Cross-Sectional Analysis," cmajo, **5**(2), pp. E301–E307.

[4] Government of Canada, S. C., 2021, "Population Estimates on July 1st, by Age and Sex" [Online]. Available: https://www150.statcan.gc.ca/t1/tbl1/en/tv.action?pid=1710000501. [Accessed: 15-Nov-2021].

[5] Fu, T. S., Jing, R., McFaull, S. R., and Cusimano, M. D., 2016, "Health & Economic Burden of Traumatic Brain Injury in the Emergency Department," Canadian Journal of Neurological Sciences, **43**(2), pp. 238–247.

[6] Canada, P. H. A. of, 2020, "Injury in Review, 2020 Edition: Spotlight on Traumatic Brain Injuries across the Life Course" [Online]. Available: https://www.canada.ca/en/public-health/services/injury-prevention/canadian-hospitals-injury-reporting-prevention-program/injury-reports/2020-spotlight-traumatic-brain-injuries-life-course.html. [Accessed: 07-Oct-2021].

[7] Centers for Disease Control and Prevention, 2015, *Report to Congress on Traumatic Brain Injury in the United States: Epidemiology and Rehabilitation*, National Center for Injury Prevention and Control; Division of Unintentional Injury Prevention, Atlanta, GA.

[8] Kay, T., Harrington, D. E., Adams, R., Anderson, T., Berrol, S., Cicerone, K., Dahlberg, C., Gerber, D., Goka, R., Harley, P., Hilt, J., Horn, L., Lehmkuhl, D., and Malec, J., 1993, "Definition of Mild Traumatic Brain Injury," Journal of Head Trauma Rehabilitation, **8**(3), pp. 86–87.

[9] McCrory, P., Meeuwisse, W., Dvorak, J., Aubry, M., Bailes, J., Broglio, S., Cantu, R. C., Cassidy, D., Echemendia, R. J., Castellani, R. J., Davis, G. A., Ellenbogen, R., Emery, C., Engebretsen, L., Feddermann-Demont, N., Giza, C. C., Guskiewicz, K. M., Herring, S., Iverson, G. L., Johnston, K. M., Kissick, J., Kutcher, J., Leddy, J. J., Maddocks, D., Makdissi, M., Manley, G. T., McCrea, M., Meehan, W. P., Nagahiro, S., Patricios, J., Putukian, M., Schneider, K. J., Sills, A., Tator, C. H., Turner, M., and Vos, P. E., 2017, "Consensus Statement on Concussion in Sport—the 5th International Conference on Concussion in Sport Held in Berlin, October 2016," Br J Sports Med, **51**(11), pp. 838–847.

[10] Gordon, K. E., and Kuhle, S., 2018, "Validation of 'Reported Concussion' within a National Health Survey," Brain Injury, **32**(1), pp. 41–48.

[11] Government of Canada, 2018, "Sport and Recreation-Related Concussions and Other Traumatic Brain Injuries Among Canada's Children and Youth" [Online]. Available: https://health-infobase.canada.ca/datalab/head-injury-interactive.html. [Accessed: 09-Nov-2021].

[12] Mainwaring, L., Ferdinand Pennock, K. M., Mylabathula, S., and Alavie, B. Z., 2018, "Subconcussive Head Impacts in Sport: A Systematic Review of the Evidence," International Journal of Psychophysiology, **132**, pp. 39–54.

[13] Bailes, J. E., Petraglia, A. L., Omalu, B. I., Nauman, E., and Talavage, T., 2013, "Role of Subconcussion in Repetitive Mild Traumatic Brain Injury: A Review," Journal of Neurosurgery, **119**(5), pp. 1235–1245.
[14] Huber, B. R., Alosco, M. L., Stein, T. D., and McKee, A. C., 2016, "Potential Long-Term Consequences of Concussive and Subconcussive Injury," Physical Medicine and Rehabilitation Clinics of North America, **27**(2), pp. 503–511.
[15] Montenigro, P. H., Alosco, M. L., Martin, B. M., Daneshvar, D. H., Mez, J., Chaisson, C. E., Nowinski, C. J., Au, R., McKee, A. C., Cantu, R. C., McClean, M. D., Stern, R. A., and Tripodis, Y., 2017, "Cumulative Head Impact Exposure Predicts Later-Life Depression, Apathy, Executive Dysfunction, and Cognitive Impairment in Former High School and College Football Players," J. Neurotrauma, **34**(2), pp. 328–340.
[16] Corbin-Berrigan, L.-A., Wagnac, É., Vinet, S.-A., Charlebois-Plante, C., Guay, S., and Beaumont, L. D., 2021, "Head Impacts in Canadian Varsity Football: An Exploratory Study," Concussion, **6**(3), p. CNC93.
[17] Muise, D. P., MacKenzie, S. J., and Sutherland, T. M., 2016, "Frequency and Magnitude of Head Accelerations in a Canadian Interuniversity Sport Football Team's Training Camp and Season," International Journal of Athletic Therapy and Training, **21**(5), pp. 36–41.
[18] Breedlove, K. M., Breedlove, E. L., Robinson, M., Poole, V. N., King, J. R., Rosenberger, P., Rasmussen, M., Talavage, T. M., Leverenz, L. J., and Nauman, E. A., 2014, "Detecting Neurocognitive and Neurophysiological Changes as a Result of Subconcussive Blows Among High School Football Athletes," Athletic Training & Sports Health Care, **6**(3), pp. 119–127.
[19] Nauman, E. A., Breedlove, K. M., Breedlove, E. L., Talavage, T. M., Robinson, M. E., and Leverenz, L. J., 2015, "Post-Season Neurophysiological Deficits Assessed by ImPACT and FMRI in Athletes Competing in American Football," Dev Neuropsychol, **40**(2), pp. 85–91.
[20] Crandall, J. R., Bose, D., Forman, J., Untaroiu, C. D., Arregui-Dalmases, C., Shaw, C. G., and Kerrigan, J. R., 2011, "Human Surrogates for Injury Biomechanics Research," Clin Anat, **24**(3), pp. 362–371.
[21] Rhule, D., Rhule, H., and Donnelly, B., 2005, "The Process of Evaluation and Documentation of Crash Test Dummies for Part 572 of the Code of Federal Regulations."
[22] Advisory Group for Aerospace Research and Development, 1996, *Anthropomorphic Dummies for Crash and Escape System Testing (Mannequins Anthropometriques Utilises Lors Des Tests D'Impact Et D'Ejection).*, Defense Technical Information Center.
[23] Melvin, J. W., 1988, *Review of Dummy Design and Use. Task D Final Report*.
[24] Kai-Uwe Schmitt, Peter F. Niederer, Markus H. Muser, and Felix Walz, 2014, "Method in Trauma Biomechanics," *Trauma Biomechanics: Accidental Injury in Traffic and Sports*, Springer-Verlag Berlin Heidelberg, pp. 63–93.
[25] Withnall, C., Shewchenko, N., Gittens, R., and Dvorak, J., 2005, "Biomechanical Investigation of Head Impacts in Football," British Journal of Sports Medicine, **39**(suppl 1), pp. i49–i57.
[26] Knowles, B. M., and Dennison, C. R., 2017, "Predicting Cumulative and Maximum Brain Strain Measures From HybridIII Head Kinematics: A Combined Laboratory Study and Post-Hoc Regression Analysis," Annals of Biomedical Engineering, **45**(9), pp. 2146–2158.
[27] Kleiven, S., 2007, "Predictors for Traumatic Brain Injuries Evaluated through Accident Reconstructions," Stapp Car Crash J, **51**, pp. 81–114.

[28] Zhang, L., Yang, K. H., and King, A. I., 2004, "A Proposed Injury Threshold for Mild Traumatic Brain Injury," J Biomech Eng, **126**(2), pp. 226–236.
[29] Pellman, E. J., Viano, D. C., Tucker, A. M., Casson, I. R., and Waeckerle, J. F., 2003, "Concussion in Professional Football: Reconstruction of Game Impacts and Injuries," Neurosurgery, **53**(4), pp. 799–812; discussion 812-814.
[30] King, A. I., Yang, K. H., Zhang, L., Hardy, W., and Viano, D. C., 2003, "Is Head Injury Caused by Linear or Angular Acceleration," *IRCOBI Conference*, pp. 1–12.
[31] Elkin, B. S., Elliott, J. M., and Siegmund, G. P., 2016, "Whiplash Injury or Concussion? A Possible Biomechanical Explanation for Concussion Symptoms in Some Individuals Following a Rear-End Collision," J Orthop Sports Phys Ther, **46**(10), pp. 874–885.
[32] Takhounts, E. G., Craig, M. J., Moorhouse, K., McFadden, J., and Hasija, V., 2013, "Development of Brain Injury Criteria (BrIC)," Stapp Car Crash J, **57**, pp. 243–266.
[33] Rowson, B., Rowson, S., and Duma, S. M., 2015, "Hockey STAR: A Methodology for Assessing the Biomechanical Performance of Hockey Helmets," Ann Biomed Eng, pp. 1–15.
[34] Funk, J., Crandall, J., Withnall, C., and Wonnacott, M., *NFL Linear Impactor Helmet Test Protocol*.
[35] National Operating Committee on Standards for Athletic Equipment (NOCSAE), 2021, "Standard Pneumatic Ram Test Method and Equipment Used in Evaluating the Performance Characteristics of Protective Headgear and Face Guards."
[36] Yu, H. Y., and Dennison, C. R., 2019, "A Laboratory Study on Effects of Cycling Helmet Fit on Biomechanical Measures Associated With Head and Neck Injury and Dynamic Helmet Retention," J Biomech Eng, **141**(1).
[37] Viano, D. C., Withnall, C., and Halstead, D., 2011, "Impact Performance of Modern Football Helmets," Annals of Biomedical Engineering, **40**(1), pp. 160–174.
[38] Cobb, B. R., Zadnik, A. M., and Rowson, S., 2016, "Comparative Analysis of Helmeted Impact Response of Hybrid III and National Operating Committee on Standards for Athletic Equipment Headforms," Proceedings of the IMechE, **230**(1), pp. 50–60.
[39] Pellman, E. J., Viano, D. C., Withnall, C., Shewchenko, N., Bir, C. A., and Halstead, P. D., 2006, "Concussion in Professional Football: Helmet Testing to Assess Impact Performance—Part 11," Neurosurgery, **58**(1), pp. 78–96.
[40] Viano, D. C., Pellman, E. J., Withnall, C., and Shewchenko, N., 2006, "Concussion in Professional Football: Performance of Newer Helmets in Reconstructed Game Impacts--Part 13," Neurosurgery, **59**(3), pp. 591–606; discussion 591-606.
[41] Foster, J. K., Kortge, J. O., and Wolanin, M. J., 1977, "Hybrid III-A Biomechanically-Based Crash Test Dummy," SAE International.
[42] Martinez, L., Vera, C., Lasaga, F., and Garcia, M., 1999, "An Advanced 50th Percentile THOR Dummy Database."
[43] Wismans, J., Bermond, F., Gertosio, G., Kreuzinger, T., Roberts, A., Ratingen, M., Svensson, M. Y., Bortenschlager, K., Öhrn, H., and Page, M., 2001, *Development and Evaluation of the ES-2 Dummy*, EEVC (European Enhanced Vehicle-safety Committee).
[44] 2013, *ISO 15830-1:2013, Road Vehicles — Design and Performance Specifications for the WorldSID 50th Percentile Male Side-Impact Dummy*, 2.
[45] NHTSA, 2004, *Technical Report - Design, Development and Evaluation of the ES-2re Side Crash Test Dummy*, NHTSA Docket No. 2004-17694-9.

[46] Friedel, B., Henssler, H., Neilson, I. D., Silvestri, G., and Wismans, J., eds., 1987, *The European Side-Impact Dummy'Eurosid'. Proceedings of the Seminar Held in Brussels, 11 December 1986. EUR 10779 EN*.
[47] Office of the Federal Register, *49 CFR § 572; Anthropomorphic Test Devices*.
[48] Sances, A., Jr., 1998, "Dynamic Comparison of the Hybrid III and Human Neck," *Frontiers in Head and Neck Trauma: Clinical and Biomechanical*, N. Yoganandan, F.A. Pintar, and S.J. Larson, eds., IOS Press, OHMSHA, pp. 73–77.
[49] Yoganandan, N., Sances, Jr., A., and Pintar, F., 1989, "Biomechanical Evaluation of the Axial Compressive Responses of the Human Cadaveric and Manikin Necks," J Biomech Eng, **111**(3), pp. 250–255.
[50] Seemann, M. R., Muzzy, W. H., and Lustick, L. S., 1986, "Comparison of Human and Hybrid III Head and Neck Dynamic Response," p. 861892.
[51] Parent, D., Craig, M., and Moorhouse, K., 2017, "Biofidelity Evaluation of the THOR and Hybrid III 50 th Percentile Male Frontal Impact Anthropomorphic Test Devices," pp. 2017-22–0009.
[52] Ogle, M., 2018, "Development and Characterization of a Mechanical Surrogate Neck Prototype for Use in Helmet Certification Applications," Master of Science, University of Alberta.
[53] MacGillivray, S., 2020, "Design and Characterization of a Novel Mechanical Surrogate Neck Model for Use in Head Impact Applications," Master of Science, University of Alberta.
[54] Menon, D. K., Schwab, K., Wright, D. W., and Maas, A. I., 2010, "Position Statement: Definition of Traumatic Brain Injury," Archives of Physical Medicine and Rehabilitation, **91**(11), pp. 1637–1640.
[55] Guskiewicz, K. M., and Mihalik, J. P., 2011, "Biomechanics of Sport Concussion: Quest for the Elusive Injury Threshold," Exercise and Sport Sciences Reviews, **39**(1), pp. 4–11.
[56] Kai-Uwe Schmitt, Peter F. Niederer, Markus H. Muser, and Felix Walz, 2014, "Head Injuries," *Trauma Biomechanics: Accidental Injury in Traffic and Sports*, Springer-Verlag Berlin Heidelberg, pp. 40–46.
[57] Melvin, J. W., and Lighthall, J. W., 1993, "Brain Injury Biomechanics," *Accidental Injury - Biomechanics and Prevention*, A.M. Nahum, and J.W. Melvin, eds., Springer cience+Business Media, New York, USA, pp. 277–302.
[58] Stålhammar, D. A., 1991, "Biomechanics of Brain Injuries," *Celebral Contusions, Lacerations and Hematomas*, R.A. Frowein, ed., Springer, Vienna, pp. 1–23.
[59] Ommaya, A. K., and Gennarelli, T. A., 1974, "Cerebral Concussion and Traumatic Unconsciousness: Correlation of Experimental and Clinical Observations on Blunt Head Injuries," Brain.
[60] Ji, S., Zhao, W., Li, Z., and McAllister, T. W., 2014, "Head Impact Accelerations for Brain Strain-Related Responses in Contact Sports: A Model-Based Investigation," Biomechanics and Modeling in Mechanobiology, **13**, pp. 1121–1136.
[61] Takhounts, E. G., Hasija, V., Ridella, S. A., Rowson, S., and Duma, S. M., 2011, "Kinematic Rotational Brain Injury Criterion (BRIC)," *Proceedings of the 22nd International Technical Conference on the Enhanced Safety of Vehicles (ESV)*, Washington, DC, pp. 11–0263.
[62] Levy, M. L., Ozgur, B. M., Berry, C., Aryan, H. E., and Apuzzo, M. L. J., 2004, "Birth and Evolution of the Football Helmet," Neurosurgery, **55**(3), pp. 656–662.
[63] Denny-Brown, D., and Russel, W. R., 1941, "Experimental Cerebral Concussion," Brain, **64**(2–3), pp. 93–164.

[64] Holbourn, A. H. S., 1943, "Mechanics of Head Injuries," The Lancet, **242**(6267), pp. 438–441.
[65] Ommaya, A. K., Rockoff, S. D., Baldwin, M., and Friauf, W. S., 1964, "Experimental Concussion: A First Report," Journal of Neurosurgery, **21**(4), pp. 249–265.
[66] Ommaya, A. K., Hirsch, A. E., Flamm, E. S., and Mahone, R. H., 1966, "Cerebral Concussion in the Monkey: An Experimental Model," Science, **153**(3732), pp. 211–212.
[67] Gurdjian, E., Roberts, V., and Thomas, L., 1966, "Tolerance Curves of Acceleration and Intracranial Pressure and Protective Index in Experimental Head Injury," Journal of Trauma, **6**(5), pp. 600–604.
[68] Hodgson, V. R., Thomas, L. M., Gurdjian, E. S., Fernando, O. U., Greenberg, S. W., and Chason, J. L., 1969, "Advances in Understanding of Experimental Concussion Mechanisms."
[69] Unterharnscheidt, F. J., 1971, *Translational versus Rotational Acceleration-Animal Experiments with Measured Input*, 710880, SAE International, Warrendale, PA.
[70] GENNERELLI, T. A., 1971, "Comparison of Translational and Rotational Head Motions in Experimental Cerebral Concussion," Proc. 15th Stapp Car Crash Conference.
[71] Gennarelli, T. A., Thibault, L. E., and Ommaya, K., 1972, "Pathophysiologic Responses to Rotational and Translational Accelerations of the Head," *16th Stapp Car Crash Conference*, SAE International.
[72] Abel, J., Gennarelli, T., and Segawa, H., 1978, "Incidence and Severity of Cerebral Concussion in the Rhesus Monkey Following Sagittal Plane Angular Acceleration," SAE Technical Paper 780886.
[73] Ono, K., Kikuchi, A., Nakamura, M., Kobayashi, H., and Nakamura, N., 1980, "Human Head Tolerance to Sagittal Impact—Reliable Estimation Deduced from Experimental Head Injury Using Subhuman Primates and Human Cadaver Skulls," SAE Transactions, **89**, pp. 3837–3866.
[74] Gennarelli, T. A., Adams, J. H., and Graham, D. I., 1981, "Acceleration Induced Head Injury in the Monkey. I. The Model, Its Mechanical and Physiological Correlates," *Experimental and Clinical Neuropathology*, K. Jellinger, F. Gullotta, and M. Mossakowski, eds., Springer, Berlin, Heidelberg, pp. 23–25.
[75] Zhang, J., Yoganandan, N., Pintar, F. A., and Gennarelli, T. A., 2006, "Role of Translational and Rotational Accelerations on Brain Strain in Lateral Head Impact," Biomed Sci Instrum, **42**, pp. 501–506.
[76] Greenwald, R. M., and Crisco, J. J., 2008, "Head Impact Severity Measures for Evaluating Mild Traumatic Brain Injury Risk Exposure," Neurosurgery, **62**, pp. 789–798.
[77] Takhounts, E. G., Ridella, S. A., Hasija, V., Tannous, R. E., Campbell, J. Q., Malone, D., Danelson, K., Stitzel, J., Rowson, S., and Duma, S., 2008, "Investigation of Traumatic Brain Injuries Using the Next Generation of Simulated Injury Monitor (SIMon) Finite Element Head Model," Stapp Car Crash Journal, **52**, pp. 1–31.
[78] "J885: Human Tolerance to Impact Conditions as Related to Motor Vehicle Design - SAE International" [Online]. Available: https://www.sae.org/standards/content/j885_201102/. [Accessed: 19-Oct-2021].
[79] Beckwith, J. G., Greenwald, R. M., Chu, J. J., Crisco, J. J., Rowson, S., Duma, S. M., Broglio, S. P., McAllister, T. W., Guskiewicz, K. M., Mihalik, J. P., Anderson, S., Schnebel, B., Brolinson, P. G., and Collins, M. W., 2013, "Head Impact Exposure Sustained by Football Players on Days of Diagnosed Concussion," Med Sci Sports Exerc, **45**(4), pp. 737–746.

[80] Rowson, S., and Duma, S. M., 2013, "Brain Injury Prediction: Assessing the Combined Probability of Concussion Using Linear and Rotational Head Acceleration," Ann Biomed Eng, **41**(5), pp. 873–882.
[81] Gabler, L. F., Crandall, J. R., and Panzer, M. B., 2016, "Assessment of Kinematic Brain Injury Metrics for Predicting Strain Responses in Diverse Automotive Impact Conditions," Annals of Biomedical Engineering, **44**(12), pp. 3705–3718.
[82] Kimpara, H., and Iwamoto, M., 2012, "Mild Traumatic Brain Injury Predictors Based on Angular Accelerations During Impacts," Annals of Biomedical Engineering, **40**(1), pp. 114–126.
[83] Wu, T., Hajiaghamemar, M., Giudice, J. S., Alshareef, A., Margulies, S. S., and Panzer, M. B., 2021, "Evaluation of Tissue-Level Brain Injury Metrics Using Species-Specific Simulations," J Neurotrauma, **38**(13), pp. 1879–1888.
[84] Margulies, S. S., Thibault, L. E., and Gennarelli, T. A., 1990, "Physical Model Simulations of Brain Injury in the Primate," J Biomech, **23**(8), pp. 823–836.
[85] Elkin, B. S., and Morrison, B., 2007, "Region-Specific Tolerance Criteria for the Living Brain," Stapp Car Crash J, **51**, pp. 127–138.
[86] Duma, S. M., and Rowson, S., 2014, "The Biomechanics of Concussion: 60 Years of Experimental Research," *Concussions in Athletics: From Brain to Behavior*, S.M. Slobounov, and W.J. Sebastianelli, eds., Springer, New York, NY, pp. 115–137.
[87] Hoshizaki, T. B., Post, A., Kendall, M., Cournoyer, J., Rousseau, P., Gilchrist, M. D., Brien, S., Cusimano, M., and Marshall, S., 2017, "The Development of a Threshold Curve for the Understanding of Concussion in Sport," Trauma, **19**(3), pp. 196–206.
[88] Fernandes, F. A., and Sousa, R. J. A. de, 2015, "Head Injury Predictors in Sports Trauma – A State-of-the-Art Review," Proc Inst Mech Eng H, **229**(8), pp. 592–608.
[89] Mertz, H. J., Irwin, A. L., and Prasad, P., 2003, "Biomechanical and Scaling Bases for Frontal and Side Impact Injury Assessment Reference Values.," Stapp Car Crash J, **47**, p. 155.
[90] "CAN-CSA-D113.2-M89 (R2009)."
[91] 2012, "CSA Z262.1-09: Standard for Ice Hockey Helmets."
[92] F08 Committee, *ASTM F1045 - 16: Performance Specification for Ice Hockey Helmets*, ASTM International.
[93] "ASTM_F717_Football_Helmets.Pdf."
[94] 2021, "Standard Performance Specification For Newly Manufactured Football Helmets - NOCSAE."
[95] McIntosh, A. S., Andersen, T. E., Bahr, R., Greenwald, R., Kleiven, S., Turner, M., Varese, M., and McCrory, P., 2011, "Sports Helmets Now and in the Future," British Journal of Sports Medicine, **45**(16), pp. 1258–1265.
[96] Mueller, F. O., 1998, "FATALITIES FROM HEAD AND CERVICAL SPINE INJURIES OCCURRING IN TACKLE FOOTBALL: 50 YEARS' EXPERIENCE," Clinics in Sports Medicine, **17**(1), pp. 169–182.
[97] Bonfield, C. M., Shin, S. S., and Kanter, A. S., 2015, "Helmets, Head Injury and Concussion in Sport," Phys Sportsmed, **43**(3), pp. 236–246.
[98] Cantu, R. C., and Mueller, F. O., 2003, "Brain Injury-Related Fatalities in American Football, 1945-1999," Neurosurgery, **52**(4), pp. 846–853.
[99] Gadd, C. W., 1966, *Use of a Weighted-Impulse Criterion for Estimating Injury Hazard*, 660793, SAE International, Warrendale, PA.

[100] Bandak, F., Eppinger, R., Haffner, M., Khaewpong, N., Kuppa, S., Maltese, M., Nguyen, T., Saul, R., Sun, E., Takhounts, E., Tannous, R., and Zhang, A., 1999, *Development of Improved Injury Criteria for the Assessment of Advanced Automotive Restraint Systems : II*.
[101] Versace, J., 1971, *A Review of the Severity Index*, 710881, SAE International, Warrendale, PA.
[102] Newman, J. A., 1986, "A Generalized Model for Brain Injury Threshold (GAMBIT)," *IRCOBI Conference Proceedings*, Zurich, Switzerland.
[103] Newman, J. A., Shewchenko, N., and Welbourne, E., 2000, "A Proposed New Biomechanical Head Injury Assessment Function - the Maximum Power Index," Stapp Car Crash J, **44**, pp. 215–47.
[104] Kimpara, H., Nakahira, Y., Iwamoto, M., Rowson, S., and Duma, S., 2011, "Head Injury Prediction Methods Based on 6 Degree of Freedom Head Acceleration Measurements during Impact," International Journal of Automotive Engineering, **2**, pp. 13–19.
[105] Yanaoka, T., Dokko, Y., and Takahashi, Y., 2015, *Investigation on an Injury Criterion Related to Traumatic Brain Injury Primarily Induced by Head Rotation*, 2015-01–1439, SAE International, Warrendale, PA.
[106] Gabler, L. F., Crandall, J. R., and Panzer, M. B., 2018, "Development of a Metric for Predicting Brain Strain Responses Using Head Kinematics," Ann Biomed Eng, **46**(7), pp. 972–985.
[107] Ommaya, A., Hirsch, A., and Martinez, J., 1966, "The Role of Whiplash in Cerebral Concussion," SAE Technical Paper 660804.
[108] Homayounpour, M., Gomez, N. G., Vasavada, A. N., and Merryweather, A. S., 2021, "The Role of Neck Muscle Co-Contraction and Postural Changes in Head Kinematics after Safe Head Impacts: Investigation of Head/Neck Injury Reduction," Journal of Biomechanics, **128**, p. 110732.
[109] Reynier, K. A., Alshareef, A., Sanchez, E. J., Shedd, D. F., Walton, S. R., Erdman, N. K., Newman, B. T., Giudice, J. S., Higgins, M. J., Funk, J. R., Broshek, D. K., Druzgal, T. J., Resch, J. E., and Panzer, M. B., 2020, "The Effect of Muscle Activation on Head Kinematics During Non-Injurious Head Impacts in Human Subjects," Ann Biomed Eng.
[110] Schmidt, J. D., Guskiewicz, K. M., Blackburn, J. T., Mihalik, J. P., Siegmund, G. P., and Marshall, S. W., 2014, "The Influence of Cervical Muscle Characteristics on Head Impact Biomechanics in Football," Am J Sports Med, **42**(9), pp. 2056–2066.
[111] Mertz, H., 1993, "Anthropomorphic Test Devices," *Accidental Injury - Biomechanics and Prevention*, Springer Science+Business Media, New York, USA.
[112] *ISO 15830-2 - Road Vehicles - Design and Performance Specifications for the WorldSID 50th Percentile Male Side-Impact Dummy - Part 2: Mechanical Subsystems - Second Edition*.
[113] *ISO TR 9790 - Road Vehicles - Anthropomorphic Side Impact Dummy - Lateral Impact Response Requirements to Assess the Biofidelity of the Dummy*.
[114] McAdams, H. T., 1973, "The Repeatability of Dummy Performance," *Human Impact Response: Measurement and Simulation*, W.F. King, and H.J. Mertz, eds., Springer US, Boston, MA, pp. 35–67.
[115] Stricklin, J., and Rhule, D., 2004, *Evaluation of the EuroSID-2re Certification Tests Repeatability and Reproducibility*, NHTSA-2004-18864-0011.
[116] Saul, R. A., 1985, *Repeatability Program Dummy Variability Analysis. Volume II. Final Report*.

[117] Janssen, E. G., and Wismans, J. S. H. M., 1987, "REPEATABILITY AND REPRODUCIBILITY OF THE EUROPEAN SIDE IMPACT DUMMY," *The European Side-Impact Dummy'Eurosid'. Proceedings of the Seminar Held in Brussels, 11 December 1986. EUR 10779 EN*, Delft, Netherlands.
[118] Saul, R. A., 1985, *Repeatability Program Dummy Variability Analysis. Volume I. Final Report*.
[119] Been, B., Philippens, M., de Lange, R., and van Ratingen, M., 2004, "WorldSID Dummy Head-Neck Biofidelity Response," Stapp Car Crash J, **48**, pp. 431–454.
[120] Scherer, R., Bortenschlager, K., Akiyama, A., Tylko, S., Hartlieb, M., and Harigae, T., 2009, "WorldSID Production Dummy Biomechanical Responses," Experimental Safety of Vehicles, pp. 18–22.
[121] NHTSA, 2018, *THOR 50th Percentile Male (THOR-50M) Qualification Procedures Manual*, NHTSA-2019-0106-0001.
[122] 2005, *Biomechanical Response Requirements of the THOR NHTSA Advanced Frontal Dummy*, GESAC-05-03, General Engineering and Systems Analysis Company, Inc., Boonsboro, MD.
[123] Millis, W., Hagedorn, A. V., Murach, M., and United States. Department of Transportation. National Highway Traffic Safety Administration. Vehicle Research and Test Center, 2020, *THOR-50M Durability Report*, DOT HS 812 869.
[124] Hubbard, R., and McLeod, D., 1974, "Definition and Development of a Crash Dummy Head," SAE Technical paper 741193.
[125] Mertz, H. J., Neathery, R. F., and Culver, C. C., 1973, "Performance Requirements and Characteristics of Mechanical Necks," *Human Impact Response: Measurement and Simulation*, W.F. King, and H.J. Mertz, eds., Springer US, Boston, MA, pp. 263–288.
[126] Wismans, J., and Spenny, C. H., 1983, "Performance Requirements for Mechanical Necks in Lateral Flexion," p. 831613.
[127] Thunnissen, J. G. M., Wismans, J. S. H. M., Ewing, C. L., and Thomas, D. J., 1995, "Human Volunteer Head-Neck Response in Frontal Flexion: A New Analysis," SAE Transactions, **104**, pp. 3065–3086.
[128] Patrick, L. M., and Chou, C. C., 1976, *Response of the Human Neck in Flexion, Extension and Lateral Flexion*, VRI-7.3, Wayne State University College of Engineering, Department of Mechanical Engineering Sciences.
[129] Ewing, C. L., D. J. Thomas, R. Black Majewski, and Lustick, L., 1977, "Measurement of Head , T1 , and Pelvic Response to -Gx Impact Acceleration," *SAE Technical Paper 770927*.
[130] Wismans, J., van Oorschot, H., and Woltring, H. J., 1986, "Omni-Directional Human Head-Neck Response," SAE Transactions, **95**, pp. 819–837.
[131] Hodgson, V., and Thomas, L., 1971, "Comparison of Head Acceleration Injury Indices in Cadaver Skull Fracture," SAE Technical Paper 710854, p. 9 pp.
[132] Ewing, C. L., Thomas, D. J., Beeler, G. W., Patrick, L. M., and Gillis, D. B., 1968, "Dynamic Response of the Head and Neck of the Living Human to -Gx Impact Acceleration," p. 680792.
[133] Ewing, C. L., Thomas, D. J., Lustick, L., Muzzy, W. H., Willems, G., and Majewski, P. L., 1976, *The Effect of Duration, Rate of Onset, and Peak Sled Acceleration on the Dynamic Response of the Human Head and Neck*, 760800, SAE International, Warrendale, PA.
[134] Mertz, H. J., 1985, "Biofidelity of the Hybrid III Head," SAE Transactions, **94**, pp. 97–105.

[135] Loyd, A. M., Nightingale, R. W., Song, Y., Luck, J. F., Cutcliffe, H., Myers, B. S., and Bass, C. 'Dale,' 2014, "The Response of the Adult and ATD Heads to Impacts onto a Rigid Surface," Accident Analysis & Prevention, **72**, pp. 219–229.
[136] Bartsch, A., Benzel, E., Miele, V., Morr, D., and Prakash, V., 2012, "Hybrid III Anthropomorphic Test Device (ATD) Response to Head Impacts and Potential Implications for Athletic Headgear Testing," Accid Anal Prev, **48**, pp. 285–291.
[137] Haffner, M., Eppinger, R., Rangarajan, N., Shams, T., Artis, M., and Beach, D., 2001, *Foundations and Elements of the NHTSA Thor ALPHA ATD Design*, 2001-06–0107, SAE International, Warrendale, PA.
[138] Yoganandan, N., Pintar, F. A., Schlick, M., Moore, J., and Maiman, D. J., 2011, "Comparison of Head-Neck Responses in Frontal Impacts Using Restrained Human Surrogates," Ann Adv Automot Med, **55**, pp. 181–191.
[139] Sandner, V., Ellway, J., and van Ratingen, M., 2017, "Euro NCAP Frontal Impact Working Group Report."
[140] Donnelly, B. R., Morgan, R. M., and Eppinger, R. H., 1983, *Durability, Repeatability and Reproducibility of the NHTSA Side Impact Dummy*, 831624, SAE International, Warrendale, PA.
[141] Byrnes, K., Abramczyk, J., Berliner, J., Irwin, A., Jensen, J., Kowsika, M., Mertz, H. J., Rouhana, S. W., Scherer, R., Shi, Y., Sutterfield, A., Xu, L., Tylko, S., and Dalmotas, D., 2002, "ES-2 Dummy Biomechanical Responses," pp. 2002-22–0018.
[142] MacGillivray, S., Wynn, G., Ogle, M., Shore, J., Carey, J. P., and Dennison, C. R., 2021, "Repeatability and Biofidelity of a Physical Surrogate Neck Model Fit to a Hybrid III Head," Ann Biomed Eng, **49**(10), pp. 2957–2972.
[143] Saari, A., Dennison, C. R., Zhu, Q., Nelson, T. S., Morley, P., Oxland, T. R., Cripton, P. A., and Itshayek, E., 2013, "Compressive Follower Load Influences Cervical Spine Kinematics and Kinetics during Simulated Head-First Impact in an in Vitro Model," J Biomech Eng, **135**(11), p. 111003.
[144] Moroney, S. P., Schultz, A. B., and Miller, J. A. A., 1988, "Analysis and Measurement of Neck Loads," Journal of Orthopaedic Research, **6**, pp. 713–720.
[145] Miura, T., Panjabi, M. M., and Cripton, P. A., 2002, "A Method to Simulate in Vivo Cervical Spine Kinematics Using in Vitro Compressive Preload," Spine, **27**, pp. 43–48.
[146] ASTM F1045-07, 2007, *Standard Performance Specification for Ice Hockey Helmets*, West Conshohocken, PA.
[147] 2018, "Standard Linear Impactor Test Method and Equipment Used in Evaluating the Performance Characteristics of Protective Headgear and Faceguards," NOCSAE.
[148] Society of Automotive Engineers, 2014, "SAE J211 Instrumentation for Impact Test - Part 1: Electronic Instrumentation."
[149] Padgaonkar, A. J., Krieger, K. W., and King, A. I., 1975, "Measurement of Angular Acceleration of a Rigid Body Using Linear Accelerometers," J. Appl. Mech, **42**(3), pp. 552–556.
[150] Pellman, E. J., Viano, D. C., Tucker, A. M., and Casson, I. R., 2003, "Concussion in Professional Football: Location and Direction of Helmet Impacts-Part 2," Neurosurgery, **53**(6), p. 1328.
[151] Karton, C., Blaine Hoshizaki, T., and Gilchrist, M. D., 2020, "A Novel Repetitive Head Impact Exposure Measurement Tool Differentiates Player Position in National Football League," Scientific Reports, **10**(1), p. 1200.

[152] Crisco, J. J., Wilcox, B. J., Beckwith, J. G., Chu, J. J., Duhaime, A.-C., Rowson, S., Duma, S. M., Maerlender, A. C., McAllister, T. W., and Greenwald, R. M., 2011, "Head Impact Exposure in Collegiate Football Players," J Biomech, **44**(15), pp. 2673–2678.
[153] Crisco, J. J., Wilcox, B. J., Machan, J. T., McAllister, T. W., Duhaime, A.-C., Duma, S. M., Rowson, S., Beckwith, J. G., Chu, J. J., and Greenwald, R. M., 2012, "Magnitude of Head Impact Exposures in Individual Collegiate Football Players," J Appl Biomech, **28**(2), pp. 174–183.
[154] Rowson, S., Duma, S. M., Beckwith, J. G., Chu, J. J., Greenwald, R. M., Crisco, J. J., Brolinson, P. G., Duhaime, A.-C., McAllister, T. W., and Maerlender, A. C., 2012, "Rotational Head Kinematics in Football Impacts: An Injury Risk Function for Concussion," Ann Biomed Eng, **40**(1), pp. 1–13.
[155] Stemper, B. D., Shah, A. S., Harezlak, J., Rowson, S., Mihalik, J. P., Duma, S. M., Riggen, L. D., Brooks, A., Cameron, K. L., Campbell, D., DiFiori, J. P., Giza, C. C., Guskiewicz, K. M., Jackson, J., McGinty, G. T., Svoboda, S. J., McAllister, T. W., Broglio, S. P., McCrea, M., and the CARE Consortium Investigators, 2019, "Comparison of Head Impact Exposure Between Concussed Football Athletes and Matched Controls: Evidence for a Possible Second Mechanism of Sport-Related Concussion," Ann Biomed Eng, **47**(10), pp. 2057–2072.
[156] Faul, F., Erdfelder, E., Lang, A.-G., and Buchner, A., 2007, "G*Power 3: A Flexible Statistical Power Analysis Program for the Social, Behavioral, and Biomedical Sciences," Behavior Research Methods, **39**(2), pp. 175–191.
[157] Schmider, E., Ziegler, M., Danay, E., Beyer, L., and Bühner, M., 2010, "Is It Really Robust?," Methodology, **6**(4), pp. 147–151.
[158] Blanca, M. J., Alarcón, R., Arnau, J., Bono, R., and Bendayan, R., 2017, "Non-Normal Data: Is ANOVA Still a Valid Option?," Psicothema, **29**(4), pp. 552–557.
[159] Cohen, J., 2013, "The Analysis of Variance," *Statistical Power Analysis for the Behavioral Sciences*, Routledge, pp. 284–288.
[160] Cohen, J., 2013, "The t Test for Means," *Statistical Power Analysis for the Behavioral Sciences*, Routledge, pp. 24–27.
[161] Cohen, J., 2013, *Statistical Power Analysis for the Behavioral Sciences*, Academic Press.